

AD-A262 363



20000920306

(2)

ARMY RESEARCH LABORATORY



Analysis of the Static and Dynamic Response of a T-38 Wing and Comparison With Experimental Data

Jong-Ho Woo

ARL-TR-99

March 1993

Reproduced From
Best Available Copy

DTIC
ELECTE
APR 05 1993
S E D

APPROVED FOR PUBLIC RELEASE; DISTRIBUTION IS UNLIMITED.

93 4 02 126

93-06967



105pg

NOTICES

Destroy this report when it is no longer needed. DO NOT return it to the originator.

Additional copies of this report may be obtained from the National Technical Information Service, U.S. Department of Commerce, 5285 Port Royal Road, Springfield, VA 22161.

The findings of this report are not to be construed as an official Department of the Army position, unless so designated by other authorized documents.

The use of trade names or manufacturers' names in this report does not constitute indorsement of any commercial product.

| REPORT DOCUMENTATION PAGE | | | Form Approved OMB No. 0704-0188 | |
|---|---|--|--|--|
| <small>Public reporting burden for this collection of information is estimated to average 1 hour per response, including the time for reviewing instructions, searching existing data sources, gathering and maintaining the data needed, and completing and reviewing the collection of information. Send comments regarding this burden estimate or any other aspect of this collection of information, including suggestions for reducing this burden, to Washington Headquarters Services, Directorate for Information Operations and Reports, 1215 Jefferson Davis Highway, Suite 1204, Arlington, VA 22202-4302, and to the Office of Management and Budget, Paperwork Reduction Project (0704-0188), Washington, DC 20503.</small> | | | | |
| 1. AGENCY USE ONLY (Leave blank) | | 2. REPORT DATE March 1993 | | 3. REPORT TYPE AND DATES COVERED Final, Aug 90-Nov 91 |
| 4. TITLE AND SUBTITLE Analysis of the Static and Dynamic Response of a T-38 Wing and Comparison With Experimental Data | | | 5. FUNDING NUMBERS PR: 1L162618AH80 | |
| 6. AUTHOR(S) Jong-Ho Woo | | | | |
| 7. PERFORMING ORGANIZATION NAME(S) AND ADDRESS(ES) U.S. Army Research Laboratory ATTN: AMSRL-SL-BA Aberdeen Proving Ground, MD 21005-5068 | | | 8. PERFORMING ORGANIZATION REPORT NUMBER | |
| 9. SPONSORING/MONITORING AGENCY NAME(S) AND ADDRESS(ES) U.S. Army Research Laboratory ATTN: AMSRL-OP-CI-B (Tech Lib) Aberdeen Proving Ground, MD 21005-5066 | | | 10. SPONSORING/MONITORING AGENCY REPORT NUMBER ARL-TR-99 | |
| 11. SUPPLEMENTARY NOTES | | | | |
| 12a. DISTRIBUTION/AVAILABILITY STATEMENT Approved for public release; distribution is unlimited. | | | 12b. DISTRIBUTION CODE | |
| 13. ABSTRACT (Maximum 200 words) <p>This report documents the investigation of a three-dimensional finite element model for calculating the static displacement and dynamic structural response of a T-38 wing and comparison of the analytical results with T-38 wing experimental data from Northrop Aircraft, Inc.</p> <p>The wing structure is modeled by rod and bar (beam), quadrilateral plate, triangular plate, and shear panel finite elements. The general structural analysis programs MSC/NASTRAN and MSC/PAL2 are used to calculate deflections, natural frequencies, and mode shapes.</p> <p>The wing finite element model yielded excellent agreement between calculated and experimental results for the eight loading conditions studied. The methodology developed in this study is expected to provide a valuable tool for the static aeroelastic response and dynamic analysis of wing structures in conjunction with aircraft ballistic vulnerability assessments.</p> | | | | |
| 14. SUBJECT TERMS T-38 wing; deflection; natural frequency; finite element methods; shear panel; MSC/NASTRAN; MSC/PAL 2; resonant frequency | | | 15. NUMBER OF PAGES 102 | |
| | | | 16. PRICE CODE | |
| 17. SECURITY CLASSIFICATION OF REPORT UNCLASSIFIED | 18. SECURITY CLASSIFICATION OF THIS PAGE UNCLASSIFIED | 19. SECURITY CLASSIFICATION OF ABSTRACT UNCLASSIFIED | 20. LIMITATION OF ABSTRACT SAR | |

INTENTIONALLY LEFT BLANK

TABLE OF CONTENTS

| | | |
|-----|--|-----|
| | LIST OF FIGURES | v |
| | LIST OF TABLES | ix |
| 1. | INTRODUCTION | 1 |
| 1.1 | General Approach to the Problem | 1 |
| 2. | WING FINITE ELEMENT MODEL ANALYSIS | 2 |
| 2.1 | Wing Description | 2 |
| 2.2 | Development of the Finite Element Model | 3 |
| 2.3 | Designation of Finite Element Model | 6 |
| 2.4 | Sizing of Rod elements | 10 |
| 2.5 | Boundary Conditions | 13 |
| 3. | GENERAL STRUCTURAL ANALYSIS | 14 |
| 3.1 | Linear Static Analysis | 14 |
| 3.2 | Dynamic Analysis | 15 |
| 4. | DISCUSSION OF RESULTS | 46 |
| 5. | CONCLUSIONS | 48 |
| 6. | RECOMMENDATIONS | 48 |
| 7. | REFERENCES | 51 |
| | APPENDIX A: Finite Element Model Numbering Details | 53 |
| | APPENDIX B: Finite Element Model for Top, Middle, and Bottom | 63 |
| | APPENDIX C: Rattinger's Wing | 73 |
| | APPENDIX D: Input Data for QSR1.DAT | 87 |
| | DISTRIBUTION LIST | 101 |

DTIC QUALITY INSPECTED 4

| | |
|--------------------|-------------------------------------|
| Accession For | |
| NTIS | <input checked="" type="checkbox"/> |
| CRA&I | <input checked="" type="checkbox"/> |
| DTIC TAB | <input type="checkbox"/> |
| Unannounced | <input type="checkbox"/> |
| Justification | |
| By _____ | |
| Distribution / | |
| Availability Codes | |
| Dist | Avail and/or Special |
| A-1 | |

INTENTIONALLY LEFT BLANK

LIST OF FIGURES

| <u>Figure</u> | <u>Page</u> |
|---|-------------|
| 1. T-38 Real Wing Structure | 3 |
| 2. T-38 Wing Internal Structure | 4 |
| 3a. Top View of Finite Element Model QSB1.DAT and QSR1.DAT | 7 |
| 3b. Top View of Finite Element Model TSB1.DAT and TSR1.DAT | 8 |
| 4a. Top View of Finite Element Model QSB2.DAT and QSR2.DAT | 8 |
| 4b. Top View of Finite Element Model TSB2.DAT and TSR2.DAT | 8 |
| 5a. Top View of Finite Element Model QSB3.DAT and QSR3.DAT | 9 |
| 5b. Top View of Finite Element Model TSB3.DAT and TSR3.DAT | 9 |
| 6. Top View of Finite Element Model QTSR4.DAT and QTSB4.DAT | 9 |
| 7. C-Beam Case | 11 |
| 8. I-Beam Case | 12 |
| 9. Loading Condition for T-38 Wing from Boundary Condition | 13 |
| 10. Position of Loading Node | 17 |
| 11a. Comparison of Displacements from TSRI.DAT and Test (500 lb at Node A) | 19 |
| 11b. Comparison of Displacements from TSBi.DAT and Test (500 lb at Node A) | 19 |
| 11c. Comparison of Displacements from QSRI.DAT and Test (500 lb at Node A) | 20 |
| 11d. Comparison of Displacements from QSBi.DAT and Test (500 lb at Node A) | 20 |
| 11e. Comparison of Displacements from SSR1.DAT and Test (500 lb at Node A) | 21 |
| 11f. Comparison of Displacements from QTSR4.DAT, QTSB4.DAT and Test (500 lb at Node A) | 21 |
| 12a. Comparison of Displacements from TSRI.DAT and Test (1,000 lb at Node B) | 22 |
| 12b. Comparison of Displacements from TSRI.DAT and Test (1,000 lb at Node B) | 22 |
| 12c. Comparison of Displacements from QSRI.DAT and Test (1,000 lb at Node B) | 23 |
| 12d. Comparison of Displacements from QSRI.DAT and Test (1,000 lb at Node B) | 23 |

| | | |
|------|--|----|
| 12e. | Comparison of Displacements from SSR1.DAT and Test (1,000 lb at Node B) | 24 |
| 12f. | Comparison of Displacements from QTSR4.DAT, QTSB4.DAT and Test (1,000 lb at Node B) | 24 |
| 13a. | Comparison of Displacements from TSRI.DAT and Test (200 lb at Node C) | 25 |
| 13b. | Comparison of Displacements from TSBI.DAT and Test (200 lb at Node C) | 25 |
| 13c. | Comparison of Displacements from QSRI.DAT and Test (200 lb at Node C) | 26 |
| 13d. | Comparison of Displacements from QSBi.DAT and Test (200 lb at Node C) | 26 |
| 13e. | Comparison of Displacements from SSR1.DAT and Test (200 lb at Node C) | 27 |
| 13f. | Comparison of Displacements from QTSR4.DAT, QTSB4.DAT and Test (200 lb at Node C) | 27 |
| 14a. | Comparison of Displacements from TSRI.DAT and Test (1,500 lb at Node D) | 28 |
| 14b. | Comparison of Displacements from TSBI.DAT and Test (1,500 lb at Node D) | 28 |
| 14c. | Comparison of Displacements from QSRI.DAT and Test (1,500 lb at Node D) | 29 |
| 14d. | Comparison of Displacements from QSBi.DAT and Test (1,500 lb at Node D) | 29 |
| 14e. | Comparison of Displacements from SSR1.DAT and Test (1,500 lb at Node D) | 30 |
| 14f. | Comparison of Displacements from QTSR4.DAT, QTSB4.DAT and Test (1,500 lb at Node D) | 30 |
| 15a. | Comparison of Displacements from TSRI.DAT and Test (2,500 lb at Node E) | 31 |
| 15b. | Comparison of Displacements from TSBI.DAT and Test (2,500 lb at Node E) | 31 |
| 15c. | Comparison of Displacements from QSRI.DAT and Test (2,500 lb at Node E) | 32 |
| 15d. | Comparison of Displacements from QSBi.DAT and Test (2,500 lb at Node E) | 32 |
| 15e. | Comparison of Displacements from SSR1.DAT and Test (2,500 lb at Node E) | 33 |
| 15f. | Comparison of Displacements from QTSR4.DAT, QTSB4.DAT and Test (2,500 lb at Node E) | 33 |
| 16a. | Comparison of Displacements from TSRI.DAT and Test (500 lb at Node F) | 34 |
| 16b. | Comparison of Displacements from TSBI.DAT and Test (500 lb at Node F) | 34 |
| 16c. | Comparison of Displacements from QSRI.DAT and Test (500 lb at Node F) | 35 |

| | | |
|------|--|----|
| 16d. | Comparison of Displacements from QSBi.DAT and Test (500 lb at Node F) | 35 |
| 16e. | Comparison of Displacements from SSR1.DAT and Test (500 lb at Node F) | 36 |
| 16f. | Comparison of Displacements from QTSR4.DAT, QTSB4.DAT and Test (500 lb at Node F) | 36 |
| 17a. | Comparison of Displacements from TSRI.DAT and Test (3,000 lb at Node G) | 37 |
| 17b. | Comparison of Displacements from TSBi.DAT and Test (3,000 lb at Node G) | 37 |
| 17c. | Comparison of Displacements from QSRi.DAT and Test (3,000 lb at Node G) | 38 |
| 17d. | Comparison of Displacements from QSBi.DAT and Test (3,000 lb at Node G) | 38 |
| 17e. | Comparison of Displacements from SSR1.DAT and Test (3,000 lb at Node G) | 39 |
| 17f. | Comparison of Displacements from QTSR4.DAT, QTSB4.DAT and Test (3,000 lb at Node G) | 39 |
| 18a. | Comparison of Displacements from TSRI.DAT and Test (5,000 lb at Node H) | 40 |
| 18b. | Comparison of Displacements from TSBi.DAT and Test (5,000 lb at Node H) | 40 |
| 18c. | Comparison of Displacements from QSRi.DAT and Test (5,000 lb at Node H) | 41 |
| 18d. | Comparison of Displacements from QSBi.DAT and Test (5,000 lb at Node H) | 41 |
| 18e. | Comparison of Displacements from SSR1.DAT and Test (5,000 lb at Node H) | 42 |
| 18f. | Comparison of Displacements from QTSR4.DAT, QTSB4.DAT and Test (5,000 lb at Node H) | 42 |
| 19a. | Numerically Predicted Mode Shape 1, $\omega_1 = 4.643$ | 43 |
| 19b. | Numerically Predicted Mode Shape 2, $\omega_2 = 6.745$ | 43 |
| 19c. | Numerically Predicted Mode Shape 3, $\omega_3 = 7.092$ | 43 |
| 19d. | Numerically Predicted Mode Shape 4, $\omega_4 = 7.105$ | 44 |
| 19e. | Numerically Predicted Mode Shape 5, $\omega_5 = 7.799$ | 44 |
| 19f. | Numerically Predicted Mode Shape 6, $\omega_6 = 7.944$ | 44 |
| 19g. | Numerically Predicted Mode Shape 7, $\omega_7 = 8.269$ | 45 |
| 19h. | Numerically Predicted Mode Shape 8, $\omega_8 = 10.681$ | 45 |
| 19i. | Numerically Predicted Mode Shape 9, $\omega_9 = 11.542$ | 45 |

| | | |
|------|--|----|
| 19j. | Numerically Predicted Mode Shape 10, $\omega_{10} = 12.655$ | 46 |
| A1. | Node Numbers, Top Surface | 55 |
| A2. | Node Numbers, Bottom Surface | 56 |
| A3. | Skin Panel Numbers, Top Surface | 57 |
| A4. | Skin Panel Numbers, Bottom Surface | 58 |
| A5. | Spar Web Element Numbers | 59 |
| A6. | Rib Web Element Numbers | 60 |
| A7. | Spar and Rib Chord Numbers, Top Surface | 61 |
| A8. | Spar and Rib Chord Numbers, Bottom Surface | 62 |
| B1. | Finite Element Model QSB1.DAT and QSR1.DAT (Top, Middle, and Bottom) | 65 |
| B2. | Finite Element Model QSB2.DAT and QSR2.DAT (Top, Middle, and Bottom) | 66 |
| B3. | Finite Element Model QSB3.DAT and QSR3.DAT (Top, Middle, and Bottom) | 67 |
| B4. | Finite Element Model TSB1.DAT and TSR1.DAT (Top, Middle, and Bottom) | 68 |
| B5. | Finite Element Model TSB2.DAT and TSR2.DAT (Top, Middle, and Bottom) | 69 |
| B6. | Finite Element Model TSB3.DAT and TSR3.DAT (Top, Middle, and Bottom) | 70 |
| B7. | Finite Element Model QTSB4.DAT and QTSR4.DAT (Top, Middle, and Bottom) . . . | 71 |
| C1. | General Box-Beam | 75 |
| C2. | Geometry of Structural Model of Rattinger's Wing | 76 |
| C3. | Finite Element Model Using Eq. C1 | 77 |
| C4. | Finite Element Model Using Eq. C2 | 78 |
| C5. | Finite Element Model SSR.1, SSR.2, SSR.3, SSR.4, QSR.1, QSR.2, QSB.1, QSB.2, QQR.1, and QQR.2 | 79 |
| C6. | Finite Element Model TSR.1, TSR.2, TSB.1, TSB.2, TQR.1, and TQR.2 | 80 |
| C7. | Finite Element Model QSR.3, QSR.4, QSB.3, and QSB.4 | 81 |
| C8. | Finite Element Model TSR.3, TSR.4, TSB.3, and TSB.4 | 82 |

LIST OF TABLES

| <u>Table</u> | <u>Page</u> |
|---|-------------|
| 1a. Designation of Finite Element Model 1 | 6 |
| 1b. Designation of Finite Element Model 2 | 6 |
| 1c. Designation of Finite Element Model 3 | 7 |
| 1d. Designation of Finite Element Model 4 | 7 |
| 2. Load Distribution at Each Node | 17 |
| 3. Natural Frequencies of T-38 Wing | 18 |
| C1. Finite Element Model Designation of Rattinger's Wing | 83 |
| C2. Comparison of Displacements from Finite Element Models of Rattinger's Wing and Test Data | 84 |

INTENTIONALLY LEFT BLANK

x

1. INTRODUCTION

This study represents the first step in the development of a methodology to analyze the structural response of aircraft wings with combat damage. An attempt is made to find an adequate structural model that could subsequently be used to accurately calculate static and dynamic aeroelastic characteristics.

The first step in this effort involved the following tasks:

- a) Develop modeling techniques for efficiency and accuracy
- b) Compare calculated deflections with experimental data
- c) Calculate natural frequencies and mode shapes

The overall objectives of this work are to:

- a) Select a finite element model and predict failure loads for a damaged wing structure
- b) Develop an aerodynamic model based on the finite element model (item a.) for static aeroelasticity, flutter analysis, and dynamic aeroelasticity.
- c) Idealize a box-beam type finite element model as a plate-beam type to save computing time and reduce the effort required to model a damaged wing.

T-38 wing deflection data from tests conducted in 1960 were obtained from the Northrop Corporation, Norair Division, See Reference [1]. During these tests, the aircraft was supported at the forward and aft fuselage by two steel jigs tied to a steel erectile structure. Wing loading was accomplished by means of hydraulic hand pumps and pressure gages, Northrop electrically-operated load maintainers, and Edison hydraulic proportioning units.

1.1 General Approach to the Problem

The MSC/NASTRAN and MSC/PAL2 finite element analysis programs were used initially to analyze the wing structure. They have special tools for the analysis of thin-skinned aircraft

structures. Following this effort, the MSC/NASTRAN Aeroelastic code was used for static aeroelastic response, flutter, and dynamic aeroelastic analyses.

The finite element model designated as Model 1, shown on pages 7 and 8, is the baseline for the study and is used in each of the analyses. These analyses and the associated MSC/NASTRAN and MSC/PAL2 solutions are approached as follows:

1. Finite element models of the structure are developed to obtain static displacements for comparison with experimental data. A static solution option is used.
2. Natural frequencies and mode shapes, involving an eigenvalue problem solution, are determined using a dynamic option.

Four finite element model variations were developed and compared with test results. Different types of wing skin elements are used for each of the models. Shear panel elements are used for the spar and rib webs. Two different finite element models are applied for the spar and rib chords, one is modeled with the beam element and the other is modeled with the rod element. To verify these finite element models, Rattinger's wing, Reference[2], is modeled and shown to have very good agreement with the test results. See Appendix C. The best structural finite element model was then used to calculate the wing static displacement, and to develop the influence coefficients needed for the aeroelastic analysis.

2. WING FINITE ELEMENT MODEL ANALYSIS

2.1 Wing Description

The T-38 wing structure is composed of aluminum panels (upper and lower surfaces) that are riveted to the root rib, main spar, auxiliary spar, and tip rib. Data necessary to describe the physical characteristics of the wing for MSC/NASTRAN and/or MSC/PAL2 were generated from engineering drawings. The numbers shown in Figure 1 represent the wing assembly parts. There are two missing parts on the drawing: the leading edge spar chord and web and the minor rib chord and

web. These two webs were reconstructed by knowledge of the dimensions of connecting rib webs and edge views of these parts. More detail is shown in Figure 2.

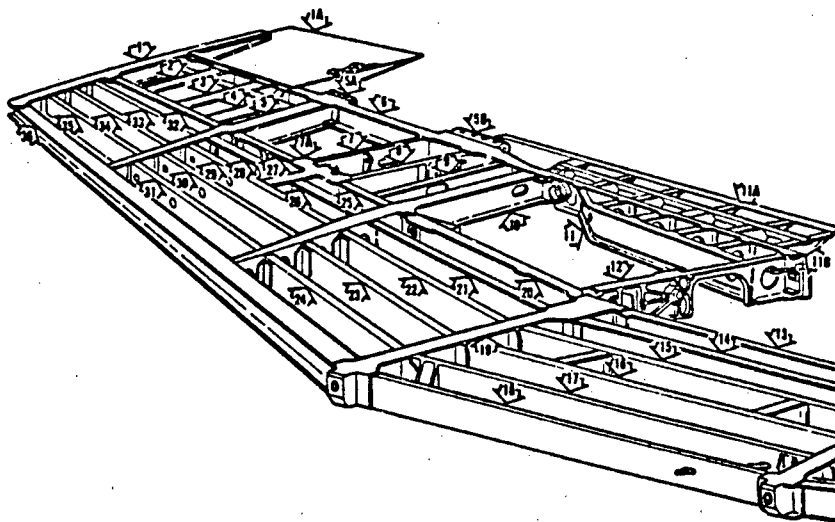


Figure 1. T-38 Real Wing Structure.

2.2 Development of the Finite Element Model

The first, and simplest, finite element model developed to describe the wing geometry shown in Figure 2 is illustrated by Figures 3a and 3b. This baseline model is labeled Model 1. The nodes in this model are located on the top and bottom surfaces of the wing at the intersection of two or more of the spar caps, rib flanges, or stringers. This model (Model 1) has a large aspect ratio quadrilateral plate. See Figures 3a and 3b. To reduce the aspect ratio, three other finite element models were created. The second model has an increased number of elements between two major ribs. For example, as seen in Figure 2, the area between ws 125.0 and ws 101.0 has an increased number of elements. The same applies between ws 101.0 and ws 64.8. See Figures 4a and 4b. The third model has an even greater number of the elements defined between the wing tip and wing root as shown in Figures 5a and 5b. The fourth model is further modified to include triangular plates and quadrilateral plates. See Figure 6. All the models used rod (beam), membrane plate, and shear panel finite elements. The element substructures that are used to model the wing skins are

triangular membrane and bending elements and quadrilateral membranes and bending elements. As shown in Figure 6 and Table 1, models QTSR4.DAT and QTSB4.DAT are composed of triangular and quadrilateral plate elements for the wing skins. Several quadrilateral elements are divided into triangular elements for geometrical reasons or to change mesh spacing between assemblies of quadrilateral plates. For models 1, 2, and 3 only triangular or quadrilateral plates are used for the wing skins. Model 1 has plate elements with large aspect ratios. To avoid large aspect ratios, model 2 and 3 have been utilized. MSC/NASTRAN and MSC/PAL2 have special rod(truss element) and shear panel model tools for the analysis of thin-skinned curved structures such as aircraft. The shear panel element does not represent bending stiffnesses. The quadrilateral SHEAR element(PSHEAR property card) supports an extensional force at grid points and a shear stress within the element. Reinforcing ROD elements are used to carry the extensional load. Consequently, SSR1.DAT is used for this treatment and represents the shear panel elements that are used for the wing skins and the spar and rib webs, while rod elements are used for the spar and rib chords.

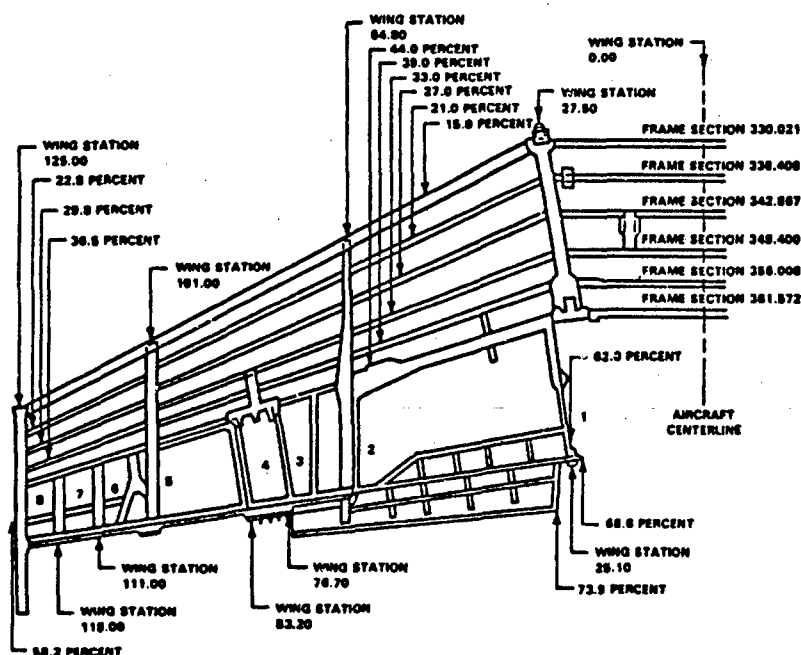


Figure 2. T-38 Wing Internal Structure.

The physical and material properties used in describing the substructure elements are defined as follows:

- a) Property cards(PSHELL, PSHEAR) identify the physical characteristics of the elements, such as thickness, material identify, inertia, and mass of the wing skin and web.
- b) Property cards(PBEAM, PROD) identify the physical characteristics of the spar and rib caps.
- c) Material card(MAT1) describes the material characteristics, such as Young's modulus, shear modulus, Poisson's ratio: MAT1 is used for isotropic material.
- d) Grid points(GRID) are assigned unique geometric locations in terms of fuselage station(FS), wing station(WS), and water line(WL). GRID identifies the appropriate coordinate system and unique constraints for the grid point.
- e) Quadrilateral plate cards(CQUAD4) identify the connection definition for an isoparametric quadrilateral with bending and membrane stiffness.
- f) Triangular plate cards(CTRIA3) identify the connection definition for an isoparametric triangle with bending and membrane stiffness.
- g) Quadrilateral plate cards(CSHEAR) identify the connection definition for shear panel.
- h) Elastic line element cards(CBEAM) identify the connection definition for general beam element.
- i) Elastic line element cards(CONROD) identify the connection and property definition for rod with axial and torsional stiffness.
- j) Load cards(FORCE) define concentrated loads at grid points.
- k) Constraint cards(SPC) define single-point constraints and enforced displacements.

The finite element models of the T-38 wing structure were used to calculate static displacements for comparison with the Northrop test results. Of these four models, the one that compares

best to test results will be used in future analyses of the damaged T-38 wing and used in the MSC/NASTRAN static and dynamic aeroelasticity and flutter solutions.

2.3 Designation of Finite Element Model

The file names for the wing models follow the format XYZI.DAT, where X represents the wing skin elements, Y the spar and rib web elements, Z the truss elements, I represents the wing model number, and DAT represents the file extension. X denotes Q for quadrilateral plate elements and T for triangular plate elements. Y denotes S for shear panel elements Z denotes R for rod elements and B for beam elements. For instance, TSR1.DAT means the triangular plate element is used for the wing skins, shear panel elements are used for the spar and rib webs, and rod elements are used for spar and rib caps for Model 1. All webs in all models are represented by shear elements. See Tables 1a and 1b.

Table 1a. Designation of Finite Element Model 1

| MODEL 1 | | | | | |
|------------------|----------|----------|----------|----------|----------|
| FILE NAME | QSB1.DAT | QSR1.DAT | TSB1.DAT | TSR1.DAT | SSR1.DAT |
| WING SKIN | CQUAD4 | CQUAD4 | CTRIA3 | CTRIA3 | CSHEAR |
| SPAR & RIB WEB | CSHEAR | CSHEAR | CSHEAR | CSHEAR | CSHEAR |
| SPAR & RIB CHORD | CBEAM | CONROD | CBEAM | CONROD | CONROD |

Table 1b. Designation of Finite Element Model 2

| MODEL 2 | | | | |
|------------------|----------|----------|----------|----------|
| FILE NAME | QSB2.DAT | QSR2.DAT | TSB2.DAT | TSR2.DAT |
| WING SKIN | CQUAD4 | CQUAD4 | CTRIA3 | CTRIA3 |
| SPAR & RIB WEB | CSHEAR | CSHEAR | CSHEAR | CSHEAR |
| SPAR & RIB CHORD | CBEAM | CONROD | CBEAM | CONROD |

Table 1c. Designation of Finite Element Model 3

| MODEL 3 | | | | |
|------------------|----------|----------|----------|----------|
| FILE NAME | QSB3.DAT | QSR3.DAT | TSB3.DAT | TSR3.DAT |
| WING SKIN | CQUAD4 | CQUAD4 | CTRIA3 | CTRIA3 |
| SPAR & RIB WEB | CSHEAR | CSHEAR | CSHEAR | CSHEAR |
| SPAR & RIB CHORD | CBEAM | CONROD | CBEAM | CONROD |

Table 1d. Designation of Finite Element Model 4

| MODEL 4 | | |
|------------------|-----------------|-----------------|
| FILE NAME | QTSB4.DAT | QTSR4.DAT |
| WING SKIN | CQUAD4 & CTRIA3 | CQUAD4 & CTRIA3 |
| SPAR & RIB WEB | CSHEAR | CSHEAR |
| SPAR & RIB CHORD | CBEAM | CONROD |

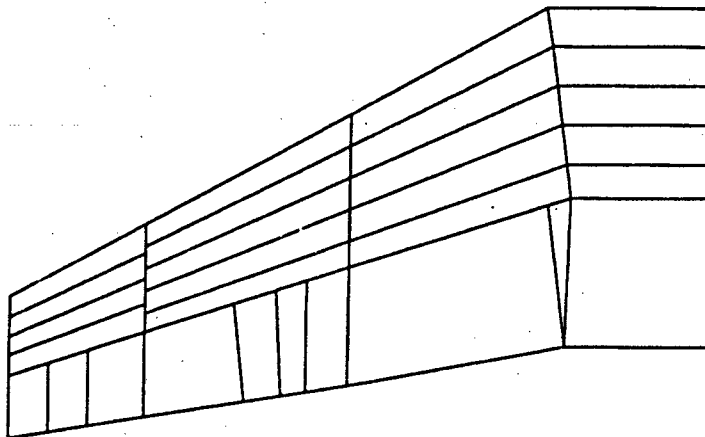


Figure 3a. Topview of Finite Element Model 1, QSB1.DAT and QSR1.DAT.

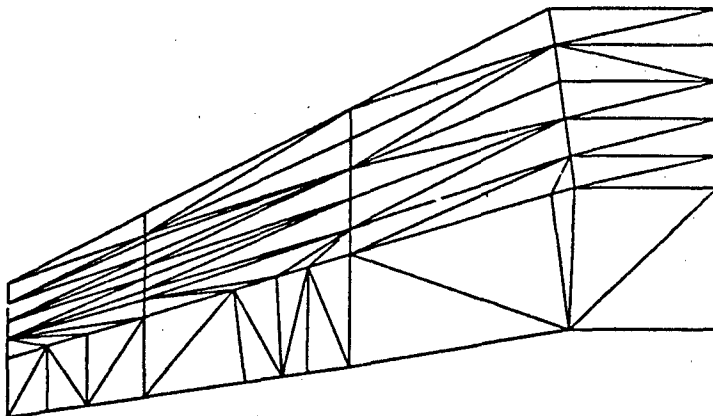


Figure 3b. Topview of Finite Element Model 1. TSB1.DAT and TSR1.DAT.

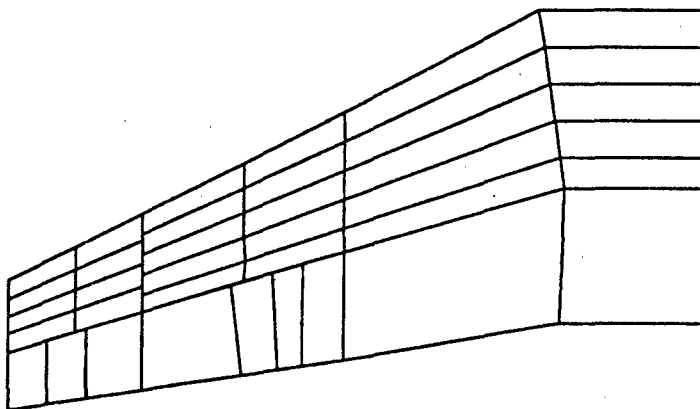


Figure 4a. Topview of Finite Element Model 2. QSB2.DAT and QSR2.DAT.

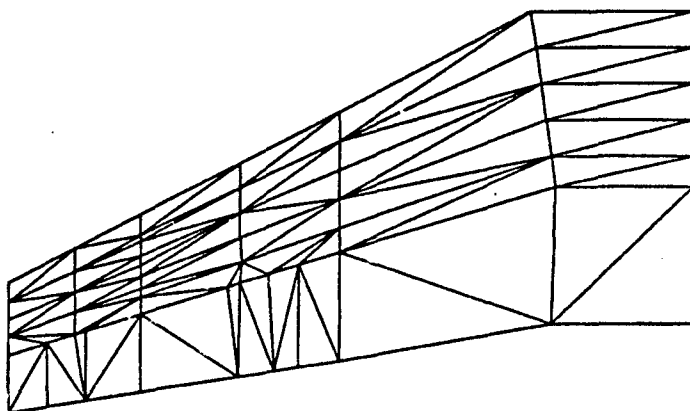


Figure 4b. Topview of Finite Element Model 2. TSB2.DAT and TSR2.DAT.

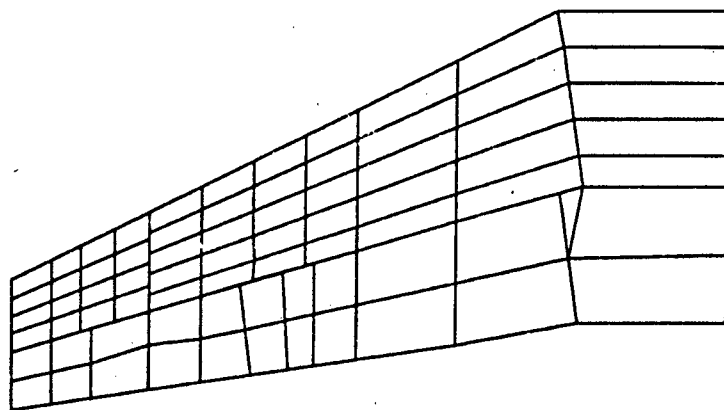


Figure 5a. Topview of Finite Element Model 3. QSB3.DAT and QSR3.DAT.

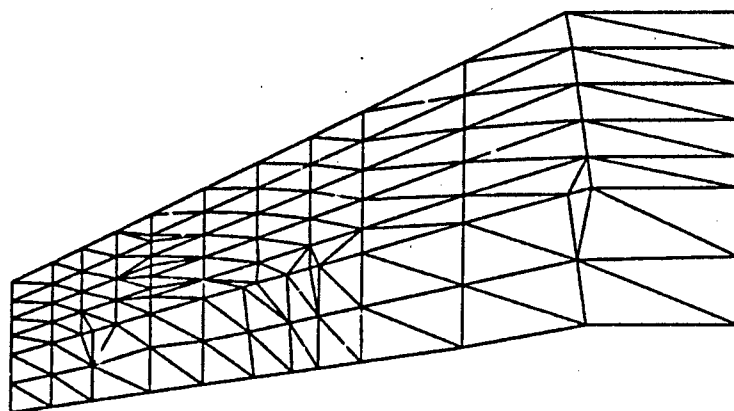


Figure 5b. Topview of Finite Element Model 3. TSB3.DAT and TSR3.DAT.

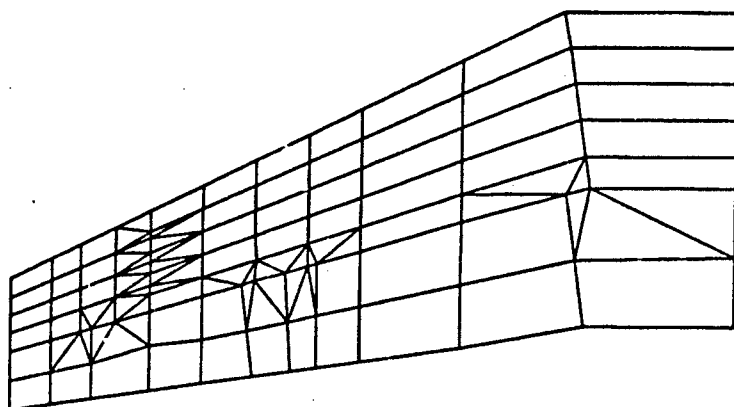


Figure 6. Topview of Finite Element Model 4. QTSB4.DAT and QTSR4.DAT.

2.4 Sizing of Rod Elements

In this study, rod and beam elements, activated through use of two optional cards (CONROD and CBEAM), are used for spar and rib caps. As shown in Figures 7 and 8, the Channel-beam and I-beam have top and bottom caps. The top and bottom caps are represented as a cross section of a rectangular beam. Areas of the cross sections, I_{xx} , and I_{yy} are input for the CBEAM option. The two caps (top and bottom) are resized as rod elements for the CONROD option. The rationale for sizing rod elements representing spar caps or rib caps is presented by Reference [3] and [4]. Property relationships are first determined for a structural member's cross section. The distance from the top surface of the section to the centroidal axis is identified as h_t . Similarly, the distance from the centroidal axis to the bottom surface of the section is h_b . Maximum bending stress at top and bottom surfaces, respectively, are:

$$\sigma_T = \frac{Mh_t}{I} \quad (1.a)$$

and

$$\sigma_B = \frac{Mh_b}{I} \quad (1.b)$$

where M is the applied bending moment, and I is the section moment of inertia about the centroidal axis.

In the four finite element models, the rod elements are assumed to be point areas and are positioned at the top and bottom surfaces of a cross section of wing skins. The rod areas are sized to maintain the location of the centroidal axis and the value of I for the section. Such a relationship yielded

$$A_t h_t = A_b h_b \quad (2)$$

with A_t and A_b being the areas of the top and bottom rods. The bending moment, M , in the model then becomes

$$M = \sigma_T A_t h_t + \sigma_B A_b h_b \quad (3)$$

Next, using actual section properties and desired model properties, the relationships of Equations (1), (2), and (3) are combined to produce

$$A_t = \frac{I}{h_t(h_t + h_b)} \quad (4.a)$$

and

$$A_b = \frac{I}{h_b(h_t + h_b)} \quad (4.b)$$

which are the rod element areas.

The actual T-38 wing has two major types of beams: C-beam and I-beam. The two different types of beams were sized as rod elements to take a CONROD option for spar and rib chords. See Figures 7 and 8. All calculated input data for rod/beam elements are presented in Appendix D.

a) C-Beam case: ws 125.0, between 15% chord and 22.75% chord

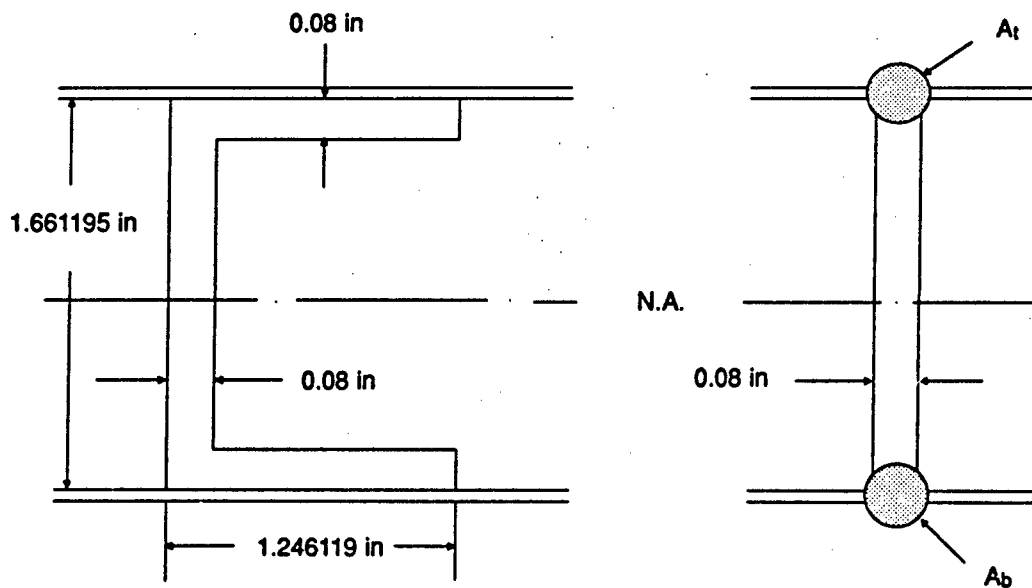


Figure 7. C-Beam Case.

$$I_{xx} = \frac{(1.246119)(1.661195)^3 - (1.246119)(1.661195 - 2 \times 0.08)^3}{12} = 0.1472808$$

$$I_{yy} = 0.04938$$

From equations (4.a) and (4.b), the rod cross-section area for top and bottom is

$$A_{tb} = \frac{0.1472808}{0.8305975 \times 1.661195} = 0.1067419$$

and the cross-section area of beam is

$$A_{cb} = 0.08 \times 1.2461188 = 0.09969$$

In the case of the CONROD option, 0.10674 in² is used for the rod area and CBEAM option 0.09969 in² is used for the beam cross area.

b) I-Beam case: ws 101.0, between 15% chord and 22.75 % chord

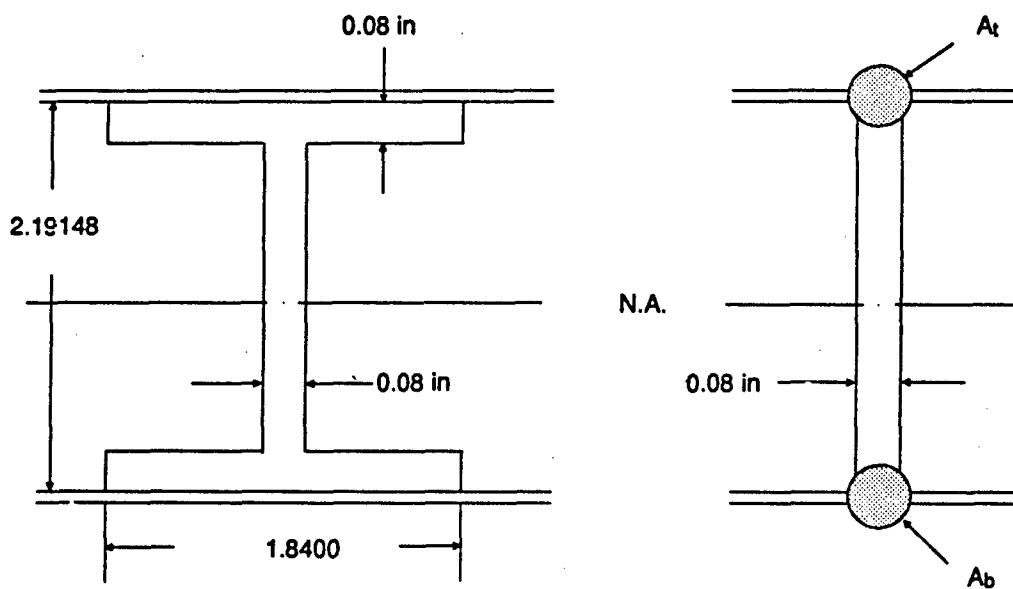


Figure 8. I-Beam Case.

$$I_{xx} = \frac{(1.84)(2.19148)^3 - (1.84 - 0.08)(2.19148 - 2 \times 0.08)^3}{12} = 0.384183$$

$$I_{yy} = \frac{2(0.08)(1.84)^3 + (2.19148 - 2 \times 0.08)(0.08)^3}{12} = 0.0831467$$

From Equations (4.a) and (4.b), the rod and beam cross-section area for top and bottom is obtained.

$$A_{tb} = \frac{0.384183}{1.09574 \times 2.19148} = 0.159778$$

$$A_{cb} = 0.08 \times 1.84 = 0.1472$$

In the above equations, the neutral axis(NA) is taken half the distance between the top and the bottom because of the symmetric beam shape.

2.5 Boundary Conditions

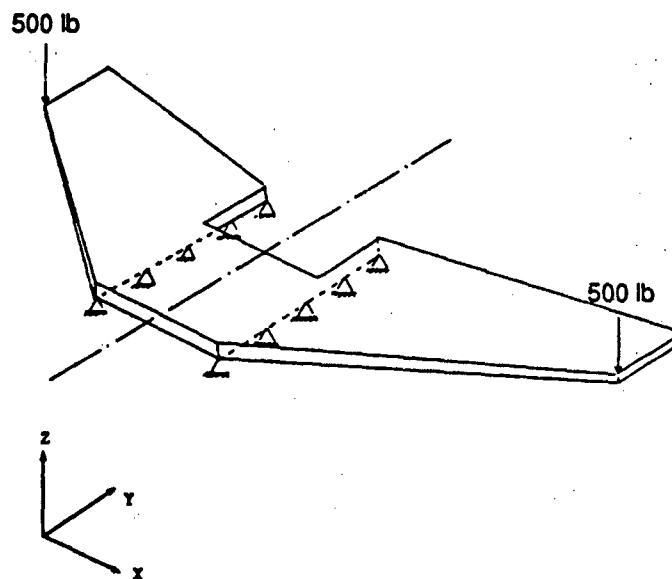


Figure 9. Loading Condition for T-38 Wing from Boundary Condition at Node A(500 lb).

The finite element model boundary conditions are based on the experimental conditions. As shown in Figure 9, the y-z plane is a plane of symmetry and therefore x-displacements in this plane are assigned zero values. The finite element models used in this report are constrained in the x-directions at the aircraft centerline and in the z-direction at the wing roots. Point loading is applied symmetrically at each of the loading points. See Figure 9.

3. GENERAL STRUCTURAL ANALYSIS EQUATION

Finite element structural analysis is a mathematical procedure to determine displacements, velocity, acceleration, stress, and support reaction forces due to applied mechanical and/or thermal loads that may or may not vary with time. The wing structures described in this study have several hundred multiple degrees of freedom(MDOF).

Equations of equilibrium may be derived for each DOF in the structure and expressed as a general structural analysis equation in matrix form:

$$[M]\{\ddot{u}\} + [B]\{\dot{u}\} + [K]\{u\} = \{P\} + \{N\} \quad (5)$$

where $[M]$, $[B]$, and $[K]$ are mass, damping, and stiffness matrices of the structure, respectively. The symbols $\{\ddot{u}\}$, $\{\dot{u}\}$, and $\{u\}$ represent acceleration, velocity, and displacement vectors, respectively, for the N degrees of freedom (N DOF) in the structure. Right hand side terms $\{P\}$ and $\{N\}$ refer to static and/or time-varying applied linear and nonlinear mechanical and/or thermal loads in Eq. 5. Constraint forces from the structure supports are obtained in the data recovery.

3.1 Linear Static Analysis

For static analysis of the T-38 wing, the solutions(SOL 24 or 101) in MSC/NASTRAN and (STAT2) in MSC/PAL2 are used. The mathematical formulation of the solution process is based on the linear theory of elasticity. The stiffness matrix is formulated and then partitioned with respect to the constrained and unconstrained degrees of freedom to be solved.

The finite element model developed allows the load(force) to be concentrated at a grid point for the static analysis. The set of forces is reduced to 1-set for the nodal forces from the constraint partitioning resulting from satisfying the equilibrium equations for stiffness versus force. In the static load case Eq. 5 reduces to

$$[K]\{u\} = \{P\} \quad (6)$$

The vectors $\{P\}$ and $\{u\}$ represent the nodal forces and displacements, respectively, and the matrix $[K]$ represents the Finite Element Model stiffness matrix. For solution of the equations, MSC/PAL2 and MSC/NASTRAN reduces the stiffness matrix into its upper and lower triangular factors. Then forward-backward substitution is performed for all the lower cases having the same constraints, which is the case here. In this study, eight different loads are applied at each different grid point as shown in Table 2. The displacement solution for each load case contains three translational values for each grid point(except those displacements which are constrained). In this manner, transverse displacements are calculated for nine grid points(A-I) shown in Figure 10. These displacements are plotted and compared with experimental data. Figures 11 through 18 present these comparisons for load applications from 200 lb to 5000 lb. Each loading has 6 plots a, b, c, d, e, and f. Plots a and b represent comparisons of displacements from models TSBI.DAT and TSRI.DAT and test data. Plots c and d represent comparisons of displacements from models QSRI.DAT and QSBI.DAT and test data. Plots e represent comparisons of displacements from models SSR1.DAT and test data and plot f represents a comparison of displacements from QTSR4.DAT and QTSB4.DAT and test data. Each plot has three stations. The top station shows deflections of grid points A, B, and C(See Figure 10), the middle station shows grid points D, E, and F, and the lower station shows the deflections of grid points G, H, and I. In other words, the top station represents three grid points on the wing station 125.0, the middle station represents three grid points on the wing station 101.0 and the lower station represents three grid points on the wing station 64.8. The three grid points at each station correspond to chord positions of 15.0 %, 44.0 %, and 66.6 % chord, respectively.

3.2 Dynamic Analysis

The modal analysis of the finite element model of T-38 wing is important to performing flutter analysis. Theoretically, this is because the response of a structure to forced vibration (i.e., flutter) is taken to be the infinite sum of the structure's free vibration mode shapes. Therefore, it is important

that verified mode shapes for the proper boundary conditions be obtained. In this report, the dynamic analysis solution DYNA2 in MSC/PAL2 is used to calculate normal mode shapes and natural frequencies.

For this analysis, applied loads, geometric stiffnesses, and structural damping are set to zero. Further assume that displacements at all locations on the structure have sinusoidal time variations with the same frequency and phase relationship:

$$\{u\} = \{\phi\} \cos \omega t \quad (7)$$

where $\{\phi\}$ is a vector of real numbers called an eigenvector. The general structural analysis Eq. 5 becomes

$$[k - \omega^2 M]\{\phi\} = 0 \quad (8)$$

where ω is the circular frequency, and k is stiffness matrix.

Roots of the matrix in Eq. 8 yield structural natural frequencies. Many numerical eigenvalue extraction techniques are available [Ref. 5] to determine the discrete set of eigen-frequencies (or natural frequencies). Substitution of a discrete frequency into Eq. 8 allows evaluation of $\{\phi\}$ if one degree of freedom is assigned an arbitrary magnitude. The column vector $\{\phi\}$ is thus a normalized eigenvector.

Individual terms in $\{\phi\}$ may be visualized as vibration displacement extremes along the structure as it vibrates sinusoidally at a specific natural frequency. Structural natural frequencies are useful to know so that applied time-varying loads do not result in resonance with the structural natural frequencies. Also, the eigenvalues and eigenvectors are useful in applying an arbitrary time history to a structure.

Mass distribution is important in a dynamic vibration analysis. The default in most finite element programs is to lump element mass into adjoining grid points. This is called a lumped mass approach and results in a diagonal mass matrix. An alternative consistent mass approach uses the same element shape functions used for element stiffness. A consistent mass matrix will have off-diagonal terms as does the stiffness matrix.

Table 2. Load Distribution at Each Node

| Node | Wing Station | Chord Percent | Load, lb |
|------|--------------|---------------|----------|
| A | 125.0 | 15.0 | 500 |
| B | 125.0 | 44.0 | 1,000 |
| C | 125.0 | 66.6 | 200 |
| D | 101.0 | 15.0 | 1,500 |
| E | 101.0 | 44.0 | 2,500 |
| F | 101.0 | 66.6 | 500 |
| G | 64.8 | 15.0 | 3,000 |
| H | 64.8 | 44.0 | 5,000 |
| I | 64.8 | 66.6 | NONE |

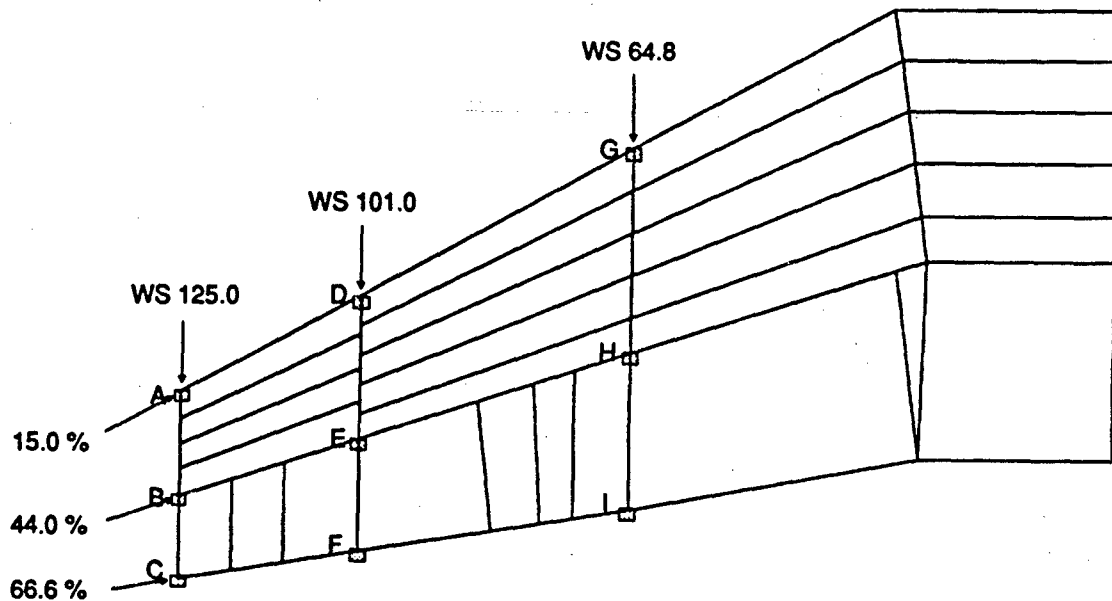


Figure 10. Position of Loading Node.

In this study, due to the software limitation of active degrees of freedom for normal modes using MSC/PAL2, the command ELIMINATE is used to reduce the number of degrees of freedom. This command(ELIMINATE) is stored in data file T38DYN.DAT(modified from data file QTSB4.DAT) for the dynamic analysis. Degree of freedom reduction is performed in order to reduce a model to a smaller size. This reduction is used primarily in the dynamic analysis, particularly to reduce the model size to one solvable in MSC/PAL2 (225 active degrees of freedom for normal modes and transient analysis). Though this reduction is not exact for the dynamic analysis, it is accurate enough that the lowest one-third of the computed resonant frequencies are accurate within 1 percent difference. The first ten natural frequencies are shown in Table 3 and the first ten mode shapes are in Figures 19a-j. The x and y translation and z rotation are constrained to calculate only the bending vibration.

Table 3. Natural Frequencies of T-38 Wing

| Mode No. | Natural Frequencies (cps) |
|----------|---------------------------|
| 1 | 4.643 |
| 2 | 6.745 |
| 3 | 7.092 |
| 4 | 7.105 |
| 5 | 7.799 |
| 6 | 7.944 |
| 7 | 8.269 |
| 8 | 10.681 |
| 9 | 11.542 |
| 10 | 12.655 |

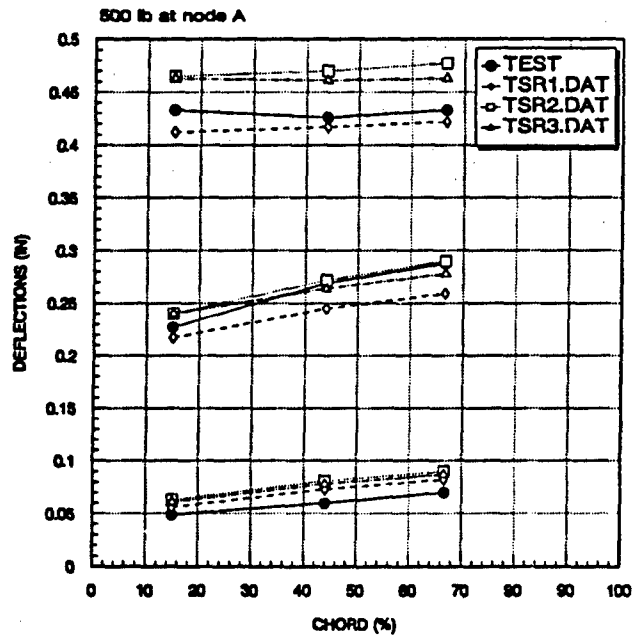


Figure 11a. Comparison of Displacements from TSRi.DAT and Test.

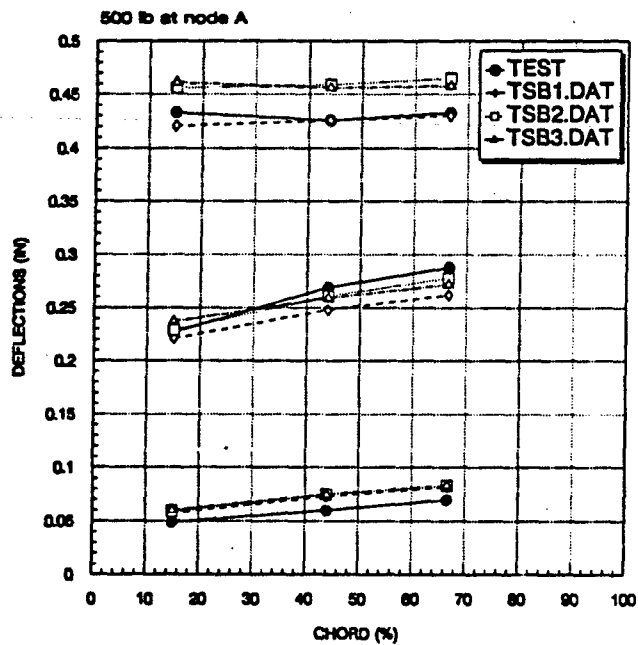


Figure 11b. Comparison of Displacements from TSBi.DAT and Test.

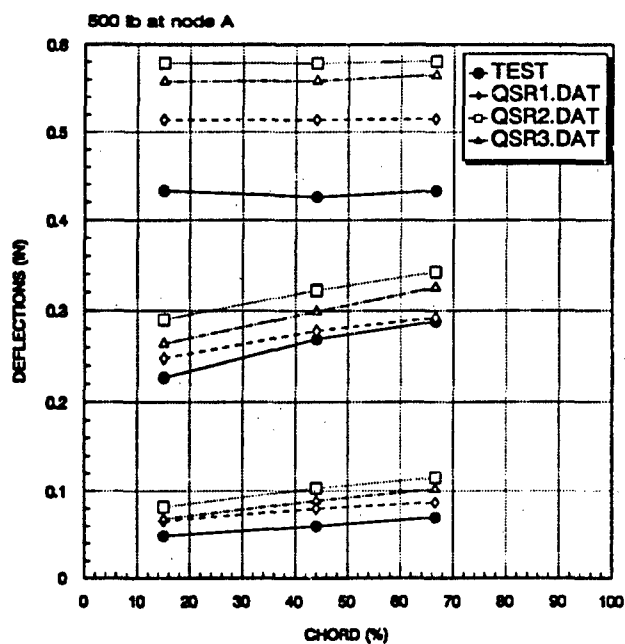


Figure 11c. Comparison of Displacements from QSRi.DAT and Test.

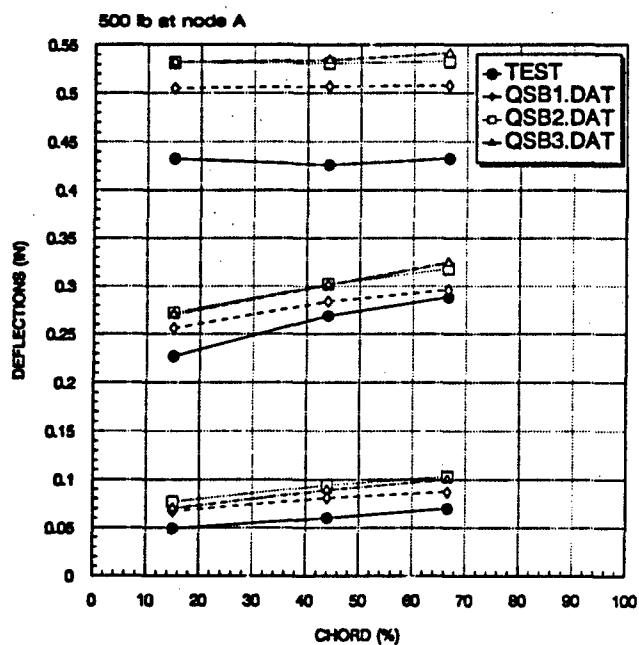


Figure 11d. Comparison of Displacements from QSBi.DAT and Test.

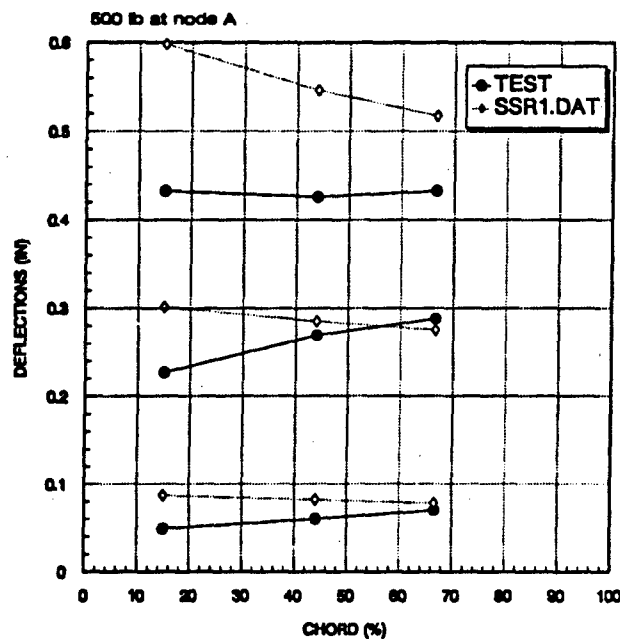


Figure 11e. Comparison of Displacements from SSR1.DAT and Test.

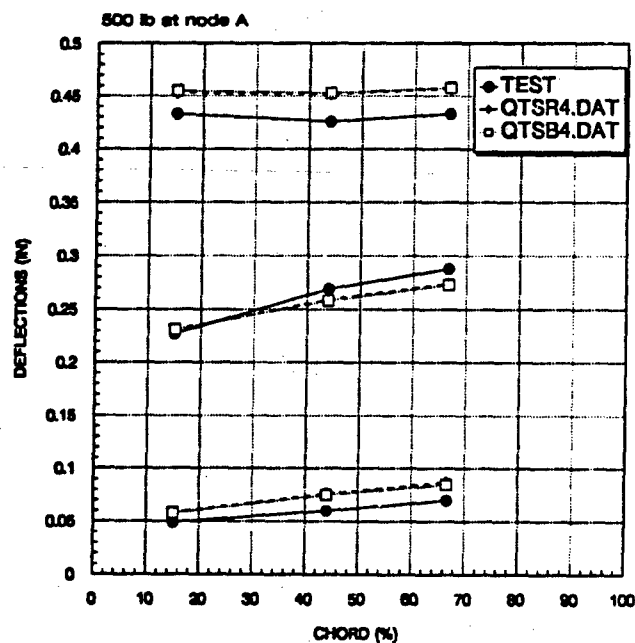


Figure 11f. Comparison of Displacements from QTSR4.DAT, QTSB4.DAT and Test.

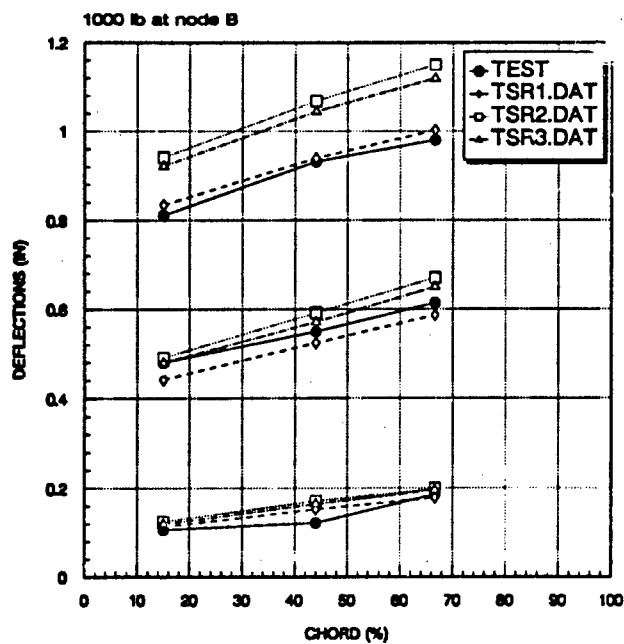


Figure 12a. Comparison of Displacements from TSRI.DAT and Test.

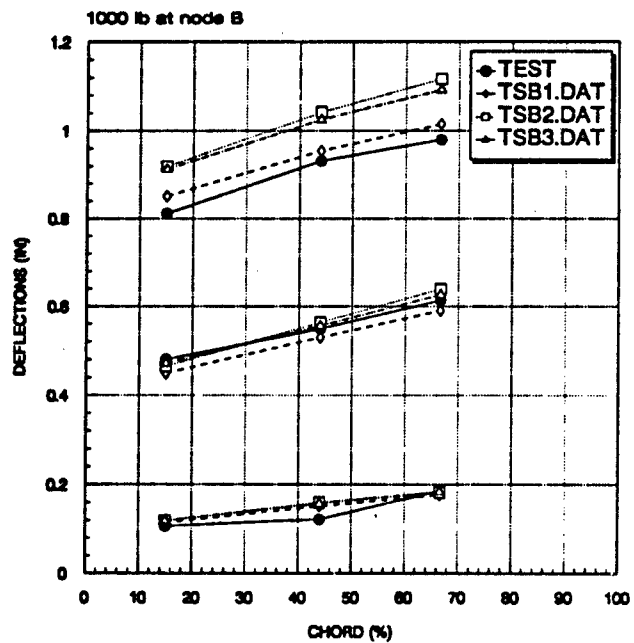


Figure 12b. Comparison of Displacements from TSBi.DAT and Test.

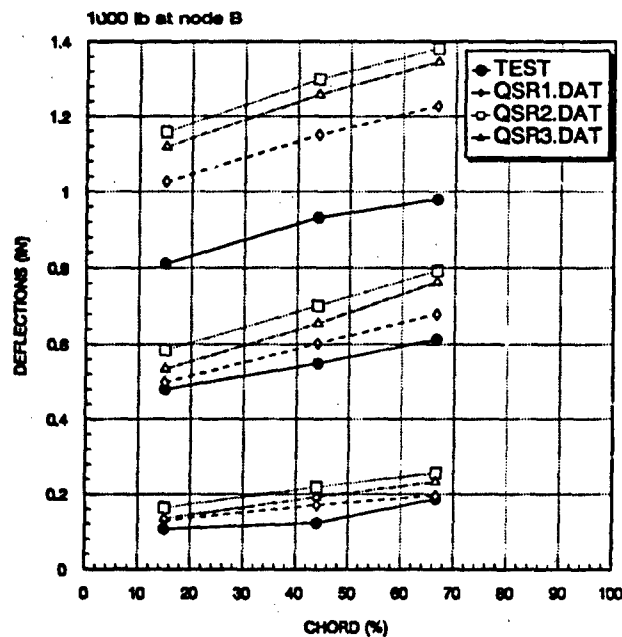


Figure 12c. Comparison of Displacements from QSRi.DAT and Test.

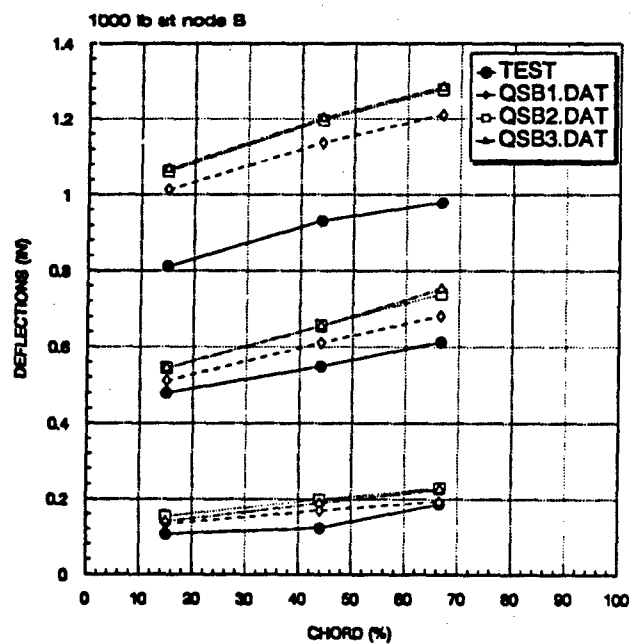


Figure 12d. Comparison of Displacements from QSBi.DAT and Test.

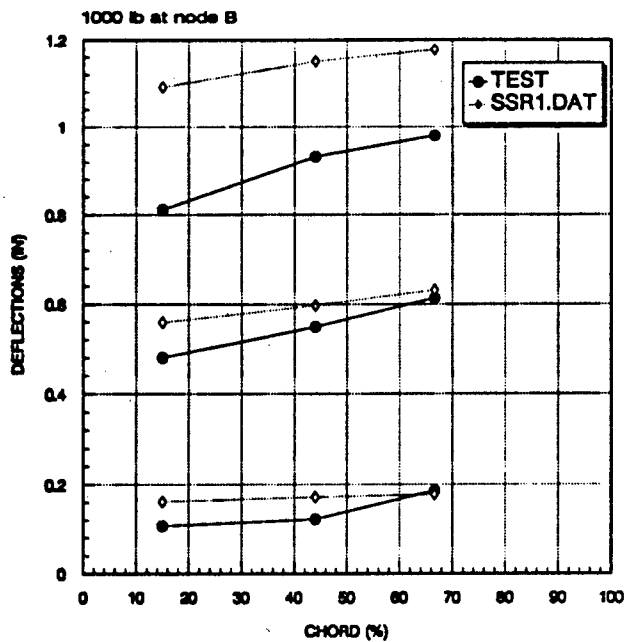


Figure 12e. Comparison of Displacements from SSR1.DAT and Test.

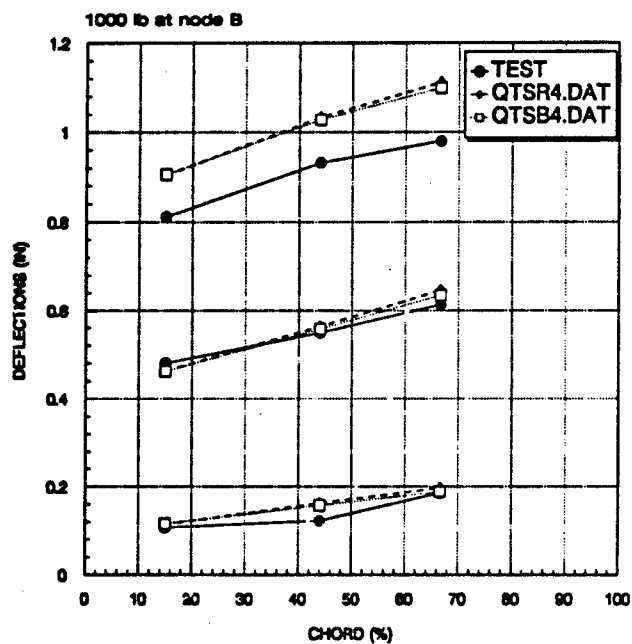


Figure 12f. Comparison of Displacements from QTSR4.DAT, QTSB4.DAT and Test.

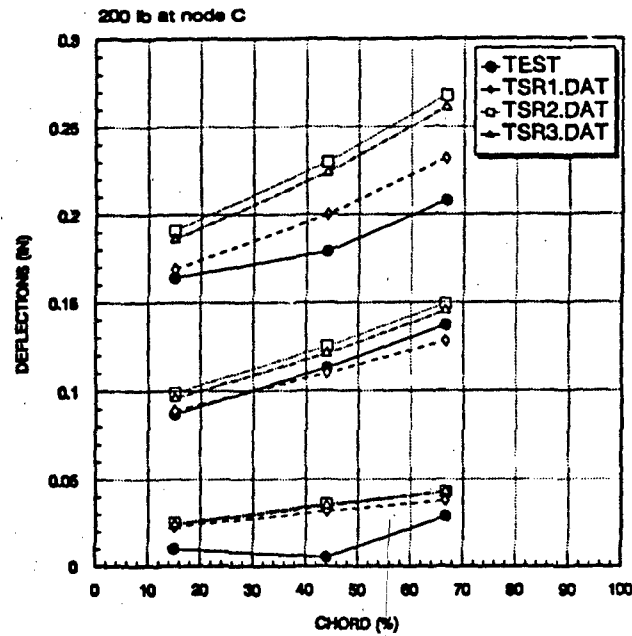


Figure 13a. Comparison of Displacements from TSRI.DAT and Test.

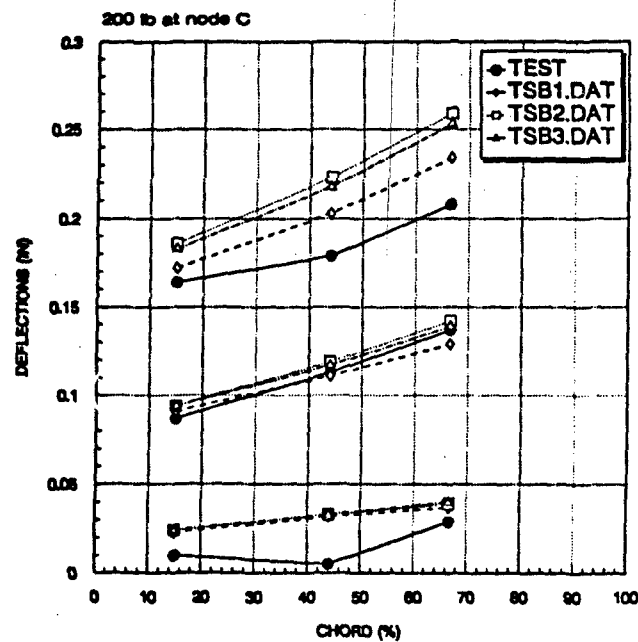


Figure 13b. Comparison of Displacements from TSBi.DAT and Test.

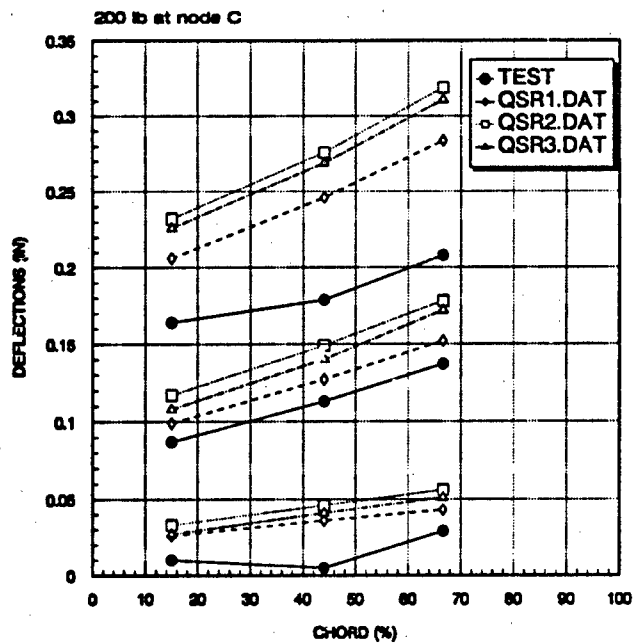


Figure 13c. Comparison of Displacements from QSRi.DAT and Test.

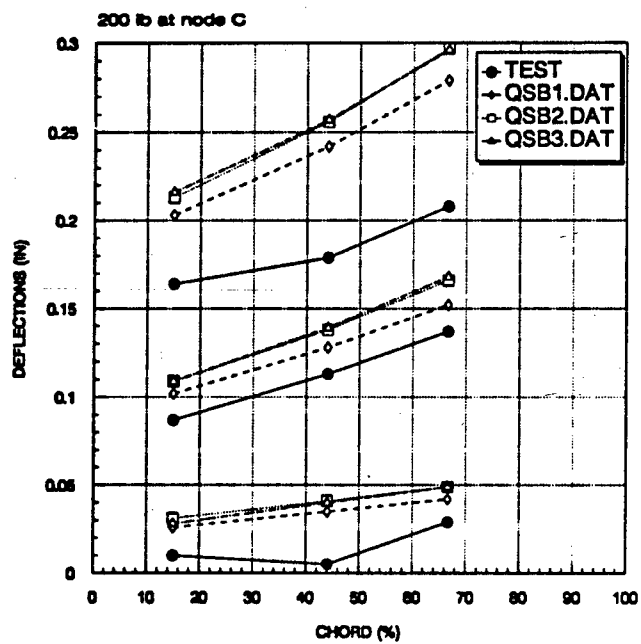


Figure 13d. Comparison of Displacements from QSBi.DAT and Test.

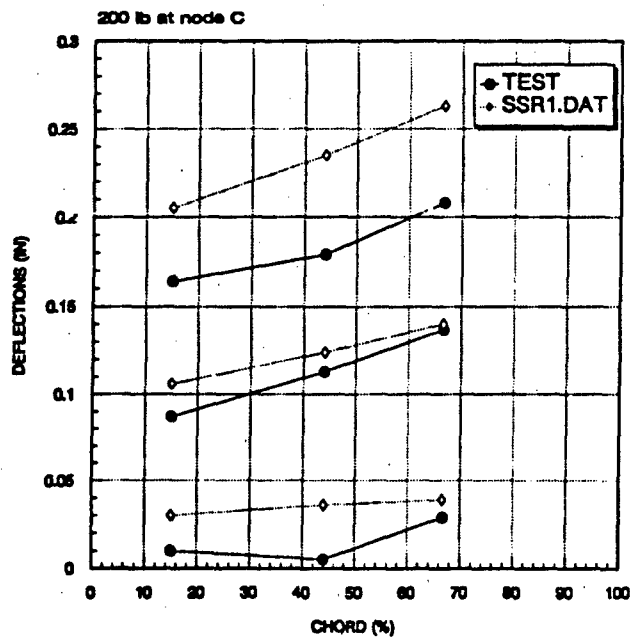


Figure 13e. Comparison of Displacements from SSR1.DAT and Test.

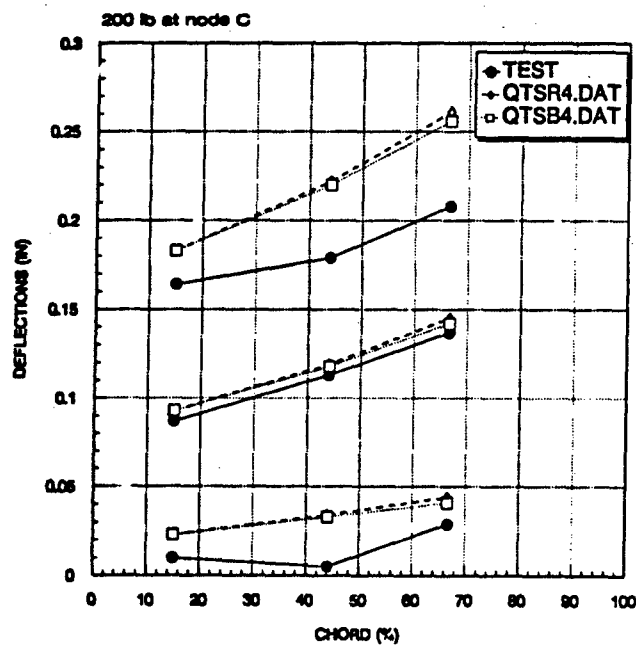


Figure 13f. Comparison of Displacements from QTSR4.DAT, QTSB4.DAT and Test.

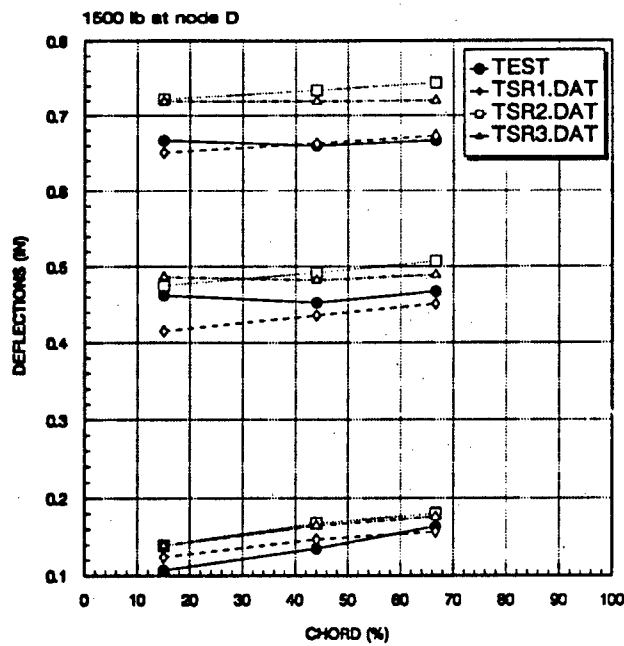


Figure 14a. Comparison of Displacements from TSRI.DAT and Test.

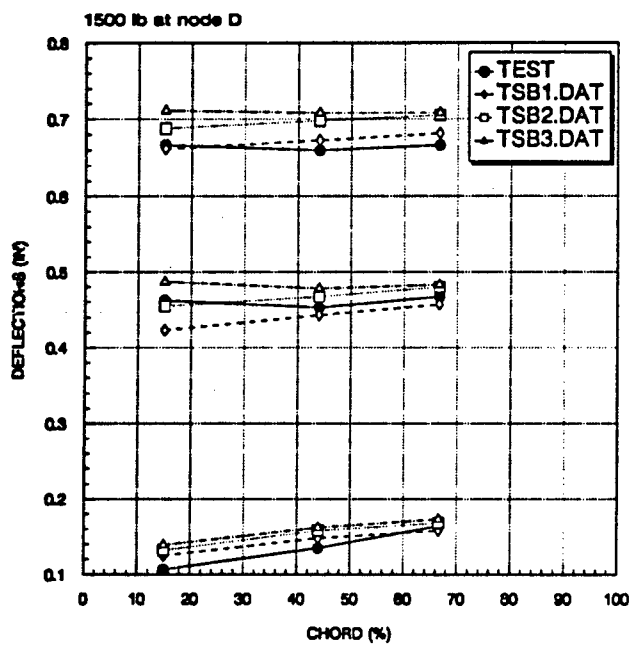


Figure 14b. Comparison of Displacements from TSBi.DAT and Test.

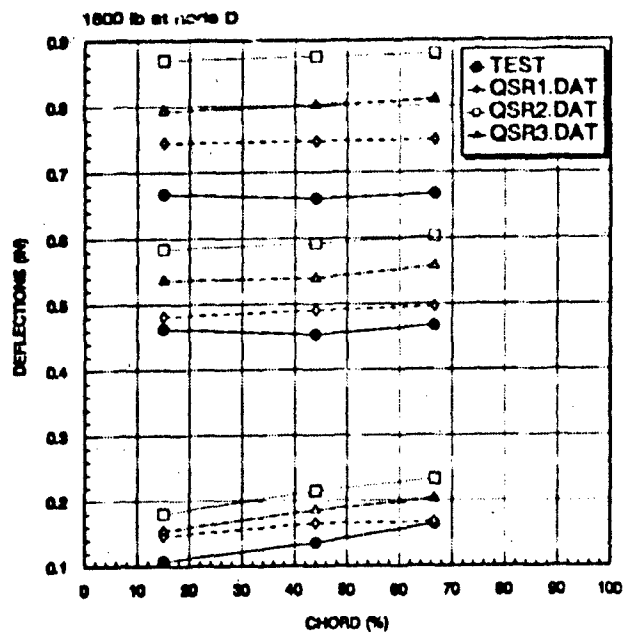


Figure 14c. Comparison of Displacements from QSRi.DAT and Test.

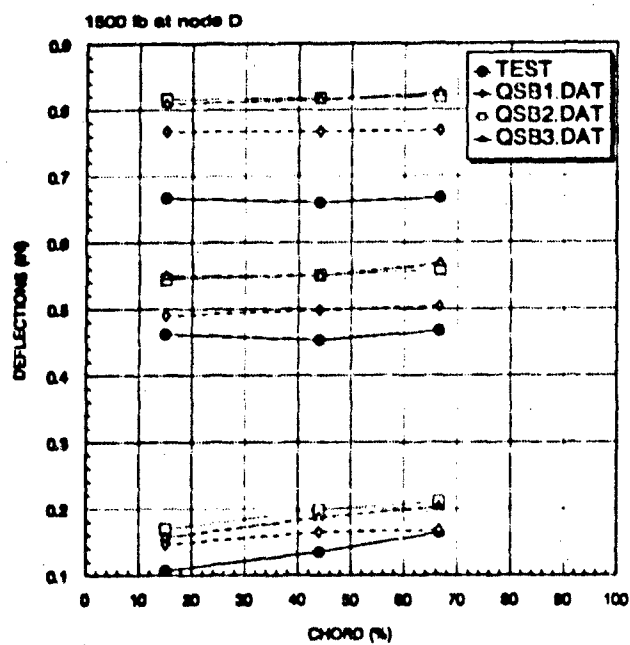


Figure 14d. Comparison of Displacements from QSBi.DAT and Test.

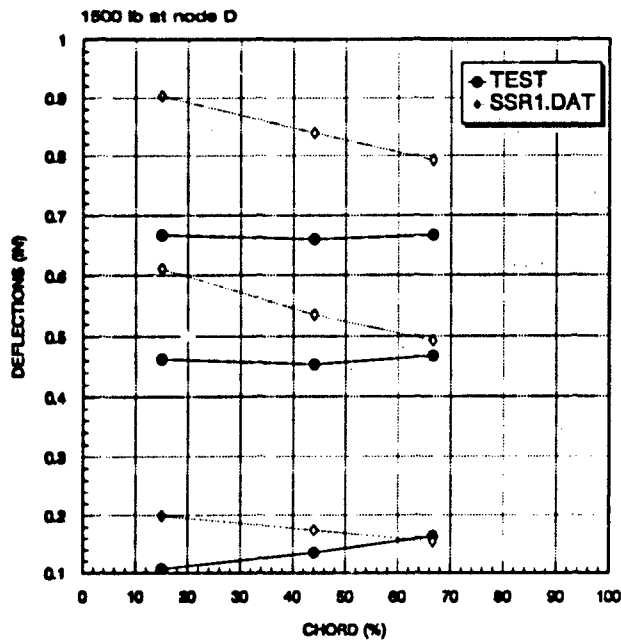


Figure 14e. Comparison of Displacements from SSR1.DAT and Test.

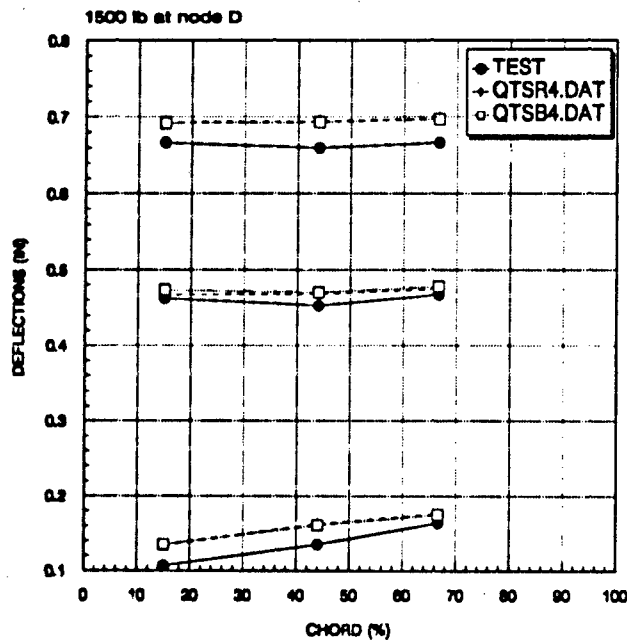


Figure 14f. Comparison of Displacements from QTSR4.DAT, QTSB4.DAT and Test.

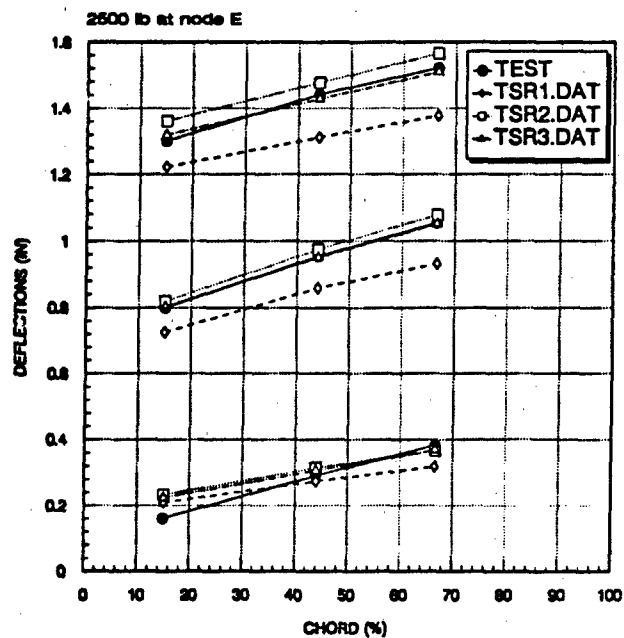


Figure 15a. Comparison of Displacements from TSRI.DAT and Test.

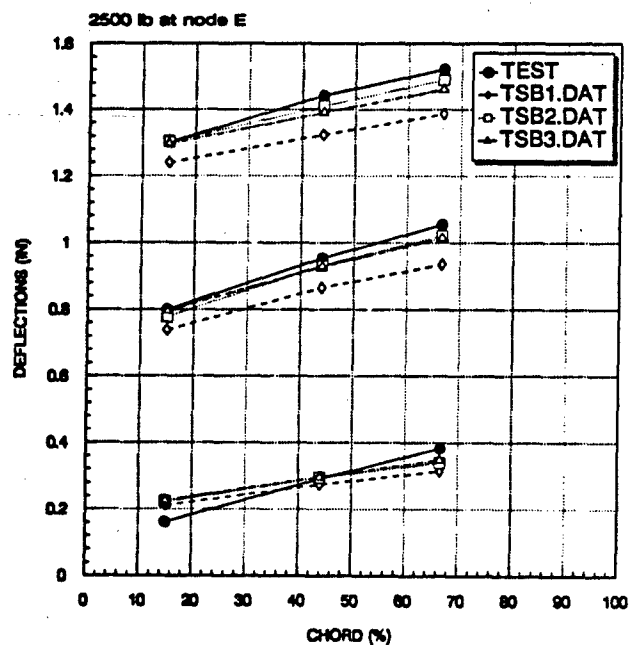


Figure 15b. Comparison of Displacements from TSB1.DAT and Test.

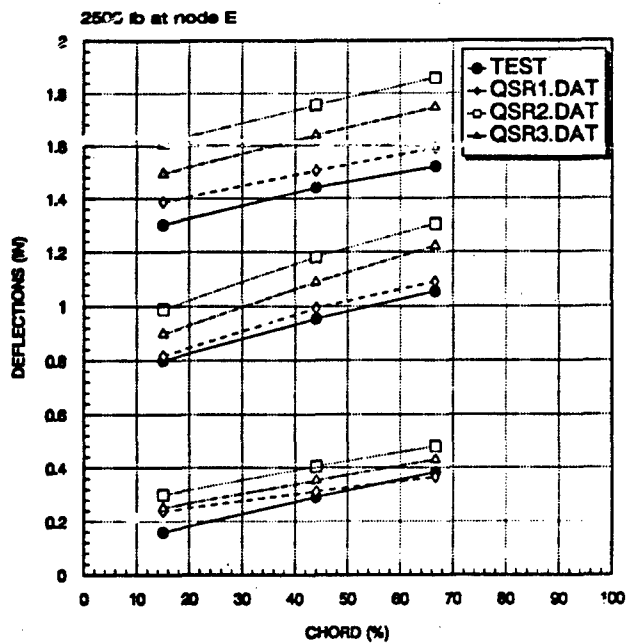


Figure 15c. Comparison of Displacements from QSRi.DAT and Test.

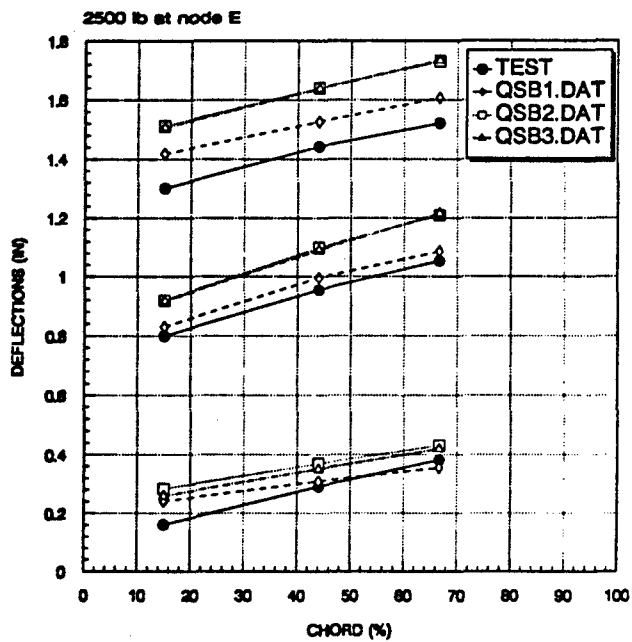


Figure 15d. Comparison of Displacements from QSBi.DAT and Test.

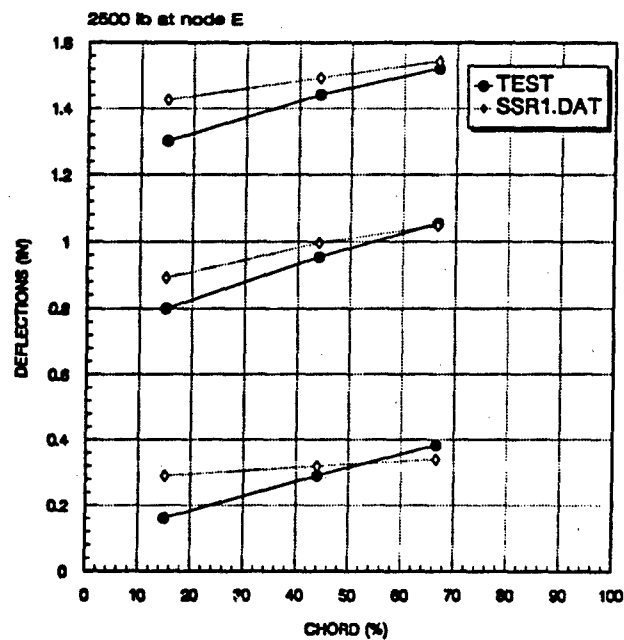


Figure 15e. Comparison of Displacements from SSR1.DAT and Test.

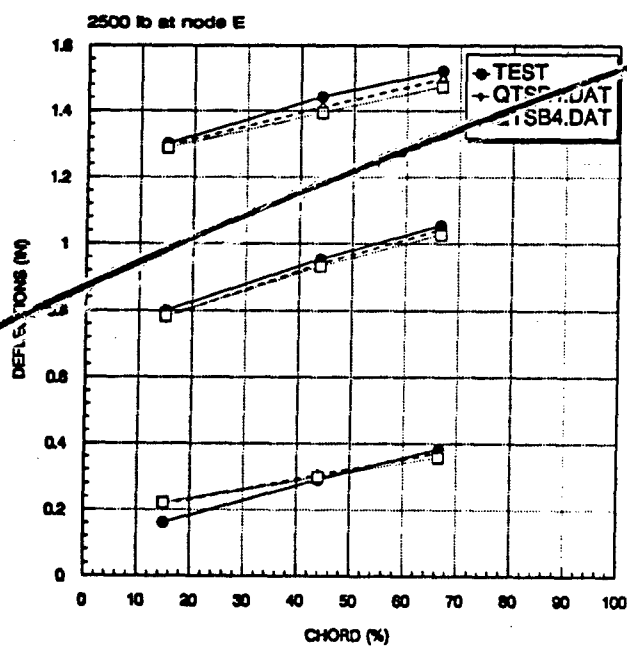


Figure 15f. Comparison of Displacements from QTSR4.DAT, QTSB4.DAT and Test.

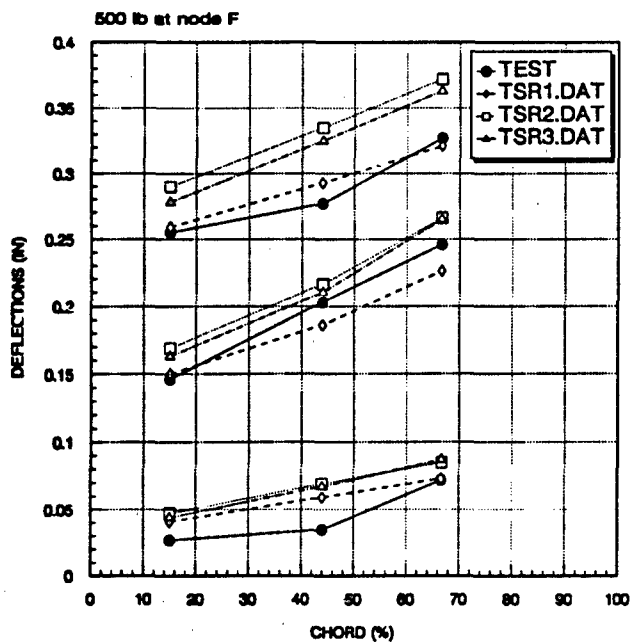


Figure 16a. Comparison of Displacements from TSRI.DAT and Test.

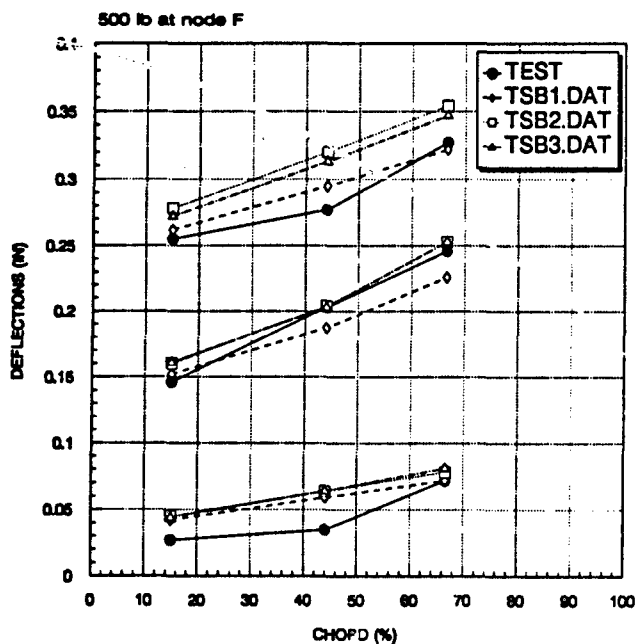


Figure 16b. Comparison of Displacements from TSBi.DAT and Test.

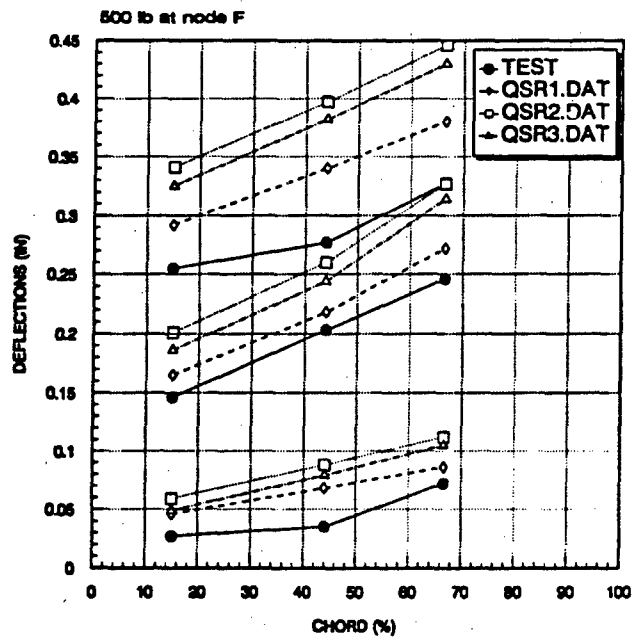


Figure 16c. Comparison of Displacements from QSRi.DAT and Test.

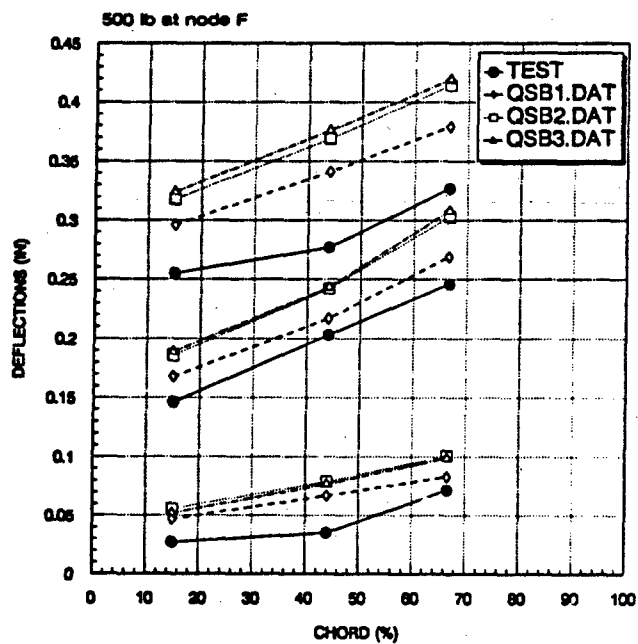


Figure 16d. Comparison of Displacements from QSBi.DAT and Test.

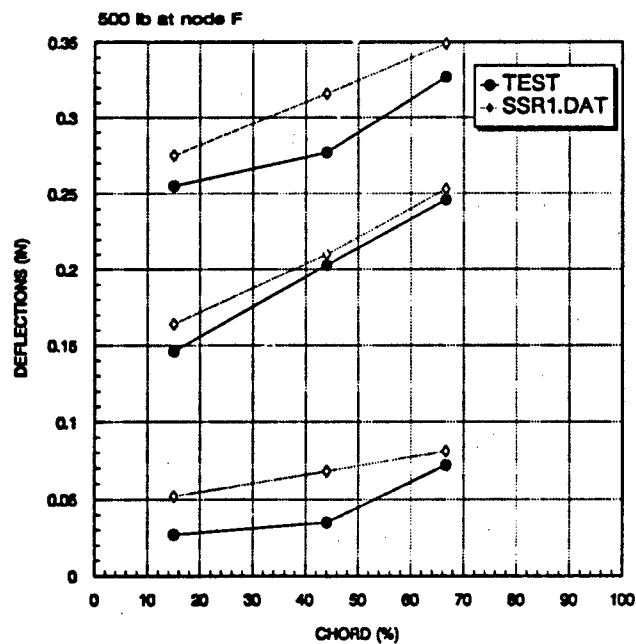


Figure 16e. Comparison of Displacements from SSR1.DAT and Test.

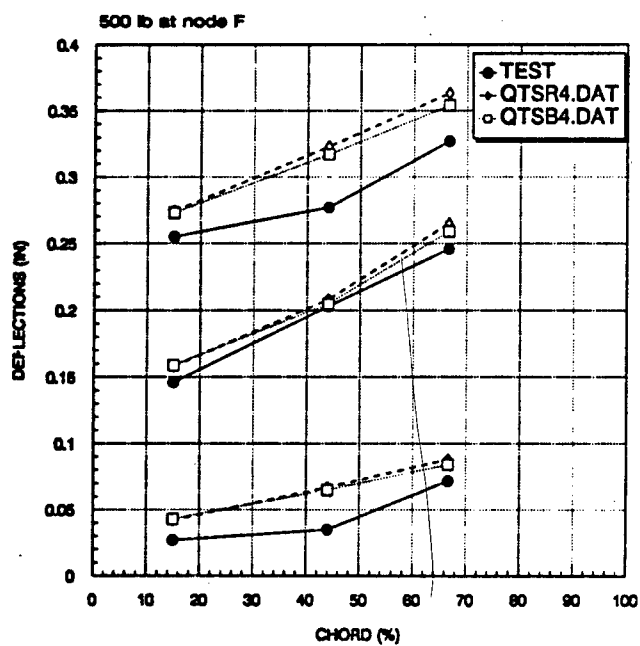


Figure 16f. Comparison of Displacements from QTSR4.DAT, QTSB4.DAT and Test.

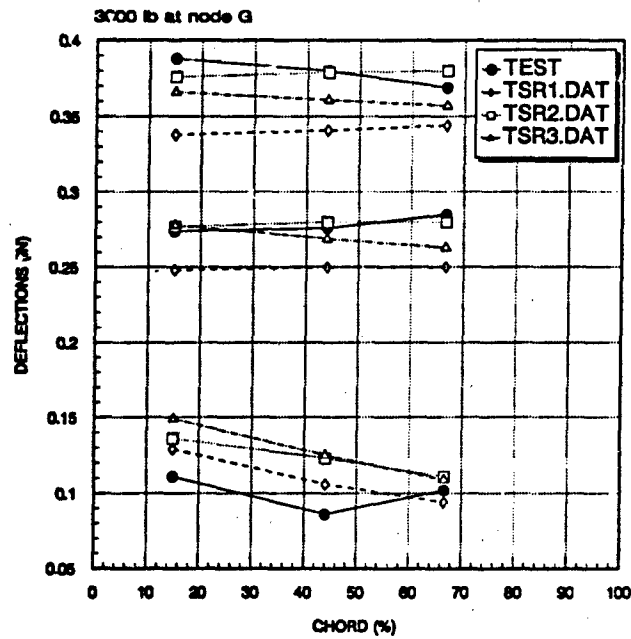


Figure 17a. Comparison of Displacements from TSRi.DAT and Test.

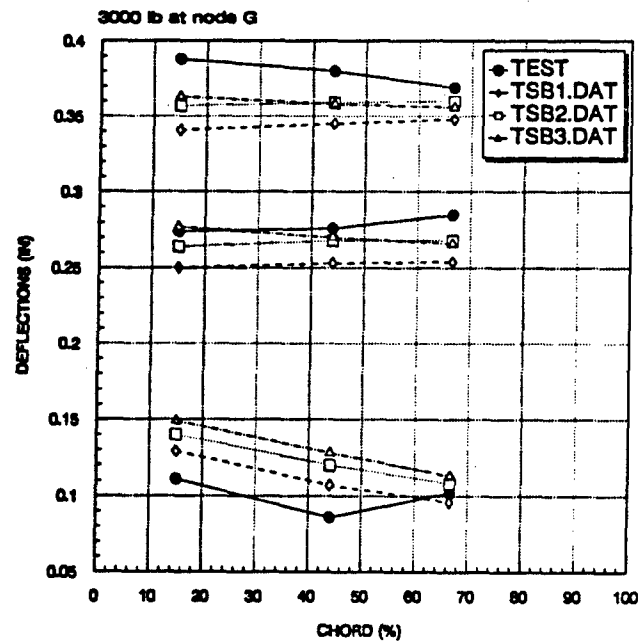


Figure 17b. Comparison of Displacements from TSBi.DAT and Test.

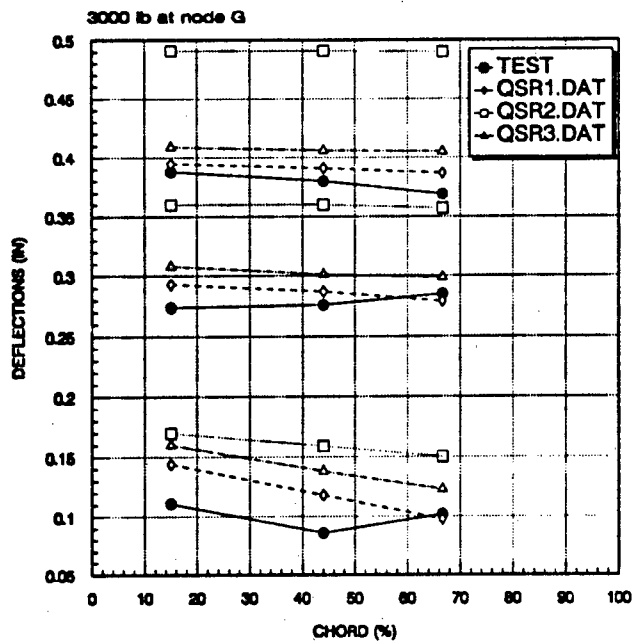


Figure 17c. Comparison of Displacements from QSRi.DAT and Test.

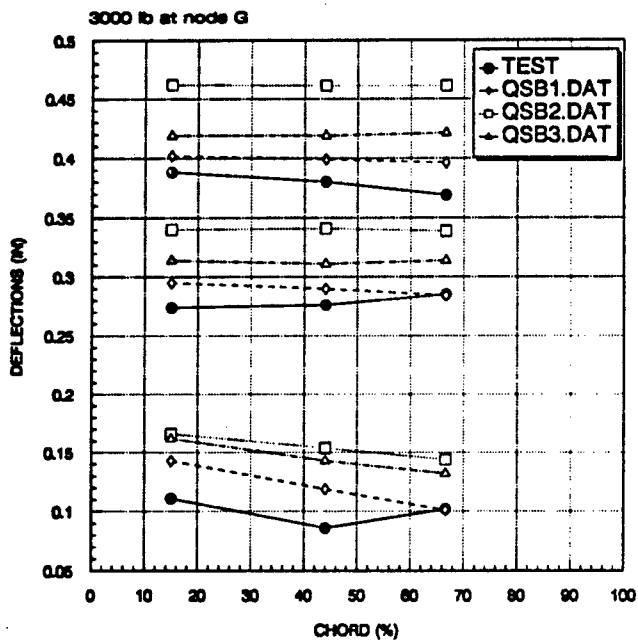


Figure 17d. Comparison of Displacements from QSBi.DAT and Test.

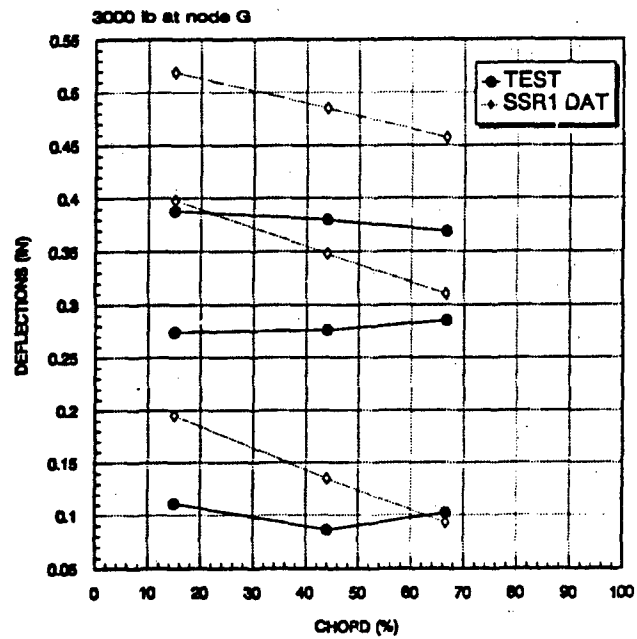


Figure 17e. Comparison of Displacements from SSR1.DAT and Test.

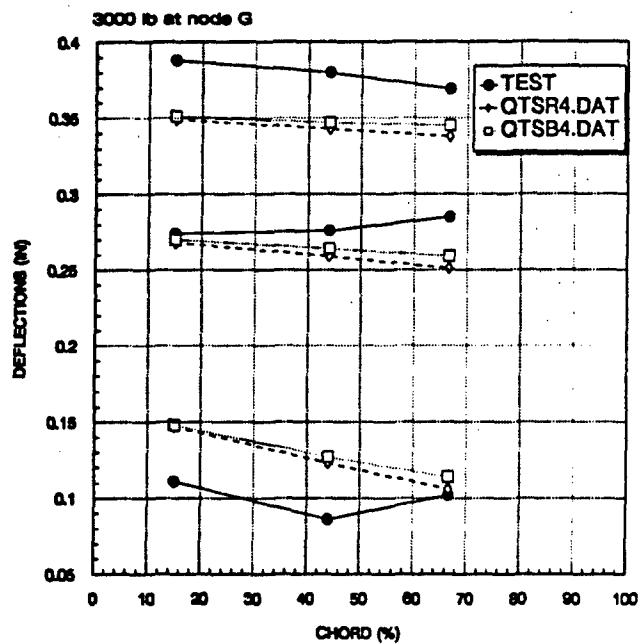


Figure 17f. Comparison of Displacements from QTSR4.DAT, QTSB4.DAT and Test.

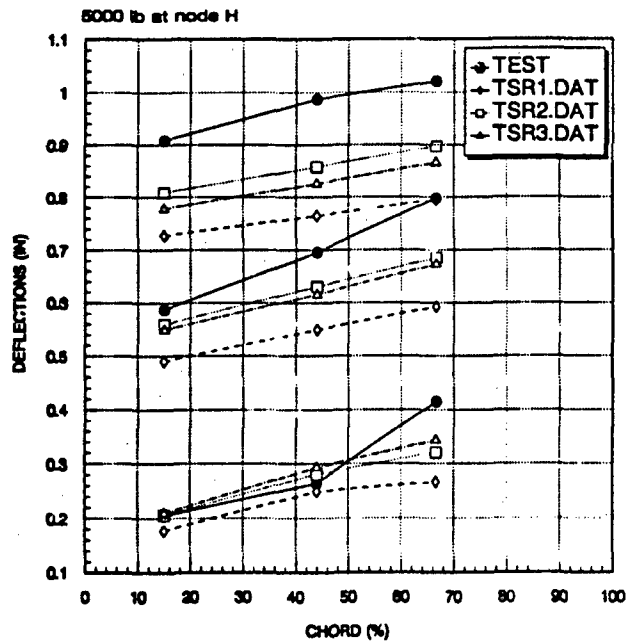


Figure 18a. Comparison of Displacements from TSRi.DAT and Test.

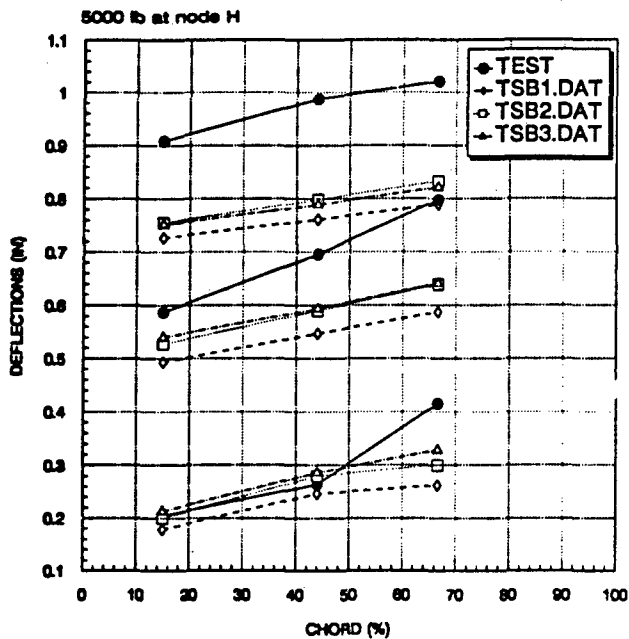


Figure 18b. Comparison of Displacements from TSBi.DAT and Test.

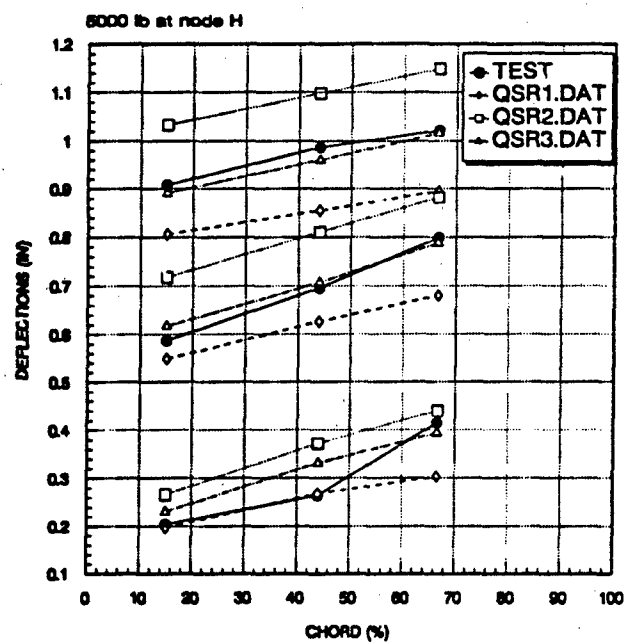


Figure 18c. Comparison of Displacements from QSRi.DAT and Test.

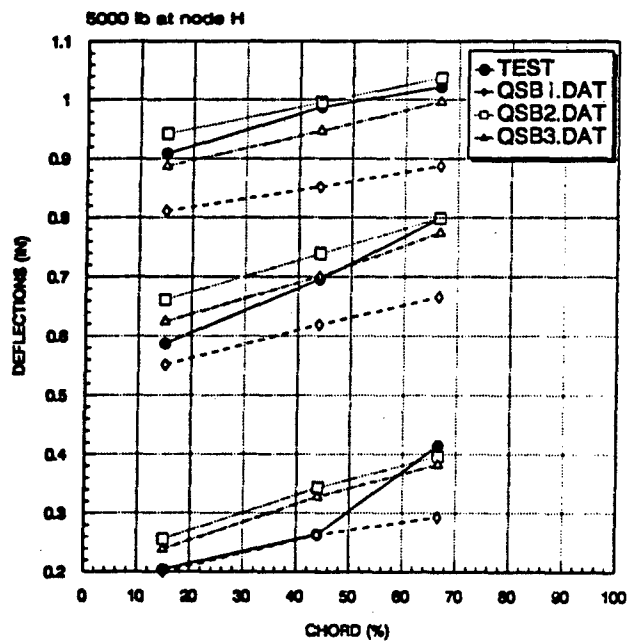


Figure 18d. Comparison of Displacements from QSBi.DAT and Test.

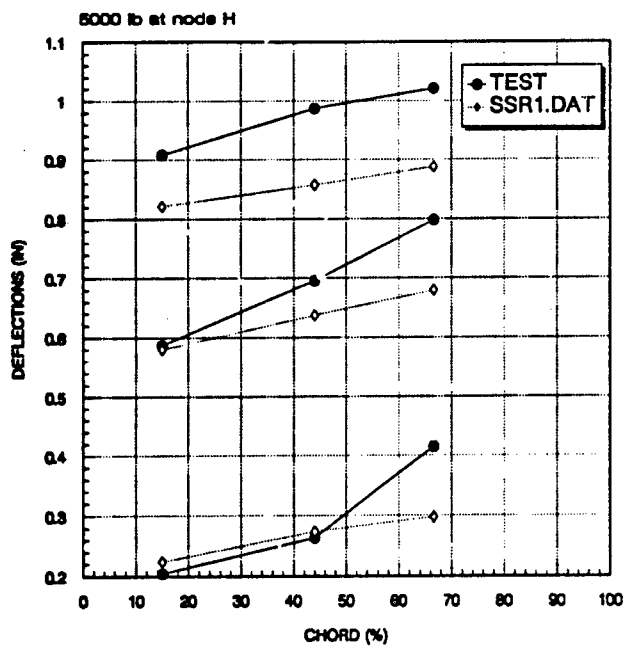


Figure 18e. Comparison of Displacements from SSR1.DAT and Test.

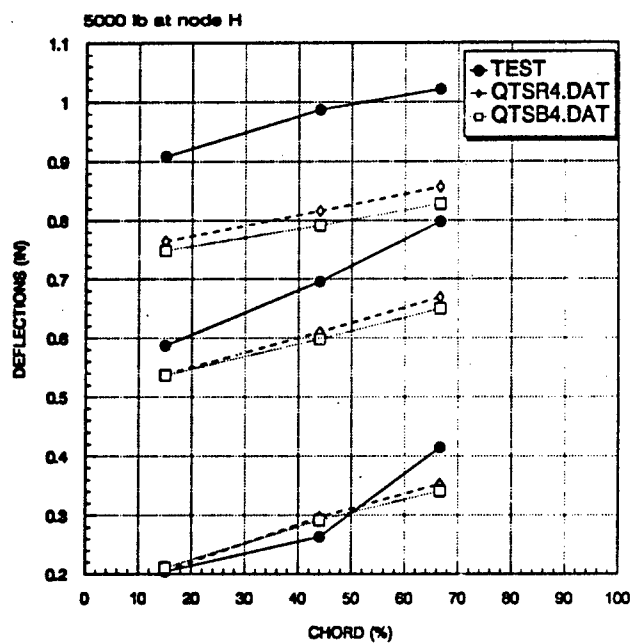


Figure 18f. Comparison of Displacements from QTSR4.DAT, QTSB4.DAT and Test.

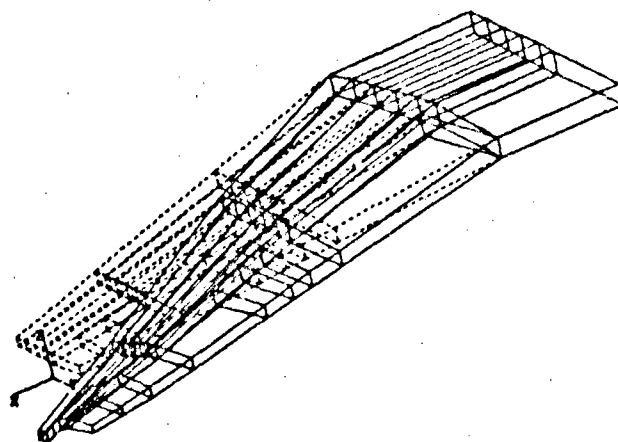


Figure 19a. Numerically Predicted Mode Shape 1. $\omega_0 \approx 4.643$.

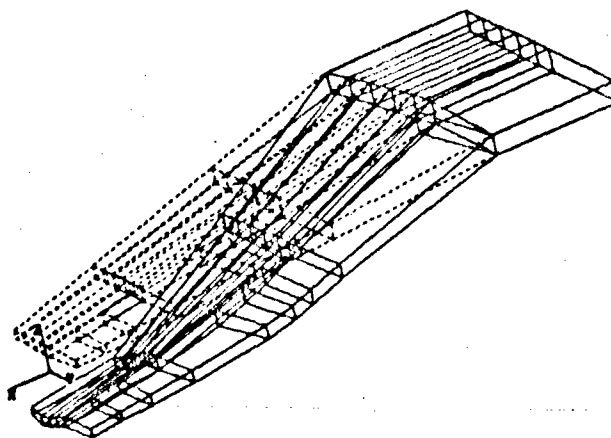


Figure 19b. Numerically Predicted Mode Shape 2. $\omega_0 \approx 6.745$.

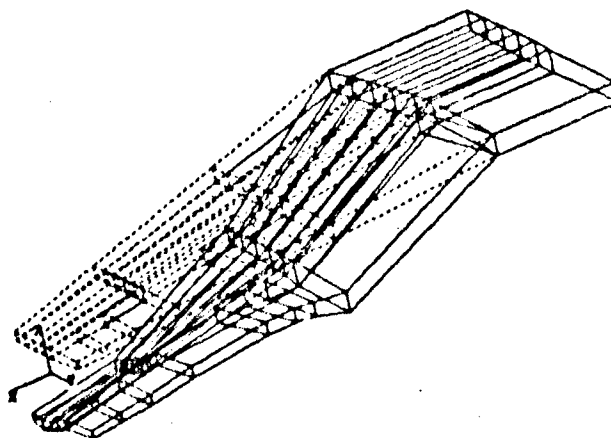


Figure 19c. Numerically Predicted Mode Shape 3. $\omega_0 \approx 7.092$.

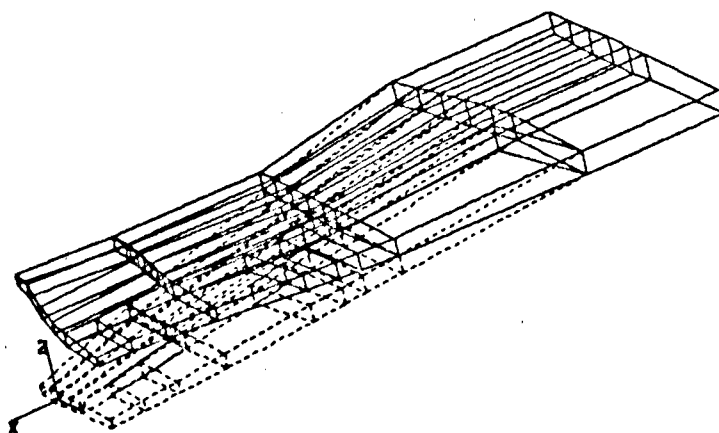


Figure 19d. Numerically Predicted Mode Shape 4. $\omega_n = 7.105$.

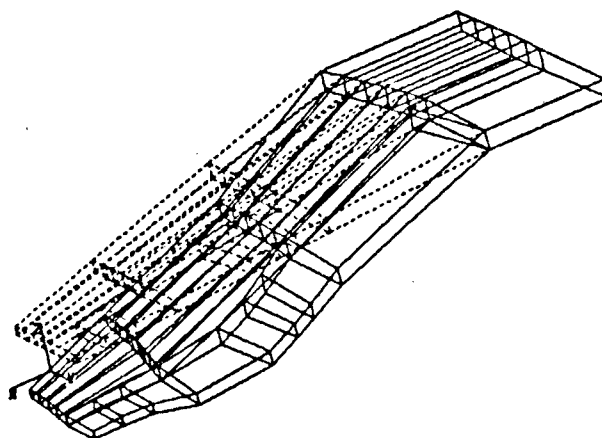


Figure 19e. Numerically Predicted Mode Shape 5. $\omega_n = 7.799$.

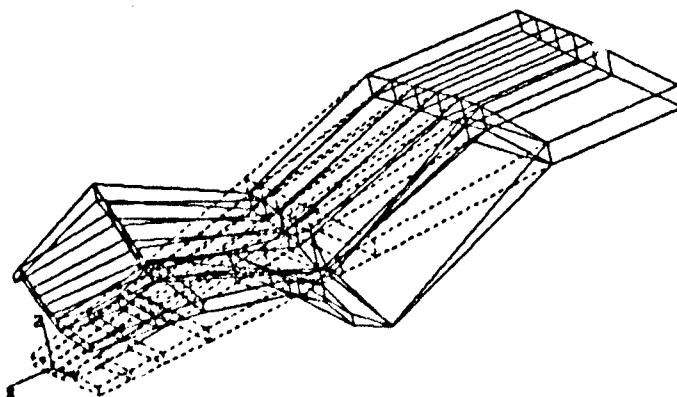


Figure 19f. Numerically Predicted Mode Shape 6. $\omega_n = 7.944$.

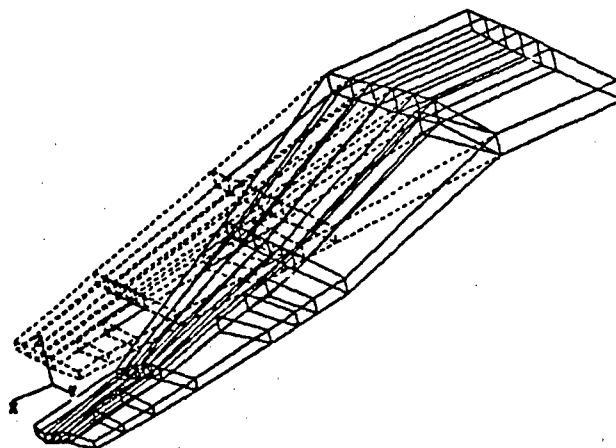


Figure 19g. Numerically Predicted Mode Shape 7. $\omega_7 = 8.269$.

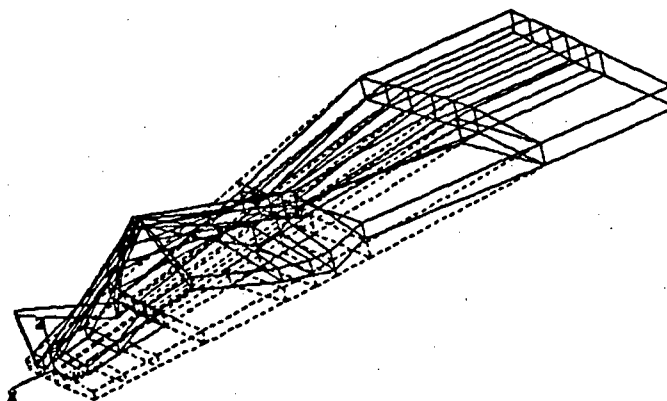


Figure 19h. Numerically Predicted Mode Shape 8. $\omega_8 = 10.681$.

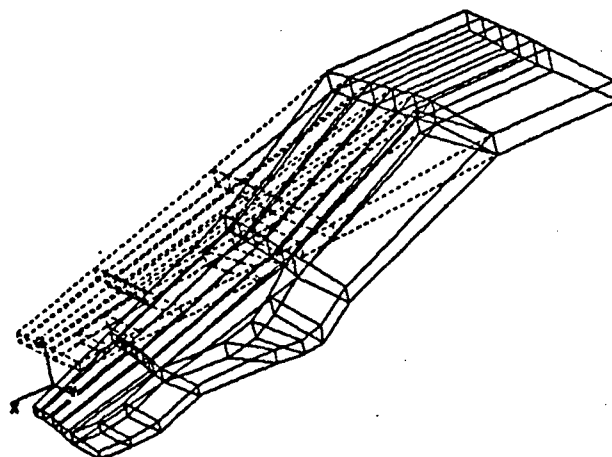


Figure 19i. Numerically Predicted Mode Shape 9. $\omega_9 = 11.542$.

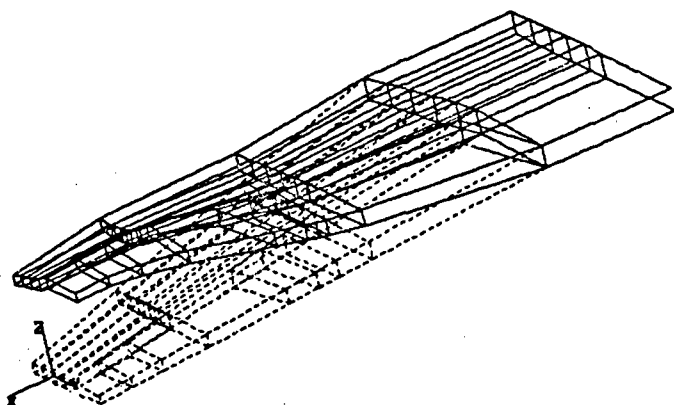


Figure 19j. Numerically Predicted Mode Shape 10. $\omega_n = 12.655$.

NOTE: - - - - - Undeformed
 ——— Mode Shape

4. DISCUSSION OF RESULTS

All results calculated by MSC/NASTRAN and MSC/PAL2 are in very good agreement with the test results. In this report, eight different loadings are applied at each node. In a few loading cases, the finite element results are slightly different from the test results, especially for the 3,000 lb and 5,000 lb loading cases. The differences are due in part to model variations and approximations relative to the actual wing structure.

The T-38 wing skin has a slight curvature, therefore, some regions of the model skin structure require finer meshing. To achieve this, triangular elements are used instead of quadrilateral elements. Sets of data files QSRI.DAT and QSBi.DAT having quadrilateral elements are modified to the sets of data files TSRI.DAT and TSBi.DAT having triangular elements. This produces better agreement. The results from TSRI.DAT and TSBi.DAT agree very well with test results for the 500 lb, 1,000 lb, 200 lb, 1,500 lb, 2,500 lb, and 500 lb loading cases as shown in Figures 11a, 11b, 12a, 12b, 13a, 13b, 14a, 14b, 15a, 15b, 16a, and 16b. The QSRI.DAT and QSBi.DAT agreement is good,

but not as good as the results of TSRI.DAT and TSBi.DAT because of large aspect ratio quadrilateral plates. For example, in the case of 2,500 lb loading at node E, the results from TSR3.DAT show that the difference between calculated and test results is 1.46 percent, and the results from QSR3.DAT has a 14.9 percent difference (In case of the deflection at node E).

In addition, the combination of quadrilateral and triangular plates is evaluated in this report. The corresponding two data files (Model 4 in Table 1) are QTSR4.DAT and QTSB4.DAT and are actually modified from QSB3.DAT and QSR3.DAT. In this case, the difference between the calculated and test results is 0.46 percent. Of particular interest, the combination of quadrilateral and triangular plate is adequate for this kind of wing skins as shown in Figures 11f-18f. In other words, use of this combination for the T-38 wing skins is significantly different as shown in Figures 15b, 15d, and 15f. Both test results and calculated results show that the loads in eight different loading cases has resulted in bending of the wing about axes parallel to the ribs and has imposed very little torsion. All results are shown in Figures 11-18.

The choice of the type of spar and rib chords depends on the wing structural model. For the current work, the spar and rib chords of the T-38 wing are modeled as beam (bar) and rod elements in separate wing models. The method of sizing the rod elements of the spar and rib of the wing is explained on pages 11-14. The results from TSBi.DAT, TSRI.DAT, QSBi.DAT, QSRi.DAT, QTSB4.DAT, and QTSR4.DAT, show the difference between the CBEAM option and the CONROD option for spar/rib chords is not significant. For example, Figures 11a and 11b show that using either option does not make any difference.

According to Reference [4], one way to treat the effective areas of the rod element is a summation of its own area, plus the additional term comprised of the skin thickness between the two rods times one half the distance between the rods. There is assumed to be no bending and membrane stiffness in the top and bottom skins (as compared to a real wing structure and box-beam). Because of this assumption, the rod element stiffness is increased. It is the author's experience that a typical difficulty exists in the calculation of the effective area of rod. For example, from equation $A_{eff} = A_f + bt/2$ (b is the distance between two spar or rib chords, t is the thickness of wing skins, and, A_f is the physical cross section area of spar and rib chords), and the value of b should be defined. In the case of the T-38 wing, it has a general quadrilateral shape, so an average

value of **b** is taken. This procedure is used in the Model SSR1.DAT (See section 2.3). SSR1.DAT has the shear panel option for the top and bottom skins and spar and rib webs: The weakness, difficulty of the calculation of the effective area of rod, in using this procedure is shown in Figures 11e-18e.

Figures 19a-j show ten flap bending modes and the associated natural frequencies. The natural frequencies for the higher modes appear in Table 3. At this time, test data are not available for correlation with dynamic test results.

5. CONCLUSIONS

In this report, results of a static and dynamic analysis of an undamaged T-38 wing have been presented. Seven different structural models of the wing have been studied. Model 4(QTSR4.DAT and QTSB4.DAT) it featured quadrilateral and triangular plate elements for the wing skins, shear panel elements for spar/rib webs and rod or bar (beam) elements for spar/rib chords gives the best comparison with the available static data. Also, this model (used to reduce the problem size) is efficient and accurate as shown in Figures 11f-18f. Model 4 will be used as the T-38 wing model for static and dynamic aeroelasticity and flutter solutions because an accurate determination of influence coefficients is needed in such analysis.

Model SSR1.DAT that used shear panel elements for the top and bottom wing skins instead of quadrilateral or triangular plate elements is not adequate for a complex wing as discussed earlier in this report as shown in Figures 11e-18e.

The CBEAM option used for the spar and rib chords instead of the CONROD option is strongly recommended to create finite structural models for the T-38 wing or similar type wings.

6. RECOMMENDATIONS

The following recommendations are based on this research.

1) Improved results can be expected by using more nodes and elements than used in models 1, 2, 3, or 4.

2) The T-38 wing skin has variable thickness, so it is recommended that the CQUAD8 card in MSC/NASTRAN be used to define a curved quadrilateral shell element with eight grid points. For the triangular plate, CTRIA6 will be used in the follow-on effort.

3) A damaged T-38 wing structural test should be performed to allow correlation with the MSC/NASTRAN finite element code predictions.

INTENTIONALLY LEFT BLANK

7. REFERENCES

1. NOR-60-6. Static Test of Complete Airframe for the T-38A Airplane. Hawthorne, California: Northrop Aircraft, Inc., March 1960.
2. Rattinger, I., Dickenson, H., Cole, C.D., "Preliminary Report Comparison with Test of Analytically Derived Influence Coefficients for a Straight Low-Aspect Ratio Model Wing," Bell Aircraft Report No. 9001-914001, 1957.
3. An Experimental and Analytical Study of the Static Response of an Undamaged and Damaged F-84 Wing, Vols I and II. 61 JTCG/ME-76-11-1 and -2. Eglin AFB, Fla.: Joint Technical Coordinating Group for Munitions Effectiveness, Aug. 24, 1976.
4. An Experimental and Analytical Study of the Dynamic Response of an Undamaged and Damaged F-84 Wing. 61 JTCG/ME-77-2. Eglin AFB, Fla.: Joint Technical Coordinating Group for Munitions Effectiveness, Feb. 27, 1977.
5. Gockel, M. A. (Ed.), MSC/NASTRAN Dynamic Handbook, MacNeal-Schwendler Corp., Los Angeles, June 1983.
6. Analysis of Progressive Collapse of Aircraft Structures. 61 JTCG/ME-84-2. Tinker AFB, OK.: Joint Technical Coordinating Group for Munitions Effectiveness, May 30, 1986.
7. Stronge, W.J. Failure Prediction for Damaged Aircraft Wings. Proceedings of the Fifth Navy-Nastran Colloquium, NSRDC, 1974.
8. Peery, David J. Aircraft Structures. New York: McGraw-Hill, 1950
9. Bruhn, E. F. Analysis and Design of Flight Vehicle Structures. Cincinnati: Tri-State Offset Company, 1973.
10. Timoshenko, S.P. and Goodier, J.N. Theory of Elasticity. New York: McGraw-Hill Book Co., 1970.
11. NASA SP-221(03). The NASTRAN Theoretical Manual. Washington DC.: Scientific and Technical Information Division, National Aeronautics and Space Administration, March 1978.
12. Oehrli, Robert, Wing Aeroelasticity Analysis: Manuevering Aerial Target, Vol. III, US Army Ballistic Research Laboratory, Aberdeen Proving Ground, Maryland, 1988.
13. Zienkiewicz, The Finite Element Method, 3rd Ed., McGraw-Hill, London, 1977.

14. Przemieniecki, J.S., Theory of Matrix Structural Analysis, McGraw-Hill, New York, 1968.
15. Tinawi, R.A., "A Study of Various Idealizations for Wing Structures and Numerical Procedures Involved Using Matrix Methods," AIAA Paper 69-26809, 1969.
16. Granger, R.A., A Unified Method of Flutter Analysis, The Martin Company, July 1959.

APPENDIX A:

Finite Element Model Numbering Details

INTENTIONALLY LEFT BLANK

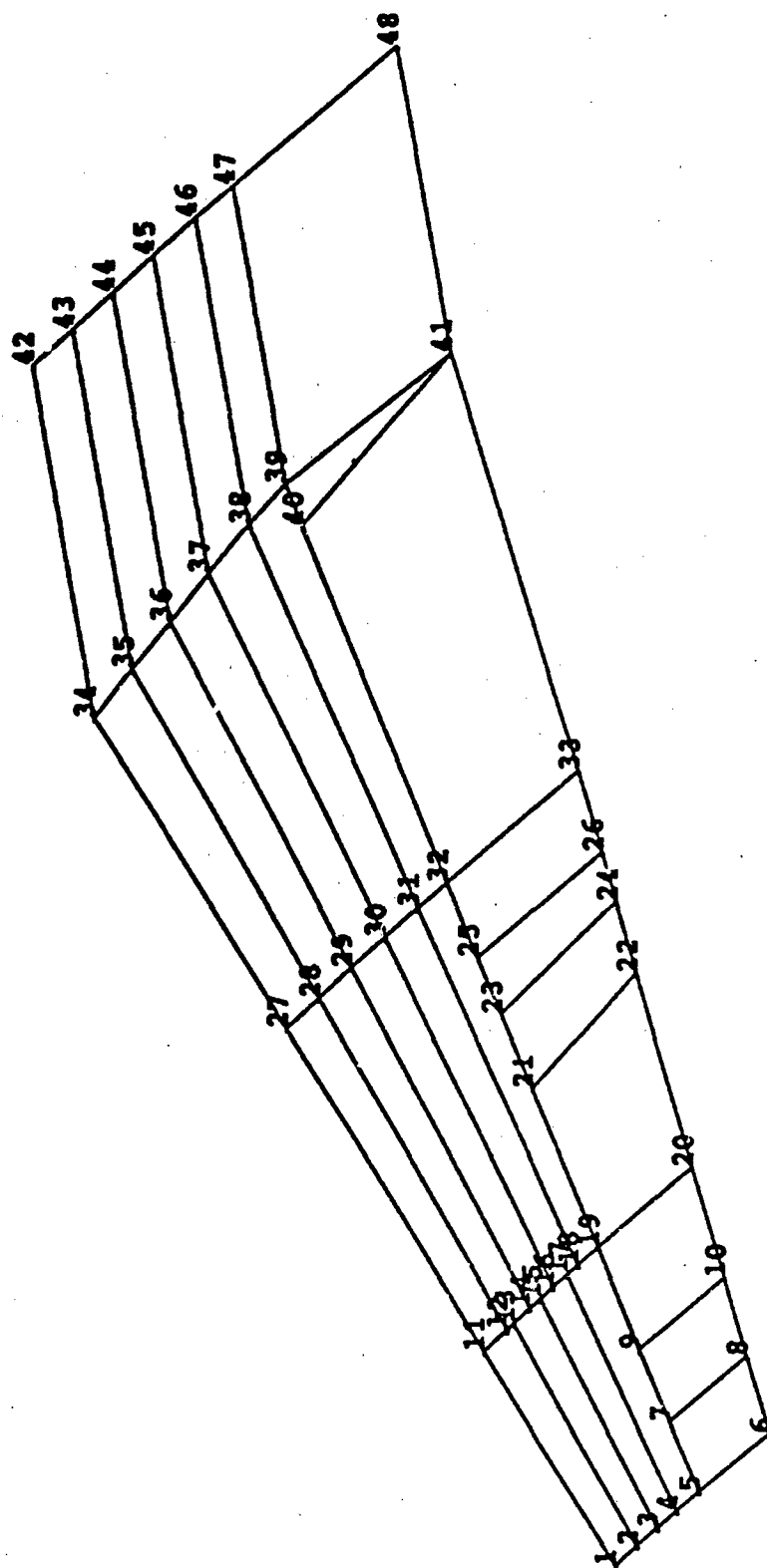


Figure A1. Node Numbers. Top Surface.

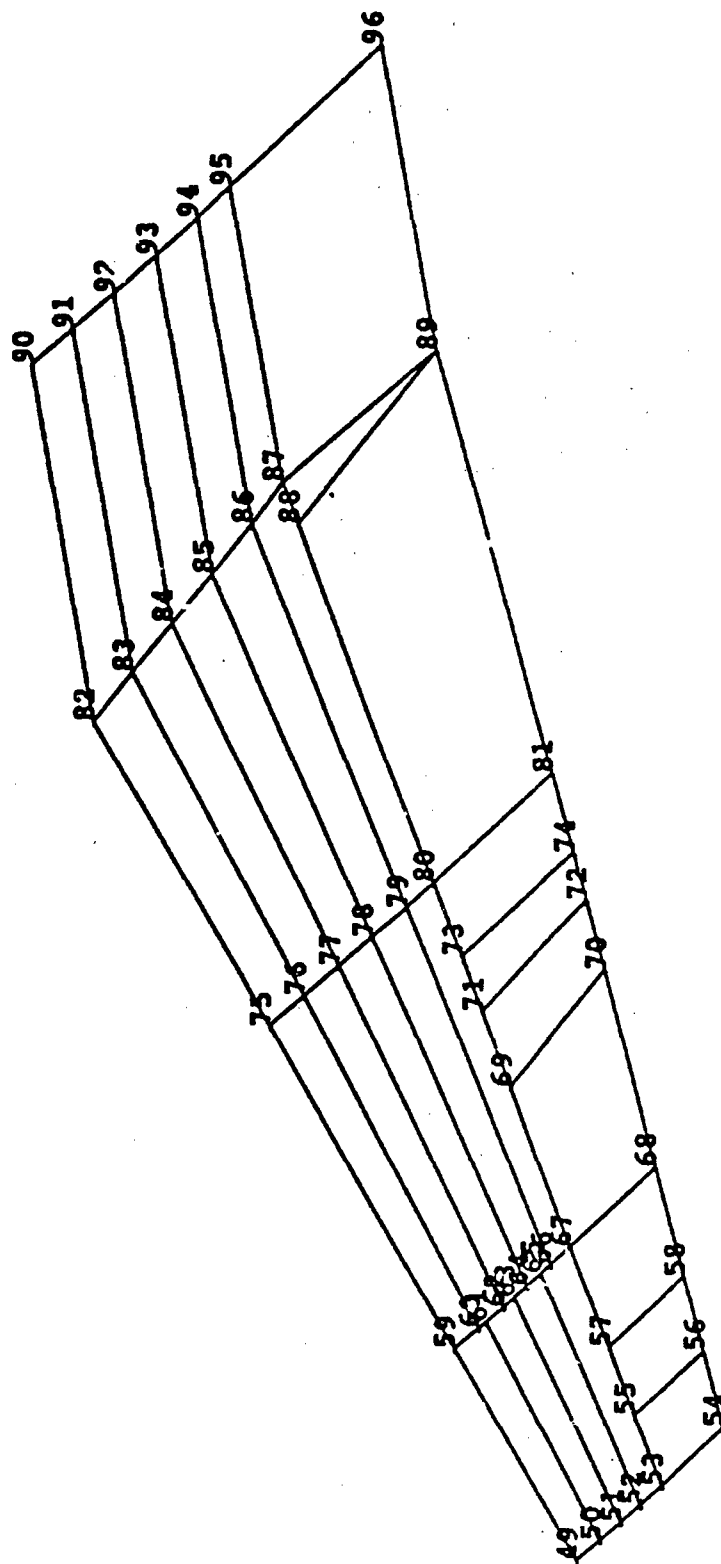


Figure A2. Node Numbers. Bottom Surface.

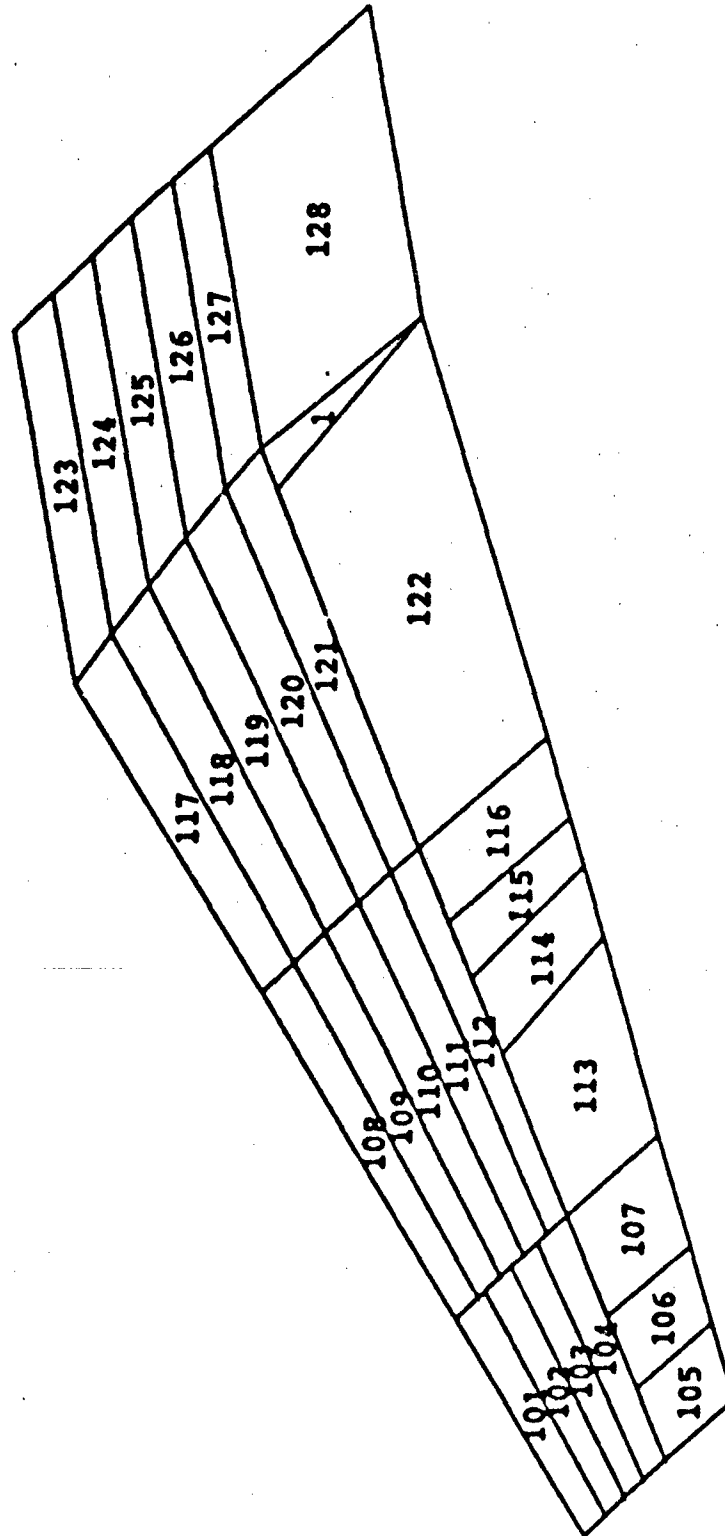


Figure A3. Skin Panel Numbers. Top Surface.

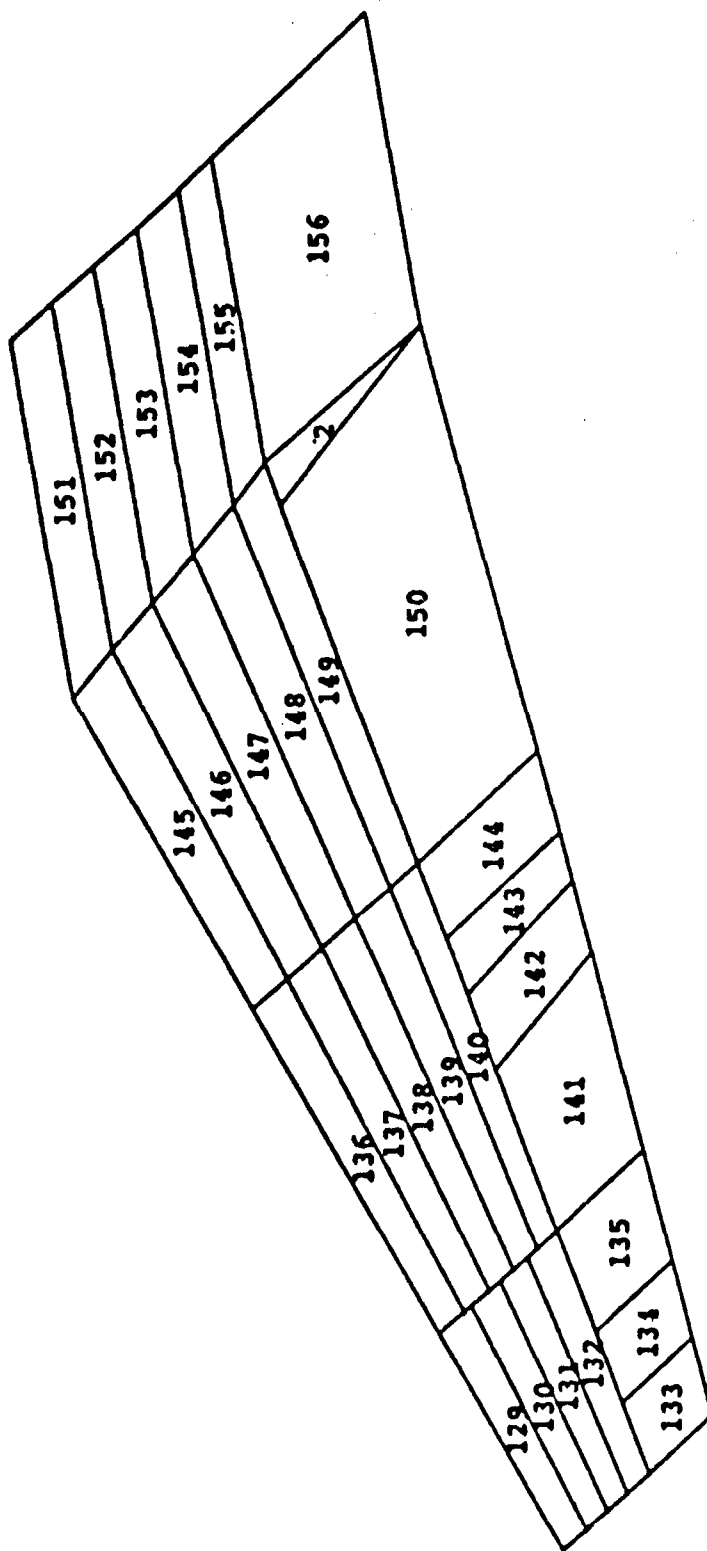


Figure A4. Skin Panel Numbers. Bottom Surface.

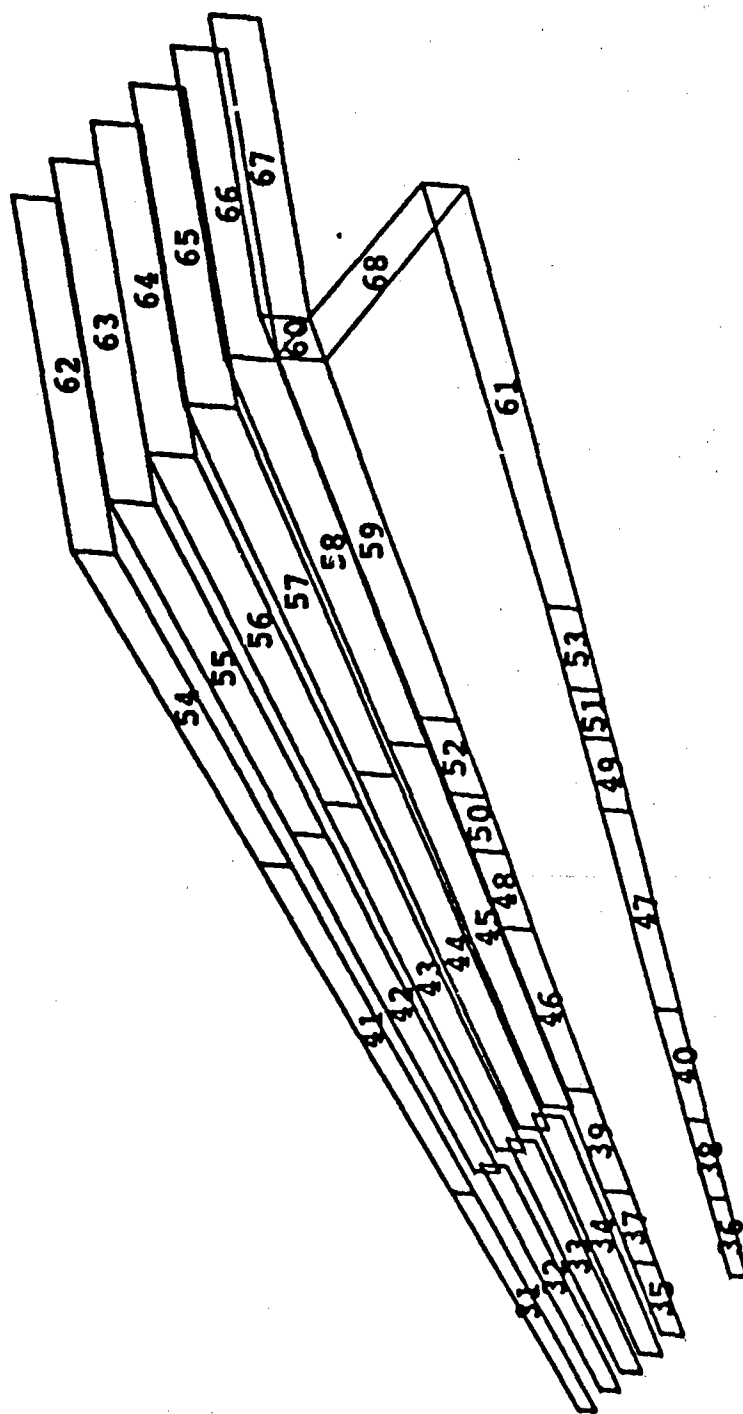


Figure A5. Spar Web Element Numbers.

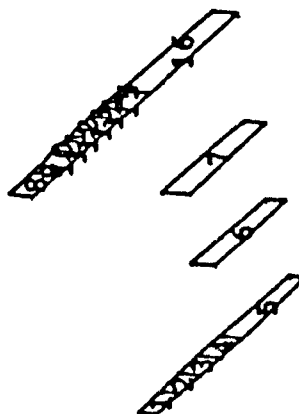
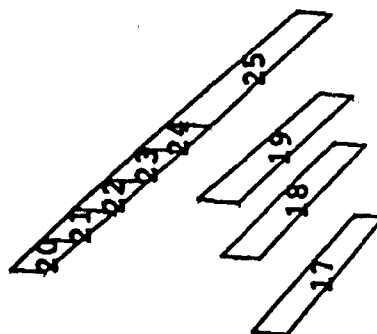
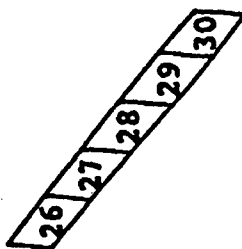


Figure A6. Rib Web Element Numbers.

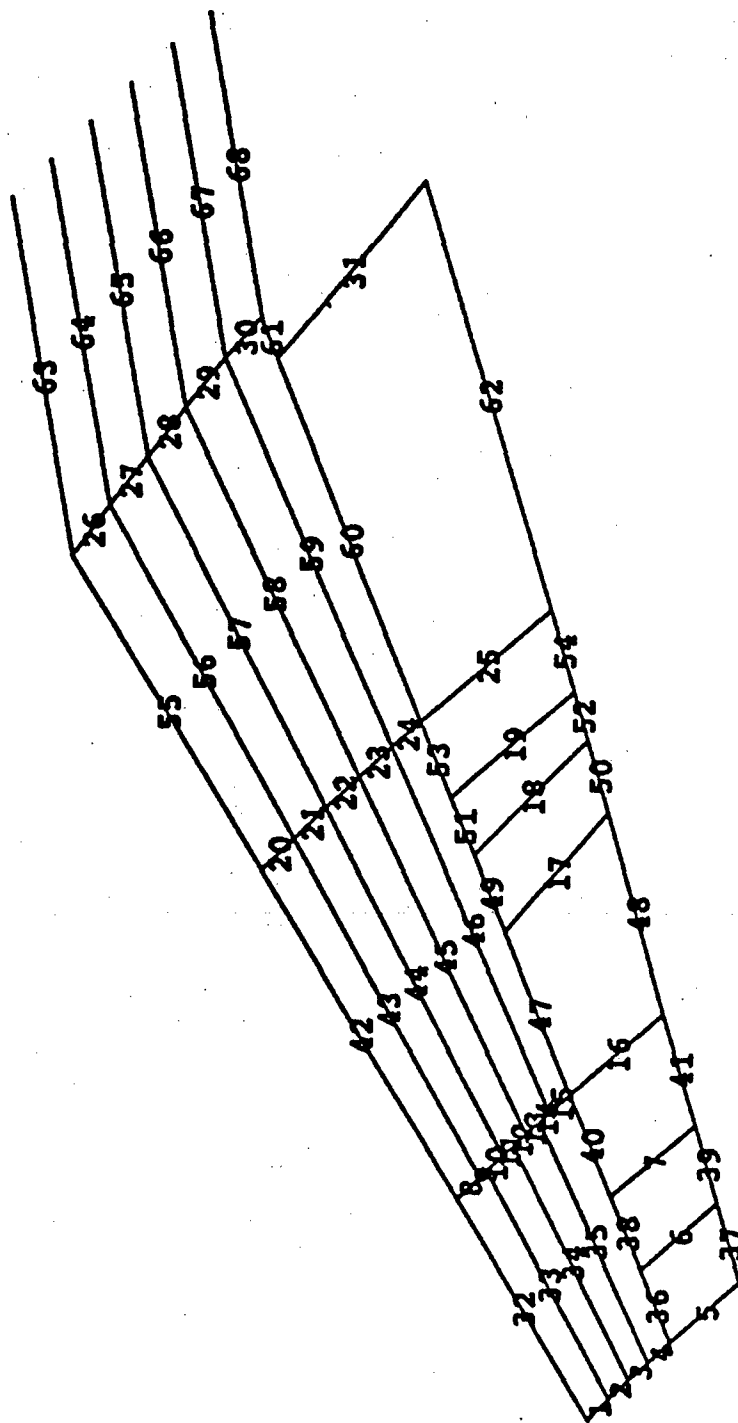


Figure A7. Spar and Rib Chord Numbers. Top Surface.

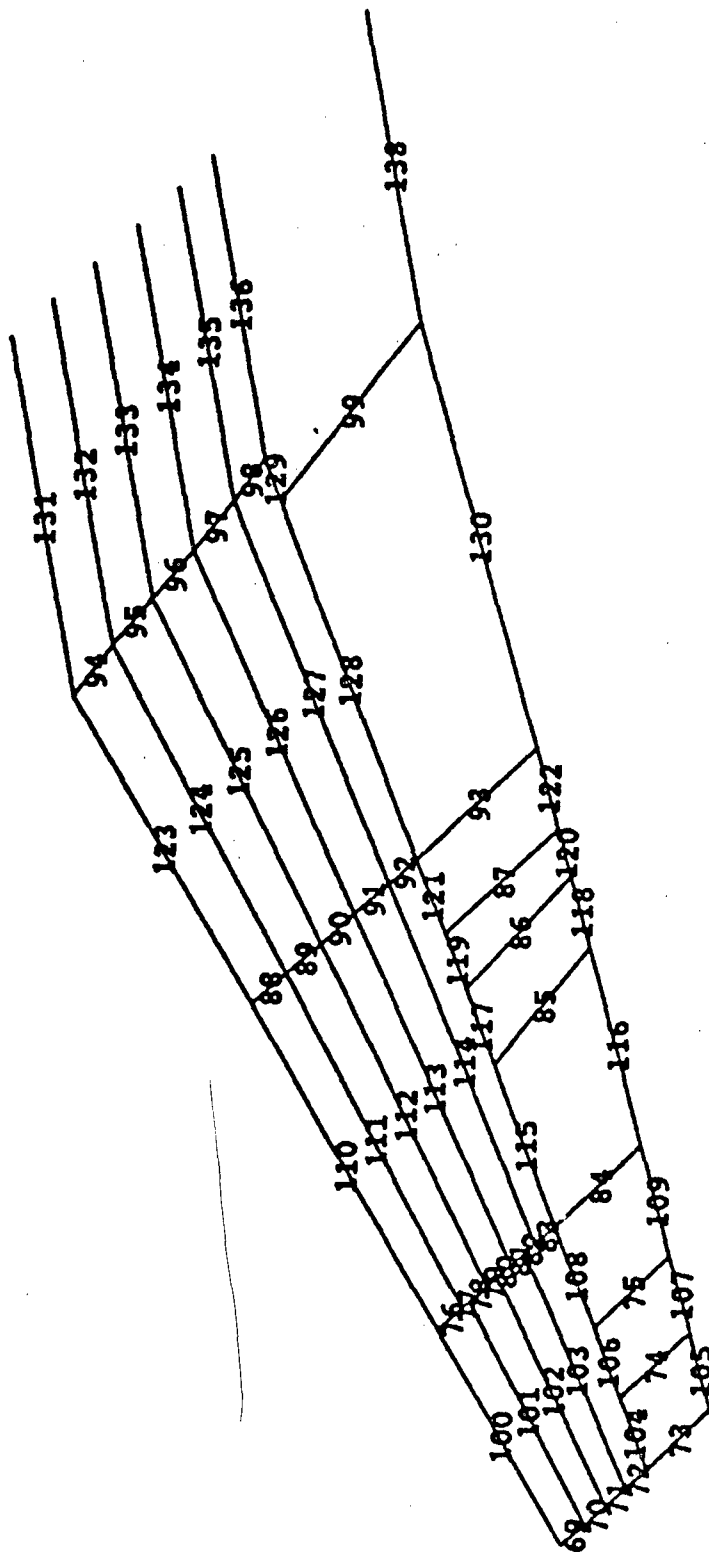


Figure A8. Spar and Rib Chord Numbers. Bottom Surface.

APPENDIX B:

Finite Element Model for Top, Middle, and Bottom

INTENTIONALLY LEFT BLANK

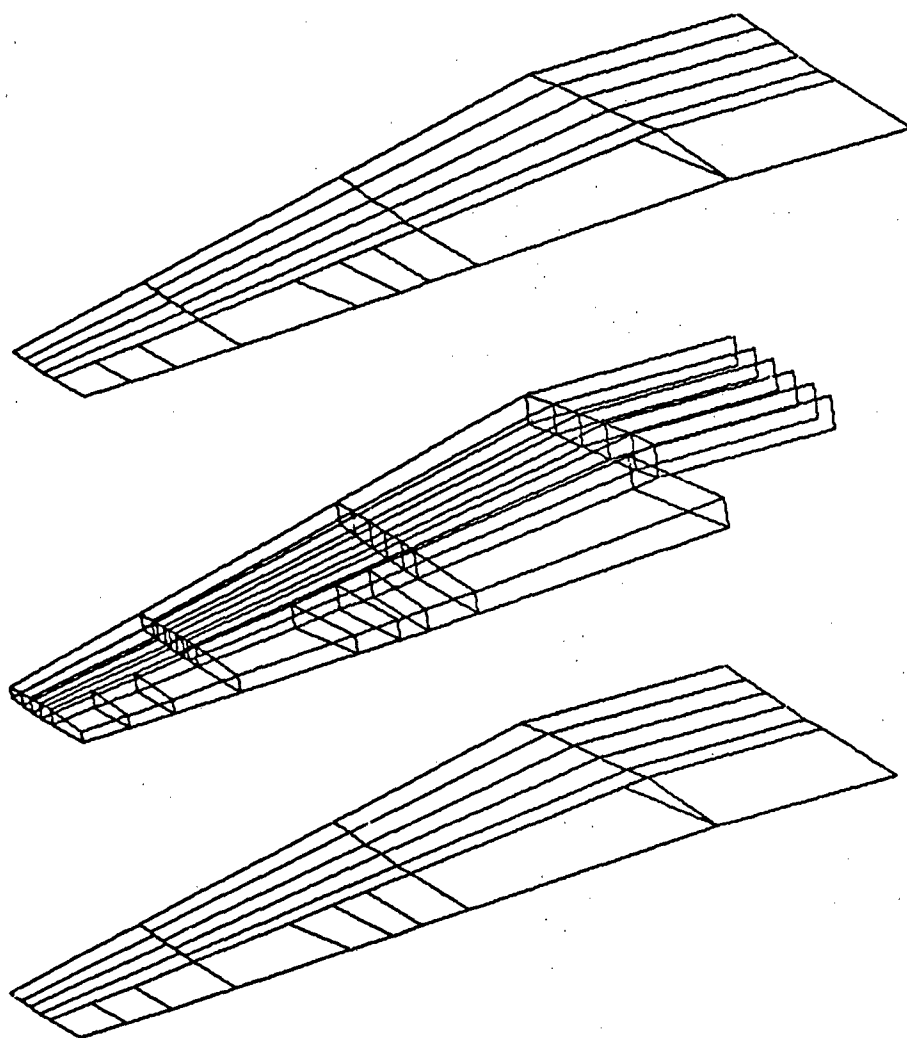


Figure B1. Finite Element Model QSB1.DAT and QSR1.DAT.

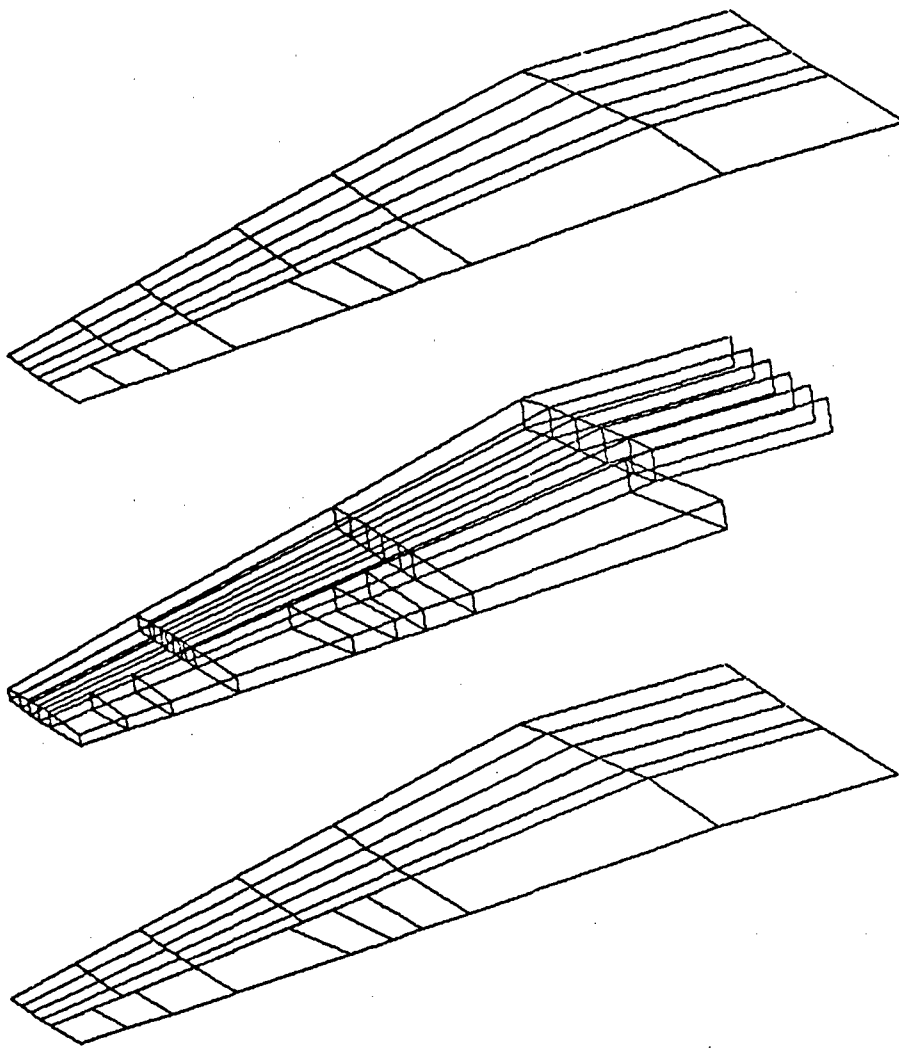


Figure B2. Finite Element Model QSB2.DAT and QSR2.DAT.

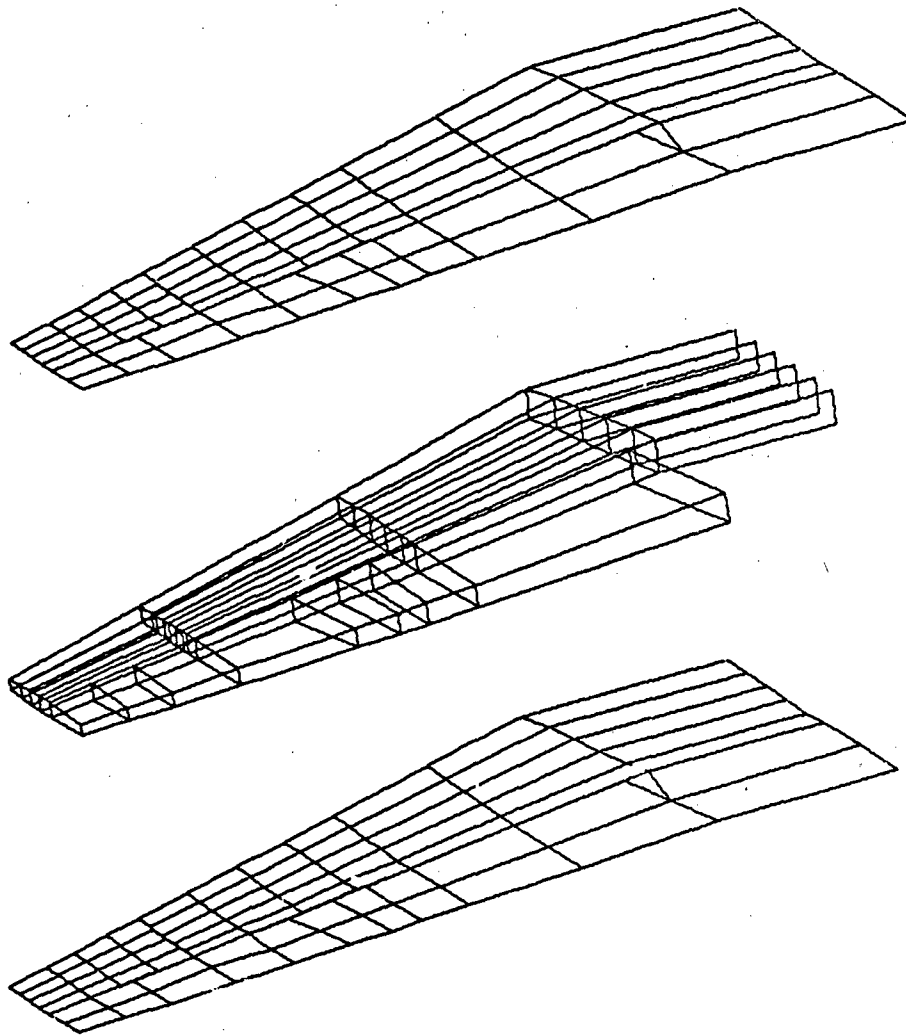


Figure B3. Finite Element Model QSB3.DAT and QSR3.DAT.

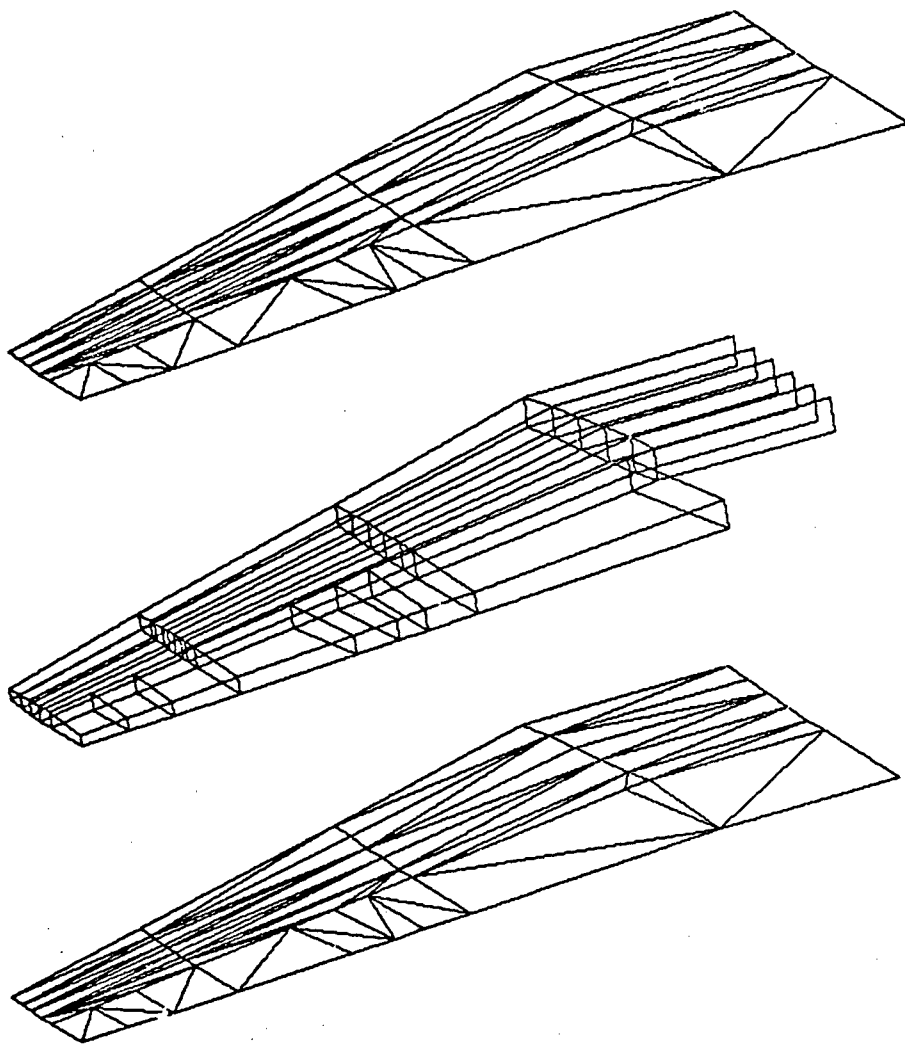


Figure B4. Finite Element Model TSB1.DAT and TSR1.DAT.

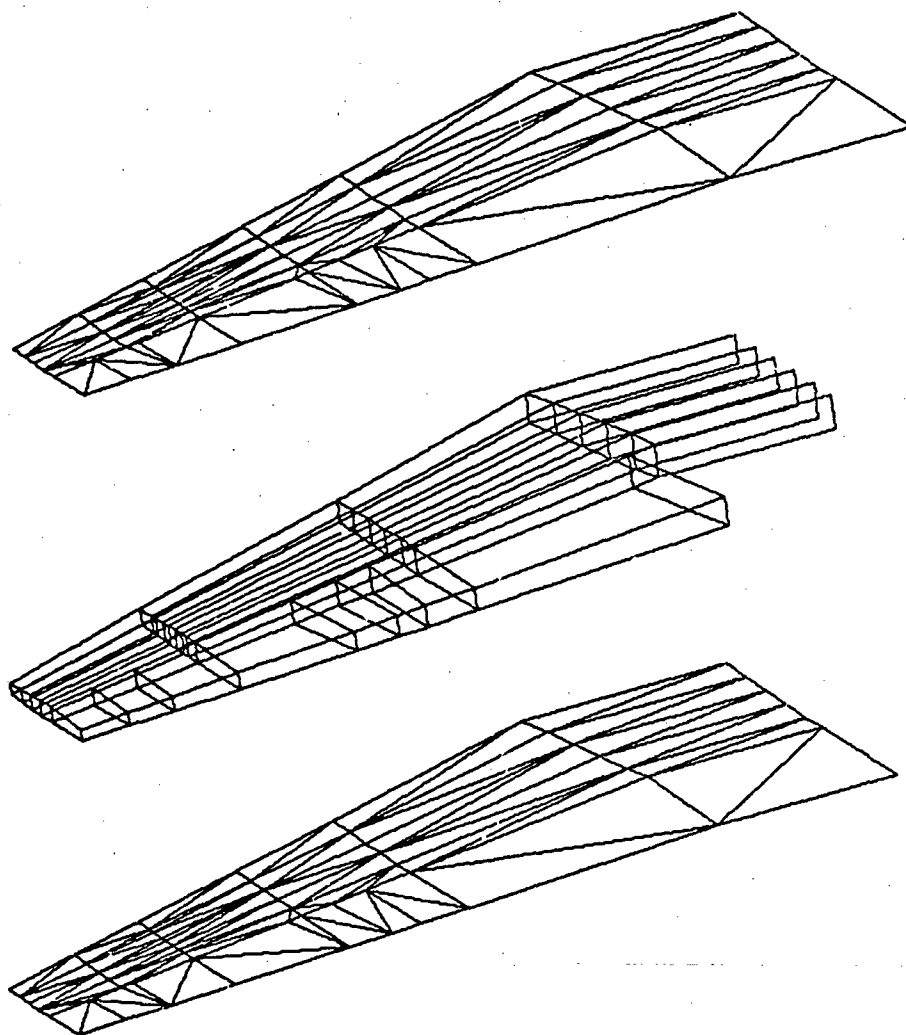


Figure B5. Finite Element Model TSB2.DAT and TSP2.DAT.

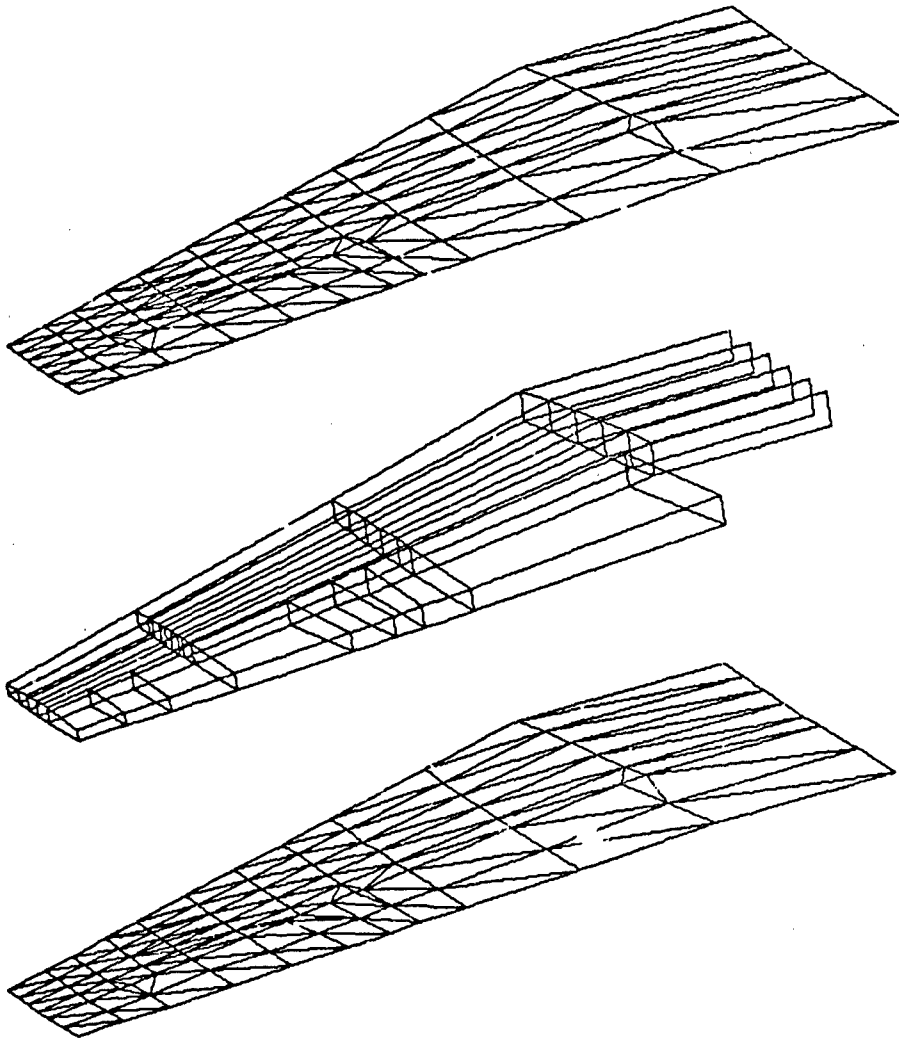


Figure B6. Finite Element Model TSB3.DAT and TSR3.DAT.

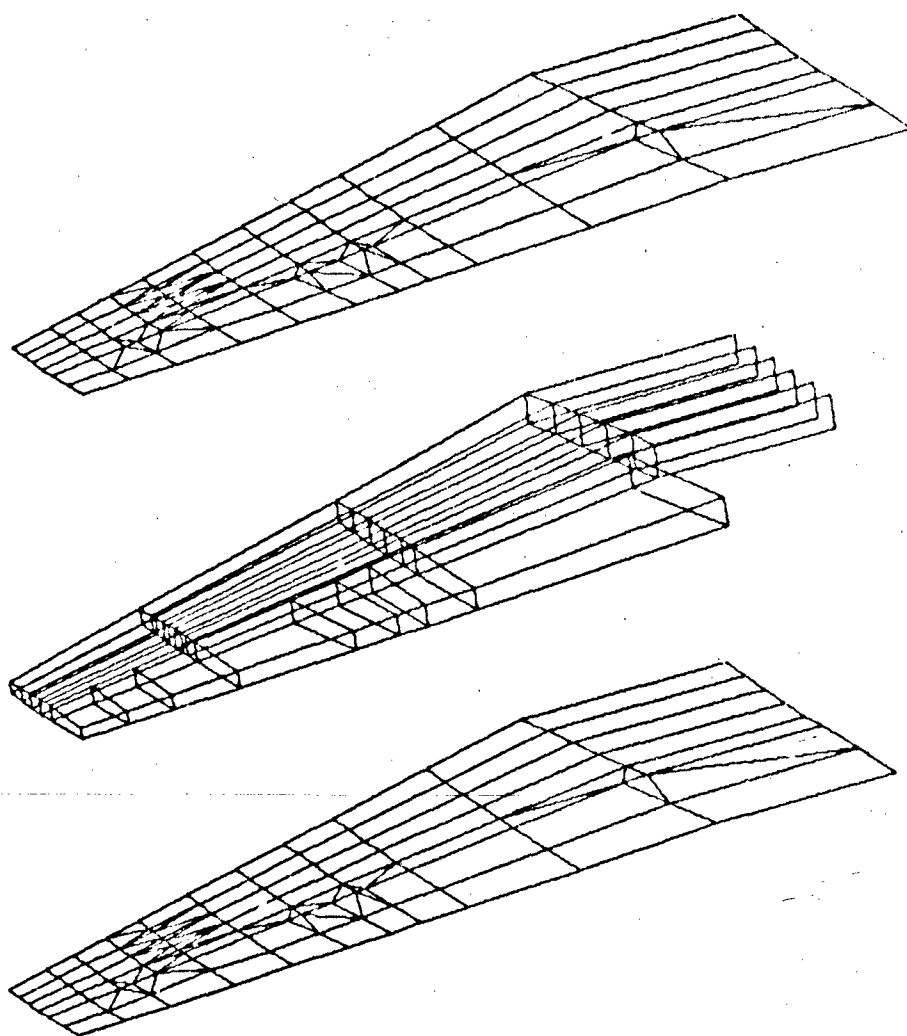


Figure B7. Finite Element Model QTSB4.DAT and QTSR4.DAT.

INTENTIONALLY LEFT BLANK

APPENDIX C:

Rattinger's Wing

INTENTIONALLY LEFT BLANK

1. Introduction

Typical static plate(box-beam) deflection analysis are sampled why different plate element are used in this report. Rattinger's wing is examined because of its structural simplicity and ease in checking out various portions of the digital program. This wing has unswept, untapered, constant-thickness, and continuous skin.

2. Boundary Conditions

This wing is considered as cantilever plate(box-beam). All fixed at wing root and all free at 15 grid points as shown in Figure C2. 100 lbs is loaded at node 3.

3. Description of Finite Element Model

Five sets of SSR.x data are used for the SHEAR panel option for the top and bottom skins as shown in Table C1. Data SSR.1 and SSR.2 are from Equation C1 and SSR.3 and SSR.4 are from Equation C2. As explained in Section 2.4, A_f is obtained and then A_{eff} is determined for the top and bottom spar/web chords.

$$A_{eff} = A_f + \frac{b_1 t_1}{2} \quad (C1)$$

$$A_{eff} = A_f + \frac{b_1 t_1}{2} + \frac{b_2 t_2}{2} \quad (C2)$$

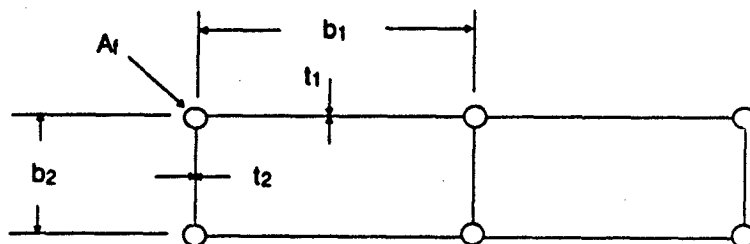
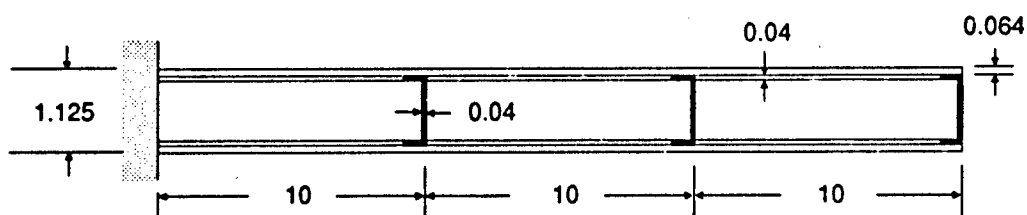
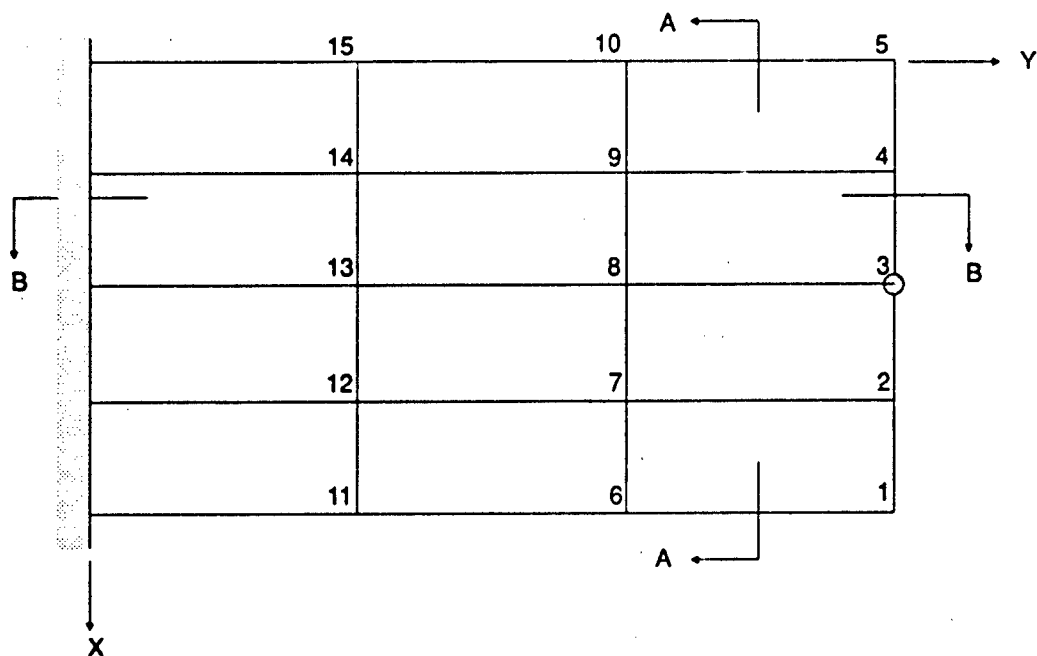
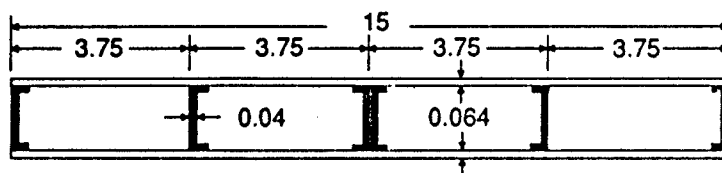


Figure C1. General Box-Beam End View.



Section BB

NOTE: All Dimensions in Inches



Section AA

Figure C2. Geometry of Structural Model.

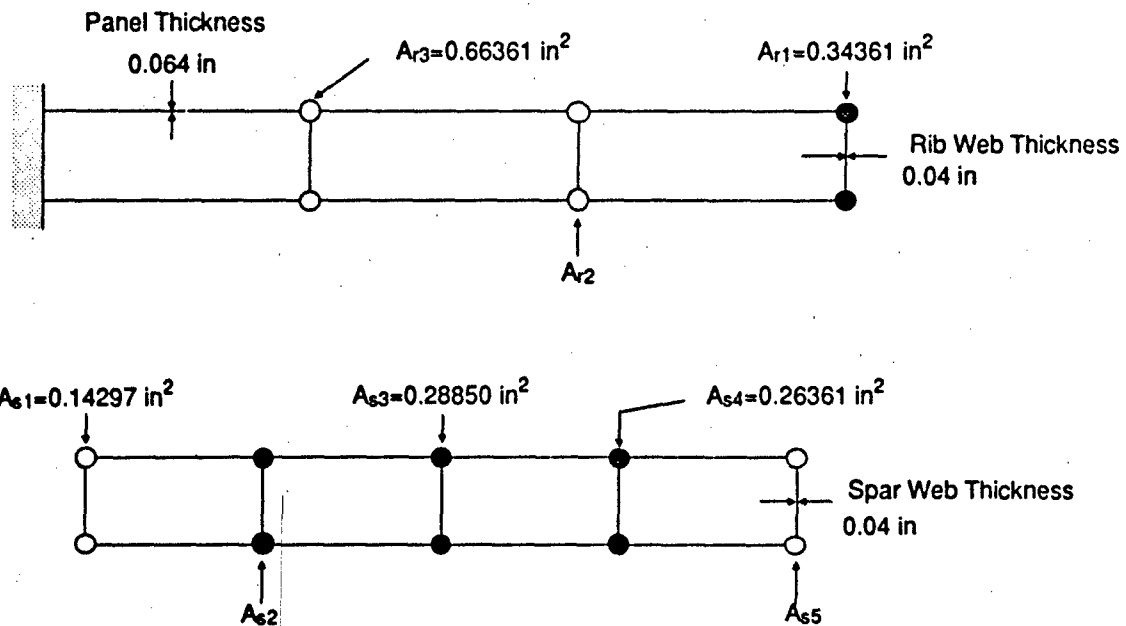


Figure C3. Finite Element Model Using Eq. C1.

Rod Element Area for SSR.3 and SSR.4

Spar Chord Area

$$A_{s1} = A_{s5} = A_f + \frac{3.75 \times 0.064}{2} = 0.14297 \text{ in}^2$$

$$A_{s2} = A_{s4} = A_f + \left(\frac{3.75 + 3.75}{2}\right) \times 0.064 = 0.26361 \text{ in}^2$$

$$A_{s3} = 2A_f + 3.75 \times 0.064 = 0.28850 \text{ in}^2$$

Rib Chord Area

$$A_{r1} = A_f + 5 \times 0.064 = 0.34361 \text{ in}^2$$

$$A_{r2} = A_{r3} = A_f + 10 \times 0.064 = 0.66361 \text{ in}^2$$

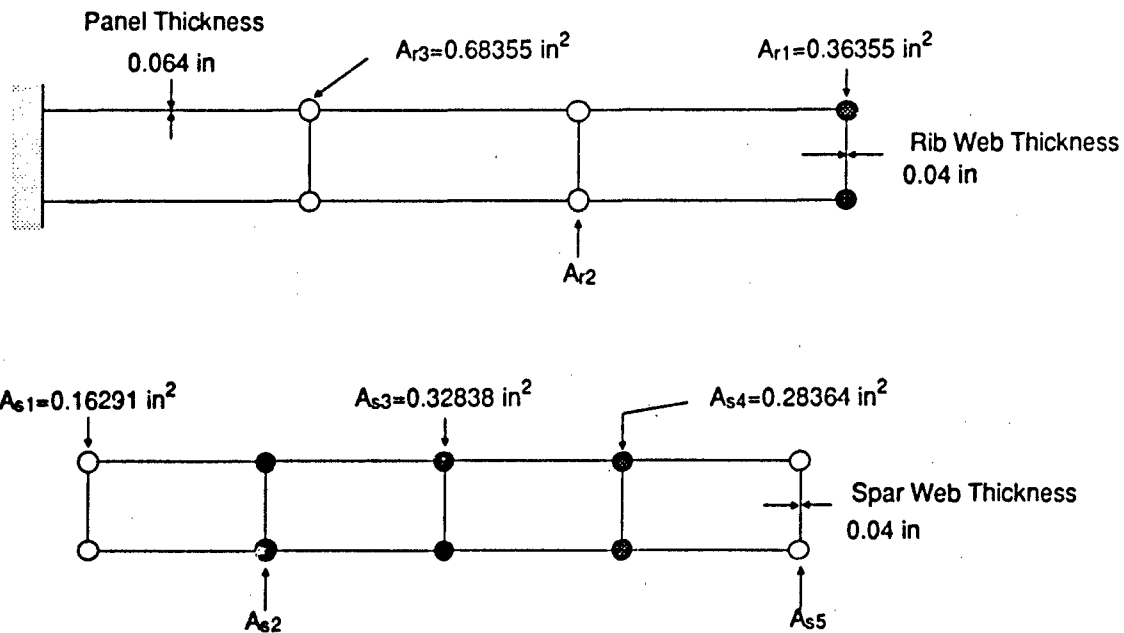


Figure C4. Finite Element Model Using Eq. C2.

Rod Element Area for SSR.1 and SSR.2

Spar Chord Area

$$A_{s1} = A_{s5} = A_f + \frac{3.75 \times 0.064}{2} + \frac{0.997 \times 0.04}{2} = 0.16291 \text{ in}^2$$

$$A_{s2} = A_{s4} = A_f + \left(\frac{3.75 + 3.75}{2}\right) \times 0.064 + \frac{0.997 \times 0.04}{2} = 0.28364 \text{ in}^2$$

$$A_{s3} = 2A_f + 3.75 \times 0.064 + \frac{0.997 \times 0.04}{2} = 0.32838 \text{ in}^2$$

Rib Chord Area

$$A_{r1} = A_f + 5 \times 0.064 + \frac{0.997 \times 0.04}{2} = 0.36355 \text{ in}^2$$

$$A_{r2} = A_{r3} = A_f + 10 \times 0.064 + \frac{0.997 \times 0.04}{2} = 0.68355 \text{ in}^2$$

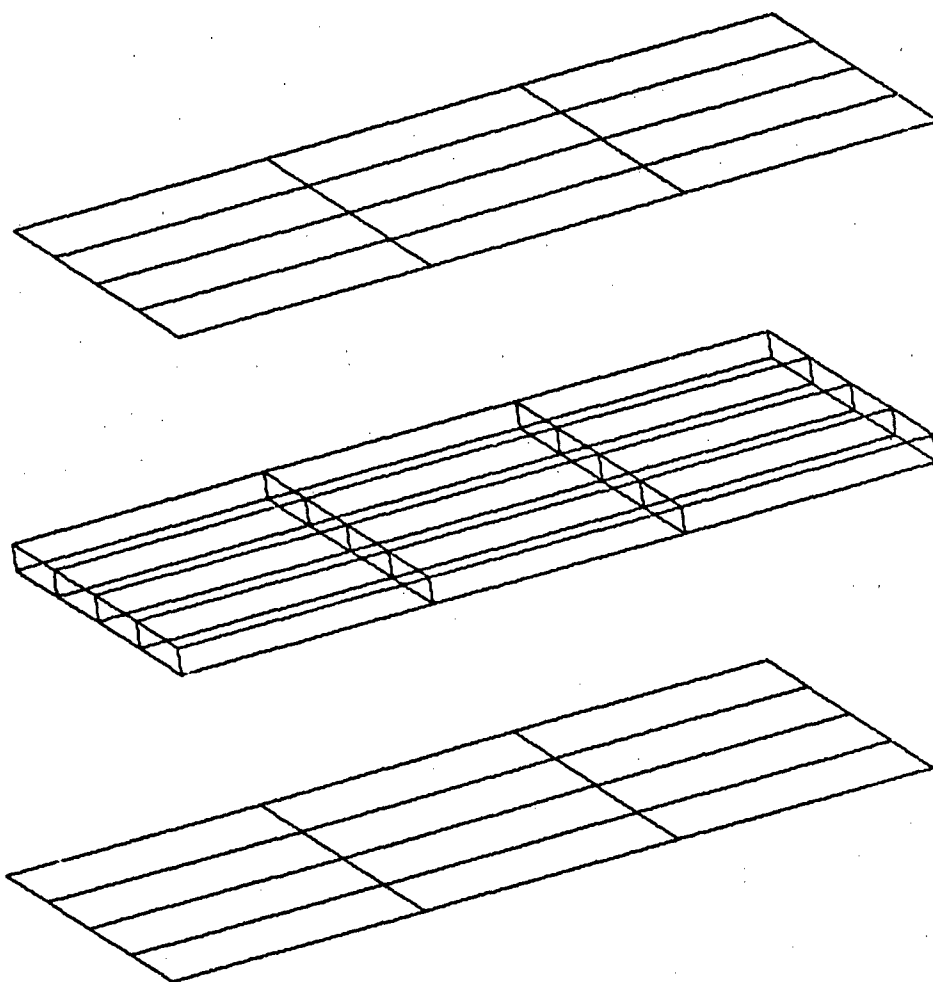


Figure C5. Finite Element Models SSR.1, SSR.2, SSR.3, SSR.4, SSR.5, QSR.1, QSR.2, QSB.1, QSB.2, QQR.1, and QQR.2.

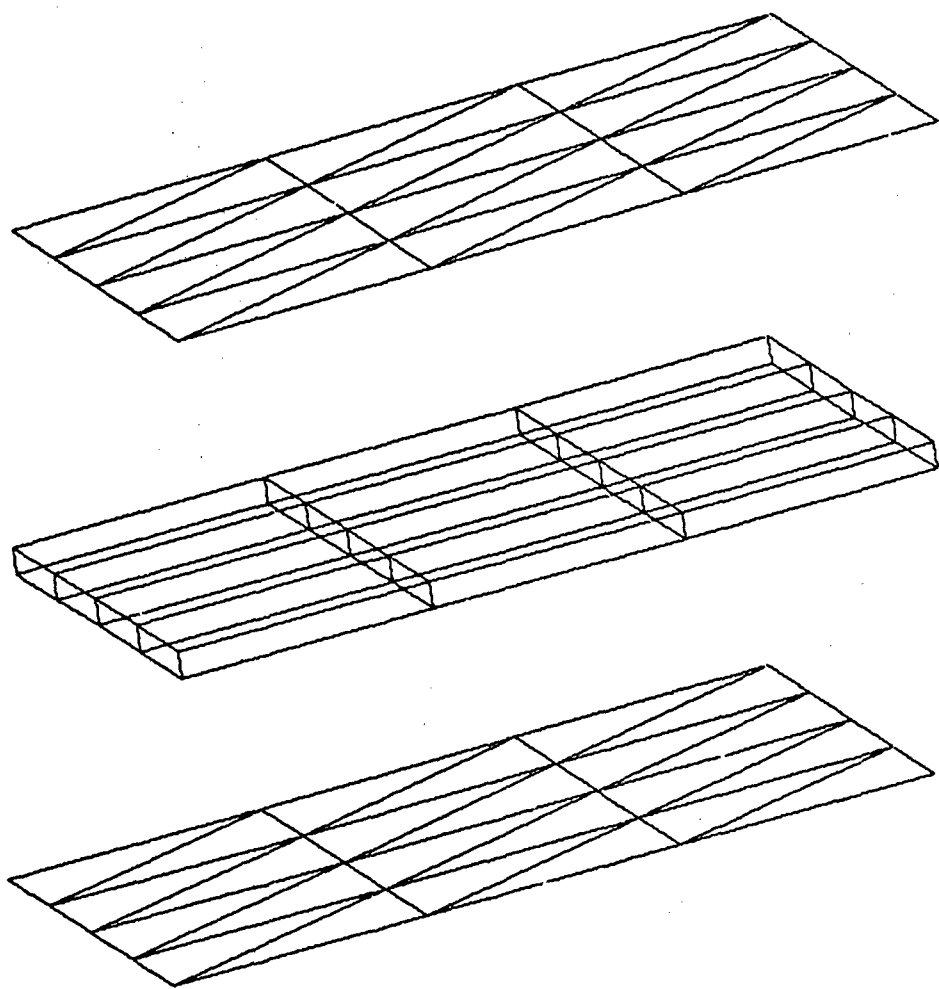


Figure C6. Finite Element Models TSR.1, TSR.2, TSB.1, TSB.2, TQR.1, and TQR.2.

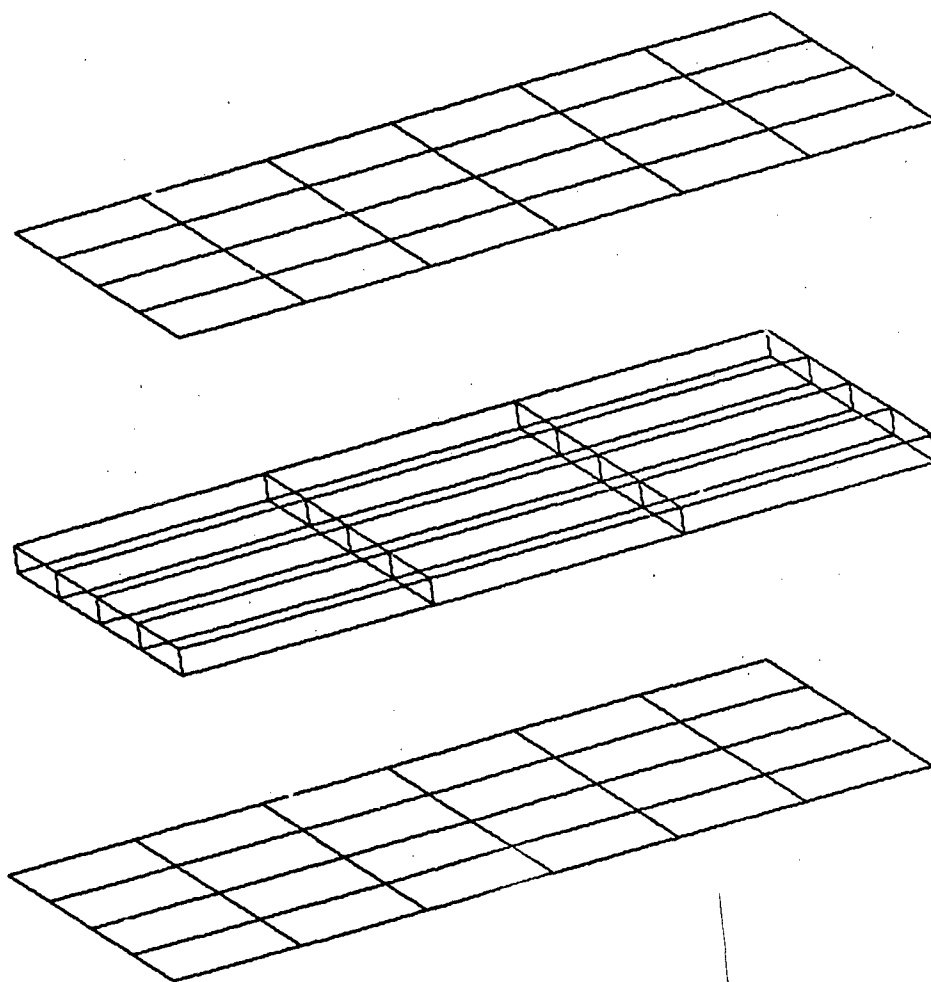


Figure C7. Finite Element Models QSR.3, QSR.4, QSB.3, and QSB.4.

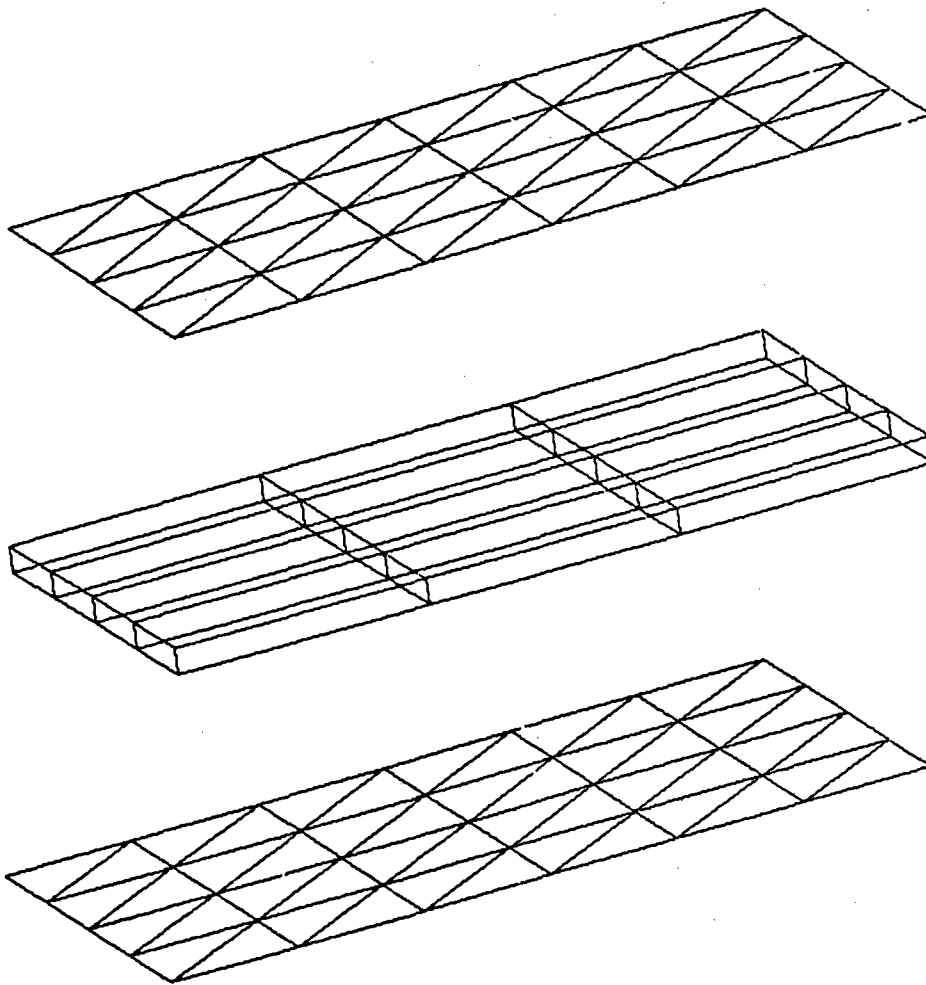


Figure C8. Finite Element Models TSR.3, TSR.4, TSB.3, and TSB.4.

Table C1. Finite Element Model Designation of Rattinger's Wing

| MODEL | SKIN ELEMENTS | STIFFNESS | WEB ELEMENTS | STIFFNESS | SPAR & RIB CHORDS |
|-------|------------------|-----------|-----------------|-----------|----------------------|
| SSR.1 | CSHEAR | NO | CSHEAR | NO | CROD |
| SSR.2 | CSHEAR | YES | CSHEAR | NO | CROD |
| SSR.3 | CSHEAR | NO | CSHEAR | NO | CROD |
| SSR.4 | CSHEAR | YES | CSHEAR | NO | CROD |
| SSR.5 | CSHEAR | NO | CSHEAR | YES | CROD |
| QSR.1 | CQUAD4 | YES | CSHEAR | NO | CROD |
| QSR.2 | CQUAD4 | NO | CSHEAR | NO | CROD |
| TSR.1 | CTRIA3 | YES | CSHEAR | NO | CROD |
| TSR.2 | CTRIA3 | NO | CSHEAR | NO | CROD |
| QSR.3 | CQUAD4 | YES | CSHEAR | NO | CROD |
| QSR.4 | CQUAD4 | NO | CSHEAR | NO | CROD |
| TSR.3 | CTRIA3 | NO | CSHEAR | NO | CROD |
| TSR.4 | CTRIA3 | NO | CSHEAR | NO | CROD |
| QSB.1 | CQUAD4 | YES | CSHEAR | NO | CBEAM |
| QSB.2 | CQUAD4 | NO | CSHEAR | NO | CBEAM |
| TSB.1 | CTRIA3 | YES | CSHEAR | NO | CBEAM |
| TSB.2 | CTRIA3 | NO | CSHEAR | NO | CBEAM |
| QSB.3 | CQUAD4 | YES | CSHEAR | NO | CBEAM |
| QSB.4 | CQUAD4 | NO | CSHEAR | NO | CBEAM |
| TSB.3 | CTRIA3 | YES | CSHEAR | NO | CBEAM |
| TSB.4 | CTRIA3 | NO | CSHEAR | NO | CBEAM |
| QQR.1 | CQUAD4 | YES | CQUAD4 | YES | CROD |
| QQR.2 | CQUAD4 | YES | CQUAD4 | NO | CROD |
| TQR.1 | CTRIA3 | YES | CQUAD4 | YES | CROD |
| TQR.2 | CTRIA3 | YES | CQUAD4 | NO | CROD |

Table C2. Comparison of Displacements from FEM and Test

| NODE MODEL | 1 | 2 | 3 | 4 | 5 | 6 | 7 |
|---------------|--------|--------|--------|--------|--------|--------|--------|
| TEST | 0.1520 | 0.1549 | 0.1572 | 0.1541 | 0.1511 | 0.0813 | 0.0833 |
| SSR.1 | 0.1457 | 0.1466 | 0.1477 | 0.1466 | 0.1457 | 0.0757 | 0.0760 |
| SSR.2 | 0.1399 | 0.1397 | 0.1408 | 0.1397 | 0.1388 | 0.0723 | 0.0725 |
| SSR.3 | 0.1622 | 0.1632 | 0.1643 | 0.1632 | 0.1622 | 0.0843 | 0.0845 |
| SSR.4 | 0.1537 | 0.1547 | 0.1558 | 0.1547 | 0.1537 | 0.0800 | 0.0802 |
| SSR.5 | 0.1486 | 0.1496 | 0.1507 | 0.1496 | 0.1486 | 0.0776 | 0.0779 |
| QSR.1 | 0.1482 | 0.1499 | 0.1513 | 0.1499 | 0.1482 | 0.0760 | 0.0773 |
| QSR.2 | 0.1563 | 0.1581 | 0.1595 | 0.1581 | 0.1563 | 0.0799 | 0.0813 |
| TSR.1 | 0.1453 | 0.1467 | 0.1479 | 0.1464 | 0.1446 | 0.0746 | 0.0757 |
| TSR.2 | 0.1556 | 0.1572 | 0.1585 | 0.1570 | 0.1551 | 0.0797 | 0.0809 |
| QSR.3 | 0.1315 | 0.1332 | 0.1347 | 0.1332 | 0.1315 | 0.0685 | 0.0697 |
| QSR.4 | 0.1610 | 0.1630 | 0.1645 | 0.1630 | 0.1610 | 0.0830 | 0.0846 |
| TSR.3 | 0.1303 | 0.1315 | 0.1325 | 0.1308 | 0.1288 | 0.0681 | 0.0689 |
| TSR.4 | 0.1604 | 0.1622 | 0.1636 | 0.1620 | 0.1601 | 0.0828 | 0.0841 |
| QSB.1 | 0.1506 | 0.1523 | 0.1537 | 0.1523 | 0.1506 | 0.0782 | 0.0785 |
| QSB.2 | 0.1589 | 0.1607 | 0.1622 | 0.1607 | 0.1589 | 0.0813 | 0.0827 |
| TSB.1 | 0.1475 | 0.1490 | 0.1502 | 0.1486 | 0.1468 | 0.0758 | 0.0769 |
| TSB.2 | 0.1581 | 0.1598 | 0.1611 | 0.1596 | 0.1577 | 0.0810 | 0.0823 |
| QSB.3 | 0.1325 | 0.1342 | 0.1357 | 0.1342 | 0.1325 | 0.0690 | 0.0702 |
| QSB.4 | 0.1625 | 0.1645 | 0.1660 | 0.1645 | 0.1625 | 0.0838 | 0.0853 |
| TSB.3 | 0.1312 | 0.1325 | 0.1335 | 0.1317 | 0.1297 | 0.0686 | 0.0694 |
| TSB.4 | 0.1619 | 0.1637 | 0.1650 | 0.1635 | 0.1615 | 0.0836 | 0.0849 |
| QQR.1 | 0.1326 | 0.1342 | 0.1335 | 0.1342 | 0.1326 | 0.0684 | 0.0695 |
| QQR.2 | 0.1435 | 0.1451 | 0.1465 | 0.1451 | 0.1435 | 0.0736 | 0.0748 |
| TQR.1 | 0.1302 | 0.1316 | 0.1328 | 0.1314 | 0.1298 | 0.0673 | 0.0683 |
| TQR.2 | 0.1407 | 0.1422 | 0.1433 | 0.1418 | 0.1401 | 0.0724 | 0.0734 |

NOTE: All Dimensions in Inches

Table C2. Comparison of Displacements from FEM and Test (Con't)

| 8 | 9 | 10 | 11 | 12 | 13 | 14 | 15 |
|--------|--------|--------|--------|--------|--------|--------|--------|
| 0.0842 | 0.0826 | 0.0816 | 0.0241 | 0.0261 | 0.0254 | 0.0249 | 0.0239 |
| 0.0761 | 0.0760 | 0.0757 | 0.0215 | 0.0216 | 0.0216 | 0.0216 | 0.0215 |
| 0.0727 | 0.0725 | 0.0723 | 0.0206 | 0.0207 | 0.0207 | 0.0207 | 0.0206 |
| 0.0847 | 0.0845 | 0.0843 | 0.0239 | 0.0240 | 0.0240 | 0.0240 | 0.0239 |
| 0.0804 | 0.0802 | 0.0800 | 0.0228 | 0.0228 | 0.0228 | 0.0228 | 0.0228 |
| 0.0780 | 0.0779 | 0.0776 | 0.0222 | 0.0222 | 0.0222 | 0.0222 | 0.0222 |
| 0.0778 | 0.0773 | 0.0760 | 0.0206 | 0.0222 | 0.0225 | 0.0222 | 0.0206 |
| 0.0819 | 0.0813 | 0.0799 | 0.0216 | 0.0233 | 0.0236 | 0.0233 | 0.0216 |
| 0.0761 | 0.0754 | 0.0739 | 0.0206 | 0.0217 | 0.0219 | 0.0215 | 0.0202 |
| 0.0814 | 0.0807 | 0.0791 | 0.0218 | 0.0231 | 0.0233 | 0.0230 | 0.0216 |
| 0.0702 | 0.0697 | 0.0685 | 0.0194 | 0.0205 | 0.0208 | 0.0205 | 0.0194 |
| 0.0852 | 0.0846 | 0.0852 | 0.0231 | 0.0245 | 0.0249 | 0.0245 | 0.0231 |
| 0.0690 | 0.0682 | 0.0667 | 0.0195 | 0.0203 | 0.0204 | 0.0200 | 0.0224 |
| 0.0846 | 0.0839 | 0.0823 | 0.0232 | 0.0244 | 0.0247 | 0.0243 | 0.0227 |
| 0.0790 | 0.0785 | 0.0782 | 0.0210 | 0.0225 | 0.0228 | 0.0225 | 0.0210 |
| 0.0833 | 0.0827 | 0.0813 | 0.0220 | 0.0236 | 0.0240 | 0.0236 | 0.0220 |
| 0.0733 | 0.0765 | 0.0750 | 0.0209 | 0.0220 | 0.0222 | 0.0219 | 0.0205 |
| 0.0827 | 0.0820 | 0.0804 | 0.0222 | 0.0235 | 0.0237 | 0.0233 | 0.0219 |
| 0.0707 | 0.0702 | 0.0690 | 0.0195 | 0.0206 | 0.0209 | 0.0206 | 0.0195 |
| 0.0860 | 0.0853 | 0.0838 | 0.0233 | 0.0247 | 0.0251 | 0.0247 | 0.0233 |
| 0.0695 | 0.0687 | 0.0672 | 0.0196 | 0.0201 | 0.0206 | 0.0201 | 0.0188 |
| 0.0854 | 0.0847 | 0.0831 | 0.0234 | 0.0247 | 0.0249 | 0.0245 | 0.0229 |
| 0.0700 | 0.0695 | 0.0684 | 0.0187 | 0.0201 | 0.0203 | 0.0201 | 0.0187 |
| 0.0754 | 0.0748 | 0.0736 | 0.0200 | 0.0215 | 0.0218 | 0.0215 | 0.0200 |
| 0.0686 | 0.0681 | 0.0668 | 0.0187 | 0.0197 | 0.0199 | 0.0196 | 0.0184 |
| 0.0738 | 0.0731 | 0.0717 | 0.0200 | 0.0211 | 0.0212 | 0.0209 | 0.0196 |

NOTE: All Dimensions in Inches

INTENTIONALLY LEFT BLANK

APPENDIX D:

Input Data for QSR1.DAT

INTENTIONALLY LEFT BLANK

ID WING T-38 DEFLECTIONS USING QUAD4 CARDS FOR SKIN AND CSHEAR FOR WEB
 SOL 24
 TIME 44
 DIAG 8
 CEND
 MAXLINES=3000
 METHOD=1
 SET 4 = 1 THRU 48
 DISPL =4
 SUBCASE 1
 LOAD = 1
 SUBCASE 2
 LOAD = 2
 SUBCASE 3
 LOAD = 3
 SUBCASE 4
 LOAD = 4
 SUBCASE 5
 LOAD = 5
 SUBCASE 6
 LOAD = 6
 SUBCASE 7
 LOAD = 7
 SUBCASE 8
 LOAD = 8
 BEGIN BULK

| \$ | EID | CD | X | Y | Z | CONSTRAINT |
|------|-----|----|-------|---------|----------|------------|
| GRID | 1 | | 125.0 | 378.467 | 0.773135 | 456 |
| GRID | 2 | | 125.0 | 381.997 | 0.888060 | 456 |
| GRID | 3 | | 125.0 | 385.186 | 0.961194 | 456 |
| GRID | 4 | | 125.0 | 388.261 | 1.002985 | 456 |
| GRID | 5 | | 125.0 | 391.678 | 0.992538 | 456 |
| GRID | 6 | | 125.0 | 401.974 | 0.721000 | 456 |
| GRID | 7 | | 118.0 | 389.538 | 1.063861 | 456 |
| GRID | 8 | | 118.0 | 400.936 | 0.852989 | 456 |
| GRID | 9 | | 111.0 | 387.398 | 1.265638 | 456 |
| GRID | 10 | | 111.0 | 399.897 | 0.937355 | 456 |
| GRID | 11 | | 101.0 | 366.238 | 1.042225 | 456 |
| GRID | 12 | | 101.0 | 369.983 | 1.149255 | 456 |
| GRID | 13 | | 101.0 | 371.076 | 1.159702 | 456 |
| GRID | 14 | | 101.0 | 373.729 | 1.272963 | 456 |
| GRID | 15 | | 101.0 | 375.445 | 1.264180 | 456 |
| GRID | 16 | | 101.0 | 377.474 | 1.328600 | 456 |
| GRID | 17 | | 101.0 | 379.659 | 1.328600 | 456 |
| GRID | 18 | | 101.0 | 381.220 | 1.337315 | 456 |
| GRID | 19 | | 101.0 | 384.341 | 1.319072 | 456 |
| GRID | 20 | | 101.0 | 398.386 | 1.093750 | 456 |
| GRID | 21 | | 85.19 | 379.507 | 1.530144 | 456 |
| GRID | 22 | | 83.2 | 395.772 | 1.273870 | 456 |
| GRID | 23 | | 77.75 | 377.232 | 1.646627 | 456 |
| GRID | 24 | | 76.7 | 394.808 | 1.331552 | 456 |
| GRID | 25 | | 72.25 | 375.551 | 1.770699 | 456 |
| GRID | 26 | | 72.25 | 394.148 | 1.397101 | 456 |
| GRID | 27 | | 64.8 | 347.793 | 1.457463 | 456 |
| GRID | 28 | | 64.8 | 353.065 | 1.572388 | 456 |
| GRID | 29 | | 64.8 | 358.337 | 1.729100 | 456 |
| GRID | 30 | | 64.8 | 363.608 | 1.736940 | 456 |
| GRID | 31 | | 64.8 | 368.880 | 1.854480 | 456 |

| | | | | | |
|------|----|--------|---------|----------|------|
| GRID | 32 | 64.8 | 373.273 | 1.828350 | 456 |
| GRID | 33 | 64.8 | 393.042 | 1.462650 | 456 |
| GRID | 34 | 29.92 | 330.021 | 1.922389 | 3456 |
| GRID | 35 | 28.777 | 336.408 | 2.037314 | 3456 |
| GRID | 36 | 27.867 | 342.867 | 2.162685 | 3456 |
| GRID | 37 | 26.946 | 349.400 | 2.340299 | 3456 |
| GRID | 38 | 26.015 | 356.008 | 2.371642 | 3456 |
| GRID | 39 | 25.231 | 361.572 | 2.194030 | 3456 |
| GRID | 40 | 29.3 | 362.731 | 2.156426 | 3456 |
| GRID | 41 | 26.06 | 386.424 | 1.947470 | 3456 |
| GRID | 42 | 0.0 | 330.021 | 1.922389 | 1456 |
| GRID | 43 | 0.0 | 336.408 | 2.037314 | 1456 |
| GRID | 44 | 0.0 | 342.867 | 2.162685 | 1456 |
| GRID | 45 | 0.0 | 349.4 | 2.340299 | 1456 |
| GRID | 46 | 0.0 | 356.008 | 2.371642 | 1456 |
| GRID | 47 | 0.0 | 361.572 | 2.194030 | 1456 |
| GRID | 48 | 0.0 | 386.424 | 1.947470 | 1456 |
| GRID | 49 | 125.0 | 378.467 | -0.77313 | 456 |
| GRID | 50 | 125.0 | 381.997 | -0.88806 | 456 |
| GRID | 51 | 125.0 | 385.186 | -0.96119 | 456 |
| GRID | 52 | 125.0 | 388.261 | -1.00298 | 456 |
| GRID | 53 | 125.0 | 391.678 | -0.99253 | 456 |
| GRID | 54 | 125.0 | 401.974 | -0.72100 | 456 |
| GRID | 55 | 118.0 | 389.538 | -1.06386 | 456 |
| GRID | 56 | 118.0 | 400.936 | -0.85299 | 456 |
| GRID | 57 | 111.0 | 387.398 | -1.26564 | 456 |
| GRID | 58 | 111.0 | 399.897 | -0.93736 | 456 |
| GRID | 59 | 101.0 | 366.238 | -1.04223 | 456 |
| GRID | 60 | 101.0 | 369.983 | -1.14926 | 456 |
| GRID | 61 | 101.0 | 371.076 | -1.15970 | 456 |
| GRID | 62 | 101.0 | 373.729 | -1.27296 | 456 |
| GRID | 63 | 101.0 | 375.445 | -1.26418 | 456 |
| GRID | 64 | 101.0 | 377.474 | -1.32860 | 456 |
| GRID | 65 | 101.0 | 379.659 | -1.32860 | 456 |
| GRID | 66 | 101.0 | 381.220 | -1.33732 | 456 |
| GRID | 67 | 101.0 | 384.341 | -1.31907 | 456 |
| GRID | 68 | 101.0 | 398.386 | -1.09375 | 456 |
| GRID | 69 | 85.19 | 379.507 | -1.53014 | 456 |
| GRID | 70 | 83.2 | 395.772 | -1.27387 | 456 |
| GRID | 71 | 77.75 | 377.232 | -1.64663 | 456 |
| GRID | 72 | 76.7 | 394.808 | -1.33155 | 456 |
| GRID | 73 | 72.25 | 375.551 | -1.77069 | 456 |
| GRID | 74 | 72.25 | 394.148 | -1.39710 | 456 |
| GRID | 75 | 64.8 | 347.793 | -1.45746 | 456 |
| GRID | 76 | 64.8 | 353.065 | -1.57239 | 456 |
| GRID | 77 | 64.8 | 358.337 | -1.72910 | 456 |
| GRID | 78 | 64.8 | 363.608 | -1.73694 | 456 |
| GRID | 79 | 64.8 | 368.880 | -1.85448 | 456 |
| GRID | 80 | 64.8 | 373.273 | -1.82835 | 456 |
| GRID | 81 | 64.8 | 393.042 | -1.46265 | 456 |
| GRID | 82 | 29.92 | 330.021 | -1.92239 | 3456 |
| GRID | 83 | 28.777 | 336.408 | -2.03731 | 3456 |
| GRID | 84 | 27.867 | 342.867 | -2.16269 | 3456 |
| GRID | 85 | 26.946 | 349.400 | -2.34029 | 3456 |
| GRID | 86 | 26.015 | 356.008 | -2.37164 | 3456 |
| GRID | 87 | 25.231 | 361.572 | -2.19403 | 3456 |
| GRID | 88 | 29.3 | 362.731 | -2.15643 | 3456 |
| GRID | 89 | 26.06 | 386.424 | -1.94747 | 3456 |

| | | | | | |
|------|----|-----|---------|----------|------|
| GRID | 90 | 0.0 | 330.021 | -1.92239 | 1456 |
| GRID | 91 | 0.0 | 336.408 | -2.03731 | 1456 |
| GRID | 92 | 0.0 | 342.867 | -2.16269 | 1456 |
| GRID | 93 | 0.0 | 349.4 | -2.34029 | 1456 |
| GRID | 94 | 0.0 | 356.008 | -2.37164 | 1456 |
| GRID | 95 | 0.0 | 361.572 | -2.19403 | 1456 |
| GRID | 96 | 0.0 | 386.424 | -1.94747 | 1456 |

| \$ | EID | G1 | G2 | MID | CSA |
|--------|-----|----|----|-----|----------|
| CONROD | 1 | 1 | 2 | 1 | 0.106742 |
| CONROD | 2 | 2 | 3 | 1 | 0.110107 |
| CONROD | 3 | 3 | 4 | 1 | 0.112086 |
| CONROD | 4 | 4 | 5 | 1 | 0.112622 |
| CONROD | 5 | 5 | 6 | 1 | 0.119206 |
| CONROD | 6 | 7 | 8 | 1 | 0.255194 |
| CONROD | 7 | 9 | 10 | 1 | 0.246097 |
| CONROD | 8 | 11 | 12 | 1 | 0.159778 |
| CONROD | 9 | 12 | 13 | 1 | 0.159778 |
| CONROD | 10 | 13 | 14 | 1 | 0.164029 |
| CONROD | 11 | 14 | 15 | 1 | 0.164029 |
| CONROD | 12 | 15 | 16 | 1 | 0.166860 |
| CONROD | 13 | 16 | 17 | 1 | 0.166860 |
| CONROD | 14 | 17 | 18 | 1 | 0.167765 |
| CONROD | 15 | 18 | 19 | 1 | 0.167765 |
| CONROD | 16 | 19 | 20 | 1 | 0.163841 |
| CONROD | 17 | 21 | 22 | 1 | 0.154423 |
| CONROD | 18 | 23 | 24 | 1 | 0.139074 |
| CONROD | 19 | 25 | 26 | 1 | 0.139074 |
| CONROD | 20 | 27 | 28 | 2 | 0.667360 |
| CONROD | 21 | 28 | 29 | 2 | 0.681896 |
| CONROD | 22 | 29 | 30 | 2 | 0.689985 |
| CONROD | 23 | 30 | 31 | 2 | 0.695839 |
| CONROD | 24 | 31 | 32 | 2 | 0.699954 |
| CONROD | 25 | 32 | 33 | 2 | 0.681363 |
| CONROD | 26 | 34 | 35 | 1 | 0.213887 |
| CONROD | 27 | 35 | 36 | 1 | 0.223157 |
| CONROD | 28 | 36 | 37 | 1 | 0.237261 |
| CONROD | 29 | 37 | 38 | 1 | 0.256984 |
| CONROD | 30 | 38 | 39 | 1 | 0.274676 |
| CONROD | 31 | 40 | 41 | 1 | 0.192684 |
| CONROD | 32 | 1 | 11 | 1 | 0.362960 |
| CONROD | 33 | 2 | 13 | 1 | 0.094927 |
| CONROD | 34 | 3 | 15 | 1 | 0.095374 |
| CONROD | 35 | 4 | 17 | 1 | 0.097067 |
| CONROD | 36 | 5 | 7 | 1 | 0.128680 |
| CONROD | 37 | 6 | 8 | 1 | 0.148729 |
| CONROD | 38 | 7 | 9 | 1 | 0.128680 |
| CONROD | 39 | 8 | 10 | 1 | 0.148729 |
| CONROD | 40 | 9 | 19 | 1 | 0.128680 |
| CONROD | 41 | 10 | 20 | 1 | 0.148729 |
| CONROD | 42 | 11 | 27 | 1 | 0.400786 |
| CONROD | 43 | 12 | 28 | 1 | 0.084990 |
| CONROD | 44 | 14 | 29 | 1 | 0.091382 |
| CONROD | 45 | 16 | 30 | 1 | 0.128673 |
| CONROD | 46 | 18 | 31 | 1 | 0.126535 |
| CONROD | 47 | 19 | 21 | 1 | 0.147487 |
| CONROD | 48 | 20 | 22 | 1 | 0.145914 |

| | | | | | |
|---------------------|-----|----|----|---|----------|
| CONROD | 49 | 21 | 23 | 1 | 0.147487 |
| CONROD | 50 | 22 | 24 | 1 | 0.145914 |
| CONROD | 51 | 23 | 25 | 1 | 0.163193 |
| CONROD | 52 | 24 | 26 | 1 | 0.145914 |
| CONROD | 53 | 25 | 32 | 1 | 0.163193 |
| CONROD | 54 | 26 | 33 | 1 | 0.145914 |
| CONROD | 55 | 27 | 34 | 1 | 0.623202 |
| CONROD | 56 | 28 | 35 | 1 | 0.136110 |
| CONROD | 57 | 29 | 36 | 1 | 0.158313 |
| CONROD | 58 | 30 | 37 | 1 | 0.196573 |
| CONROD | 59 | 31 | 38 | 1 | 0.198040 |
| CONROD | 60 | 32 | 40 | 1 | 0.390376 |
| CONROD | 61 | 40 | 39 | 1 | 0.390376 |
| CONROD | 62 | 33 | 41 | 1 | 0.104919 |
| CONROD | 63 | 34 | 42 | 1 | 0.172374 |
| CONROD | 64 | 35 | 43 | 1 | 0.145401 |
| CONROD | 65 | 36 | 44 | 1 | 0.167005 |
| CONROD | 66 | 37 | 45 | 1 | 0.184835 |
| CONROD | 67 | 38 | 46 | 1 | 0.216165 |
| CONROD | 68 | 39 | 47 | 1 | 0.243853 |
| \$lower skin chords | | | | | |
| CONROD | 69 | 49 | 50 | 1 | 0.106742 |
| CONROD | 70 | 50 | 51 | 1 | 0.110107 |
| CONROD | 71 | 51 | 52 | 1 | 0.112086 |
| CONROD | 72 | 52 | 53 | 1 | 0.112622 |
| CONROD | 73 | 53 | 54 | 1 | 0.119206 |
| CONROD | 74 | 55 | 56 | 1 | 0.255194 |
| CONROD | 75 | 57 | 58 | 1 | 0.246097 |
| CONROD | 76 | 59 | 60 | 1 | 0.159778 |
| CONROD | 77 | 60 | 61 | 1 | 0.159778 |
| CONROD | 78 | 61 | 62 | 1 | 0.164029 |
| CONROD | 79 | 62 | 63 | 1 | 0.164029 |
| CONROD | 80 | 63 | 64 | 1 | 0.166860 |
| CONROD | 81 | 64 | 65 | 1 | 0.166860 |
| CONROD | 82 | 65 | 66 | 1 | 0.167765 |
| CONROD | 83 | 66 | 67 | 1 | 0.167765 |
| CONROD | 84 | 67 | 68 | 1 | 0.163841 |
| CONROD | 85 | 69 | 70 | 1 | 0.154423 |
| CONROD | 86 | 71 | 72 | 1 | 0.139074 |
| CONROD | 87 | 73 | 74 | 1 | 0.139074 |
| CONROD | 88 | 75 | 76 | 2 | 0.667360 |
| CONROD | 89 | 76 | 77 | 2 | 0.681896 |
| CONROD | 90 | 77 | 78 | 2 | 0.689985 |
| CONROD | 91 | 78 | 79 | 2 | 0.695839 |
| CONROD | 92 | 79 | 80 | 2 | 0.699954 |
| CONROD | 93 | 80 | 81 | 2 | 0.681363 |
| CONROD | 94 | 82 | 83 | 1 | 0.213887 |
| CONROD | 95 | 83 | 84 | 1 | 0.223157 |
| CONROD | 96 | 84 | 85 | 1 | 0.237261 |
| CONROD | 97 | 85 | 86 | 1 | 0.256984 |
| CONROD | 98 | 86 | 87 | 1 | 0.274676 |
| CONROD | 99 | 88 | 89 | 1 | 0.192684 |
| CONROD | 100 | 49 | 59 | 1 | 0.362960 |
| CONROD | 101 | 50 | 61 | 1 | 0.094927 |
| CONROD | 102 | 51 | 63 | 1 | 0.095374 |
| CONROD | 103 | 52 | 65 | 1 | 0.097067 |
| CONROD | 104 | 53 | 55 | 1 | 0.128680 |
| CONROD | 105 | 54 | 56 | 1 | 0.148729 |

| | | | | | |
|----------|-----|----|----|---|----------|
| CONROD | 106 | 55 | 57 | 1 | 0.128680 |
| CONROD | 107 | 56 | 58 | 1 | 0.148729 |
| CONROD | 108 | 57 | 67 | 1 | 0.128680 |
| CONROD | 109 | 58 | 68 | 1 | 0.148729 |
| CONROD | 110 | 59 | 75 | 1 | 0.400786 |
| CONROD | 111 | 60 | 76 | 1 | 0.084990 |
| CONROD | 112 | 62 | 77 | 1 | 0.091382 |
| CONROD | 113 | 64 | 78 | 1 | 0.128673 |
| CONROD | 114 | 66 | 79 | 1 | 0.126535 |
| CONROD | 115 | 67 | 69 | 1 | 0.147487 |
| CONROD | 116 | 68 | 70 | 1 | 0.145914 |
| CONROD | 117 | 69 | 71 | 1 | 0.147487 |
| CONROD | 118 | 70 | 72 | 1 | 0.145914 |
| CONROD | 119 | 71 | 73 | 1 | 0.163193 |
| CONROD | 120 | 72 | 74 | 1 | 0.145914 |
| CONROD | 121 | 73 | 80 | 1 | 0.163193 |
| CONROD | 122 | 74 | 81 | 1 | 0.145914 |
| CONROD | 123 | 75 | 82 | 1 | 0.623202 |
| CONROD | 124 | 76 | 83 | 1 | 0.136110 |
| CONROD | 125 | 77 | 84 | 1 | 0.158313 |
| CONROD | 126 | 78 | 85 | 1 | 0.196573 |
| CONROD | 127 | 79 | 86 | 1 | 0.198040 |
| CONROD | 128 | 80 | 88 | 1 | 0.390376 |
| CONROD | 129 | 88 | 87 | 1 | 0.390376 |
| CONROD | 130 | 81 | 89 | 1 | 0.104919 |
| CONROD | 131 | 82 | 90 | 1 | 0.172374 |
| CONROD | 132 | 83 | 91 | 1 | 0.145401 |
| CONROD | 133 | 84 | 92 | 1 | 0.167005 |
| CONROD | 134 | 85 | 93 | 1 | 0.164835 |
| CONROD | 135 | 86 | 94 | 1 | 0.216165 |
| CONROD | 136 | 87 | 95 | 1 | 0.243853 |
| \$CONROD | 137 | 41 | 48 | 1 | 0.24 |
| \$CONROD | 138 | 89 | 96 | 1 | 0.24 |

| \$ | EID | G1 | G2 | MID | CSA |
|--------|-----|----|----|-----|------|
| CONROD | 201 | 1 | 49 | 1 | 0.24 |
| CONROD | 202 | 2 | 50 | 1 | 0.24 |
| CONROD | 203 | 3 | 51 | 1 | 0.24 |
| CONROD | 204 | 4 | 52 | 1 | 0.24 |
| CONROD | 205 | 5 | 53 | 1 | 0.24 |
| CONROD | 206 | 6 | 54 | 1 | 0.24 |
| CONROD | 207 | 7 | 55 | 1 | 0.24 |
| CONROD | 208 | 8 | 56 | 1 | 0.24 |
| CONROD | 209 | 9 | 57 | 1 | 0.24 |
| CONROD | 210 | 10 | 58 | 1 | 0.24 |
| CONROD | 211 | 11 | 59 | 1 | 0.24 |
| CONROD | 212 | 12 | 60 | 1 | 0.24 |
| CONROD | 213 | 13 | 61 | 1 | 0.24 |
| CONROD | 214 | 14 | 62 | 1 | 0.24 |
| CONROD | 215 | 15 | 63 | 1 | 0.24 |
| CONROD | 216 | 16 | 64 | 1 | 0.24 |
| CONROD | 217 | 17 | 65 | 1 | 0.24 |
| CONROD | 218 | 18 | 66 | 1 | 0.24 |
| CONROD | 219 | 19 | 67 | 1 | 0.24 |
| CONROD | 220 | 20 | 68 | 2 | 0.24 |
| CONROD | 221 | 21 | 69 | 2 | 0.24 |
| CONROD | 222 | 22 | 70 | 2 | 0.24 |
| CONROD | 223 | 23 | 71 | 2 | 0.24 |

| | | | | | |
|----------|-----|----|----|---|------|
| CONROD | 224 | 24 | 72 | 2 | 0.24 |
| CONROD | 225 | 25 | 73 | 2 | 0.24 |
| CONROD | 226 | 26 | 74 | 1 | 0.24 |
| CONROD | 227 | 27 | 75 | 1 | 0.24 |
| CONROD | 228 | 28 | 76 | 1 | 0.24 |
| CONROD | 229 | 29 | 77 | 1 | 0.24 |
| CONROD | 230 | 30 | 78 | 1 | 0.24 |
| CONROD | 231 | 31 | 79 | 1 | 0.24 |
| CONROD | 232 | 32 | 80 | 1 | 0.24 |
| CONROD | 233 | 33 | 81 | 1 | 0.24 |
| CONROD | 234 | 34 | 82 | 1 | 0.24 |
| CONROD | 235 | 35 | 83 | 1 | 0.24 |
| CONROD | 236 | 36 | 84 | 1 | 0.24 |
| CONROD | 237 | 37 | 85 | 1 | 0.24 |
| CONROD | 238 | 38 | 86 | 1 | 0.24 |
| CONROD | 239 | 39 | 87 | 1 | 0.24 |
| CONROD | 240 | 40 | 88 | 1 | 0.24 |
| CONROD | 241 | 41 | 89 | 1 | 0.24 |
| \$CONROD | 242 | 42 | 90 | 1 | 0.24 |
| \$CONROD | 243 | 43 | 91 | 1 | 0.24 |
| \$CONROD | 244 | 44 | 92 | 1 | 0.24 |
| \$CONROD | 245 | 45 | 93 | 1 | 0.24 |
| \$CONROD | 246 | 46 | 94 | 1 | 0.24 |
| \$CONROD | 247 | 47 | 95 | 1 | 0.24 |
| \$CONROD | 248 | 48 | 96 | 1 | 0.24 |

| \$ | EID | PID | G1 | G2 | G3 | G4 |
|--------|-----|-----|----|----|----|----|
| CQUAD4 | 101 | 101 | 2 | 13 | 11 | 1 |
| CQUAD4 | 102 | 102 | 3 | 15 | 13 | 2 |
| CQUAD4 | 103 | 103 | 4 | 17 | 15 | 3 |
| CQUAD4 | 104 | 104 | 5 | 19 | 17 | 4 |
| CQUAD4 | 105 | 105 | 6 | 8 | 7 | 5 |
| CQUAD4 | 106 | 106 | 8 | 10 | 9 | 7 |
| CQUAD4 | 107 | 107 | 10 | 20 | 19 | 9 |
| CQUAD4 | 108 | 108 | 12 | 28 | 27 | 11 |
| CQUAD4 | 109 | 109 | 14 | 29 | 28 | 12 |
| CQUAD4 | 110 | 110 | 16 | 30 | 29 | 14 |
| CQUAD4 | 111 | 111 | 18 | 31 | 30 | 16 |
| CQUAD4 | 112 | 112 | 19 | 32 | 31 | 18 |
| CQUAD4 | 113 | 113 | 20 | 22 | 21 | 19 |
| CQUAD4 | 114 | 114 | 22 | 24 | 23 | 21 |
| CQUAD4 | 115 | 115 | 24 | 26 | 25 | 23 |
| CQUAD4 | 116 | 116 | 26 | 33 | 32 | 25 |
| CQUAD4 | 117 | 117 | 28 | 35 | 34 | 27 |
| CQUAD4 | 118 | 118 | 29 | 36 | 35 | 28 |
| CQUAD4 | 119 | 119 | 30 | 37 | 36 | 29 |
| CQUAD4 | 120 | 120 | 31 | 38 | 37 | 30 |
| CQUAD4 | 121 | 121 | 32 | 39 | 38 | 31 |
| CQUAD4 | 122 | 122 | 33 | 41 | 40 | 32 |
| CQUAD4 | 123 | 123 | 35 | 43 | 42 | 34 |
| CQUAD4 | 124 | 124 | 36 | 44 | 43 | 35 |
| CQUAD4 | 125 | 125 | 37 | 45 | 44 | 36 |
| CQUAD4 | 126 | 126 | 38 | 46 | 45 | 37 |
| CQUAD4 | 127 | 127 | 39 | 47 | 46 | 38 |
| CQUAD4 | 128 | 128 | 50 | 61 | 59 | 49 |
| CQUAD4 | 129 | 129 | 51 | 63 | 61 | 50 |
| CQUAD4 | 130 | 130 | 52 | 65 | 63 | 51 |
| CQUAD4 | 131 | 131 | 53 | 67 | 65 | 52 |

| | | | | | | |
|--------|-----|-----|----|----|----|----|
| CQUAD4 | 132 | 132 | 54 | 56 | 55 | 53 |
| CQUAD4 | 133 | 133 | 56 | 58 | 57 | 55 |
| CQUAD4 | 134 | 134 | 58 | 68 | 67 | 57 |
| CQUAD4 | 135 | 135 | 60 | 76 | 75 | 59 |
| CQUAD4 | 136 | 136 | 62 | 77 | 76 | 60 |
| CQUAD4 | 137 | 137 | 64 | 78 | 77 | 62 |
| CQUAD4 | 138 | 138 | 66 | 79 | 78 | 64 |
| CQUAD4 | 139 | 139 | 67 | 80 | 79 | 66 |
| CQUAD4 | 140 | 140 | 68 | 70 | 69 | 67 |
| CQUAD4 | 141 | 141 | 70 | 72 | 71 | 69 |
| CQUAD4 | 142 | 142 | 72 | 74 | 73 | 71 |
| CQUAD4 | 143 | 143 | 74 | 81 | 80 | 73 |
| CQUAD4 | 144 | 144 | 76 | 83 | 82 | 75 |
| CQUAD4 | 145 | 145 | 77 | 84 | 83 | 76 |
| CQUAD4 | 146 | 146 | 78 | 85 | 84 | 77 |
| CQUAD4 | 147 | 147 | 79 | 86 | 85 | 78 |
| CQUAD4 | 148 | 148 | 80 | 87 | 86 | 79 |
| CQUAD4 | 149 | 149 | 81 | 89 | 88 | 80 |
| CQUAD4 | 150 | 150 | 83 | 91 | 90 | 82 |
| CQUAD4 | 151 | 151 | 84 | 92 | 91 | 83 |
| CQUAD4 | 152 | 152 | 85 | 93 | 92 | 84 |
| CQUAD4 | 153 | 153 | 86 | 94 | 93 | 85 |
| CQUAD4 | 154 | 154 | 87 | 95 | 94 | 86 |
| CQUAD4 | 155 | 155 | 41 | 48 | 47 | 39 |
| CQUAD4 | 156 | 156 | 89 | 96 | 95 | 87 |

| \$ | PID | MID1 | TH | MID2 | 12I/T3 |
|--------|-----|------|--------|------|--------|
| PSHELL | 101 | 4 | 0.09 | 4 | |
| PSHELL | 102 | 4 | 0.0625 | 4 | |
| PSHELL | 103 | 4 | 0.0645 | 4 | |
| PSHELL | 104 | 4 | 0.067 | 4 | |
| PSHELL | 105 | 4 | 0.06 | 4 | |
| PSHELL | 106 | 4 | 0.065 | 4 | |
| PSHELL | 107 | 4 | 0.07 | 4 | |
| PSHELL | 108 | 4 | 0.1415 | 4 | |
| PSHELL | 109 | 4 | 0.116 | 4 | |
| PSHELL | 110 | 4 | 0.1255 | 4 | |
| PSHELL | 111 | 4 | 0.13 | 4 | |
| PSHELL | 112 | 4 | 0.133 | 4 | |
| PSHELL | 113 | 4 | 0.04 | 4 | |
| PSHELL | 114 | 4 | 0.11 | 4 | |
| PSHELL | 115 | 4 | 0.095 | 4 | |
| PSHELL | 116 | 4 | 0.095 | 4 | |
| PSHELL | 117 | 4 | 0.175 | 4 | |
| PSHELL | 118 | 4 | 0.195 | 4 | |
| PSHELL | 119 | 4 | 0.2055 | 4 | |
| PSHELL | 120 | 4 | 0.216 | 4 | |
| PSHELL | 121 | 4 | 0.2395 | 4 | |
| PSHELL | 122 | 4 | 0.025 | 4 | |
| PSHELL | 123 | 4 | 0.207 | 4 | |
| PSHELL | 124 | 4 | 0.230 | 4 | |
| PSHELL | 125 | 4 | 0.244 | 4 | |
| PSHELL | 126 | 4 | 0.258 | 4 | |
| PSHELL | 127 | 4 | 0.290 | 4 | |
| PSHELL | 128 | 4 | 0.065 | 4 | |
| PSHELL | 129 | 4 | 0.055 | 4 | |
| PSHELL | 130 | 4 | 0.055 | 4 | |
| PSHELL | 131 | 4 | 0.055 | 4 | |

| | | | | |
|--------|-----|---|--------|---|
| PSHELL | 132 | 4 | 0.058 | 4 |
| PSHELL | 133 | | 0.038 | 4 |
| PSHELL | 134 | | 0.038 | 4 |
| PSHELL | 135 | | 0.1115 | 4 |
| PSHELL | 136 | 4 | 0.1065 | 4 |
| PSHELL | 137 | 4 | 0.115 | 4 |
| PSHELL | 138 | 4 | 0.1215 | 4 |
| PSHELL | 139 | 4 | 0.1215 | 4 |
| PSHELL | 140 | 4 | 0.038 | 4 |
| PSHELL | 141 | 4 | 0.038 | 4 |
| PSHELL | 142 | 4 | 0.08 | 4 |
| PSHELL | 143 | 4 | 0.08 | 4 |
| PSHELL | 144 | 4 | 0.1725 | 4 |
| PSHELL | 145 | 4 | 0.132 | 4 |
| PSHELL | 146 | 4 | 0.1965 | 4 |
| PSHELL | 147 | 4 | 0.2215 | 4 |
| PSHELL | 148 | 4 | 0.239 | 4 |
| PSHELL | 149 | 4 | 0.04 | 4 |
| PSHELL | 150 | 4 | 0.21 | 4 |
| PSHELL | 151 | 4 | 0.22 | 4 |
| PSHELL | 152 | 4 | 0.24 | 4 |
| PSHELL | 153 | 4 | 0.27 | 4 |
| PSHELL | 154 | 4 | 0.298 | 4 |
| PSHELL | 155 | 4 | 0.3 | 4 |
| PSHELL | 156 | 4 | 0.3 | 4 |

| \$ | EID | PID | G1 | G2 | G3 | G4 |
|--------|-----|-----|----|----|----|----|
| CSHEAR | 1 | 1 | 49 | 50 | 2 | 1 |
| CSHEAR | 2 | 2 | 50 | 51 | 3 | 2 |
| CSHEAR | 3 | 3 | 51 | 52 | 4 | 3 |
| CSHEAR | 4 | 4 | 52 | 53 | 5 | 4 |
| CSHEAR | 5 | 5 | 53 | 54 | 6 | 5 |
| CSHEAR | 6 | 6 | 55 | 56 | 8 | 7 |
| CSHEAR | 7 | 7 | 57 | 58 | 10 | 9 |
| CSHEAR | 8 | 8 | 59 | 60 | 12 | 11 |
| CSHEAR | 9 | 9 | 60 | 61 | 13 | 12 |
| CSHEAR | 10 | 10 | 61 | 62 | 14 | 13 |
| CSHEAR | 11 | 11 | 62 | 63 | 15 | 14 |
| CSHEAR | 12 | 12 | 63 | 64 | 16 | 15 |
| CSHEAR | 13 | 13 | 64 | 65 | 17 | 16 |
| CSHEAR | 14 | 14 | 65 | 66 | 18 | 17 |
| CSHEAR | 15 | 15 | 66 | 67 | 19 | 18 |
| CSHEAR | 16 | 16 | 67 | 68 | 20 | 19 |
| CSHEAR | 17 | 17 | 69 | 70 | 22 | 21 |
| CSHEAR | 18 | 18 | 71 | 72 | 24 | 23 |
| CSHEAR | 19 | 19 | 73 | 74 | 26 | 25 |
| CSHEAR | 20 | 20 | 75 | 76 | 28 | 27 |
| CSHEAR | 21 | 21 | 76 | 77 | 29 | 28 |
| CSHEAR | 22 | 22 | 77 | 78 | 30 | 29 |
| CSHEAR | 23 | 23 | 78 | 79 | 31 | 30 |
| CSHEAR | 24 | 24 | 79 | 80 | 32 | 31 |
| CSHEAR | 25 | 25 | 80 | 81 | 33 | 32 |
| CSHEAR | 26 | 26 | 82 | 83 | 35 | 34 |
| CSHEAR | 27 | 27 | 83 | 84 | 36 | 35 |
| CSHEAR | 28 | 28 | 84 | 85 | 37 | 36 |
| CSHEAR | 29 | 29 | 85 | 86 | 38 | 37 |
| CSHEAR | 30 | 30 | 86 | 87 | 39 | 38 |
| CSHEAR | 31 | 31 | 49 | 59 | 11 | 1 |

| | | | | | | |
|--------|----|----|----|----|----|----|
| CSHEAR | 32 | 32 | 50 | 61 | 13 | 2 |
| CSHEAR | 33 | 33 | 51 | 63 | 15 | 3 |
| CSHEAR | 34 | 34 | 52 | 65 | 17 | 4 |
| CSHEAR | 35 | 35 | 53 | 55 | 7 | 5 |
| CSHEAR | 36 | 36 | 54 | 56 | 8 | 6 |
| CSHEAR | 37 | 37 | 55 | 57 | 9 | 7 |
| CSHEAR | 38 | 38 | 56 | 58 | 10 | 8 |
| CSHEAR | 39 | 39 | 57 | 67 | 19 | 9 |
| CSHEAR | 40 | 40 | 58 | 68 | 20 | 10 |
| CSHEAR | 41 | 41 | 59 | 75 | 27 | 11 |
| CSHEAR | 42 | 42 | 60 | 76 | 28 | 12 |
| CSHEAR | 43 | 43 | 62 | 77 | 29 | 14 |
| CSHEAR | 44 | 44 | 64 | 78 | 30 | 16 |
| CSHEAR | 45 | 45 | 66 | 79 | 31 | 18 |
| CSHEAR | 46 | 46 | 67 | 69 | 21 | 19 |
| CSHEAR | 47 | 47 | 68 | 70 | 22 | 20 |
| CSHEAR | 48 | 48 | 69 | 71 | 23 | 21 |
| CSHEAR | 49 | 49 | 70 | 72 | 24 | 22 |
| CSHEAR | 50 | 50 | 71 | 73 | 25 | 23 |
| CSHEAR | 51 | 51 | 72 | 74 | 26 | 24 |
| CSHEAR | 52 | 52 | 73 | 80 | 32 | 25 |
| CSHEAR | 53 | 53 | 74 | 81 | 33 | 26 |
| CSHEAR | 54 | 54 | 75 | 82 | 34 | 27 |
| CSHEAR | 55 | 55 | 76 | 83 | 35 | 28 |
| CSHEAR | 56 | 56 | 77 | 84 | 36 | 29 |
| CSHEAR | 57 | 57 | 78 | 85 | 37 | 30 |
| CSHEAR | 58 | 58 | 79 | 86 | 38 | 31 |
| CSHEAR | 59 | 59 | 80 | 88 | 40 | 32 |
| CSHEAR | 60 | 60 | 88 | 87 | 39 | 40 |
| CSHEAR | 61 | 61 | 81 | 89 | 41 | 33 |
| CSHEAR | 62 | 62 | 82 | 90 | 42 | 34 |
| CSHEAR | 63 | 63 | 83 | 91 | 43 | 35 |
| CSHEAR | 64 | 64 | 84 | 92 | 44 | 36 |
| CSHEAR | 65 | 65 | 85 | 93 | 45 | 37 |
| CSHEAR | 66 | 66 | 86 | 94 | 46 | 38 |
| CSHEAR | 67 | 67 | 87 | 95 | 47 | 39 |
| CSHEAR | 68 | 68 | 88 | 89 | 41 | 40 |

| S | PID | MID1 | TH |
|--------|-----|------|------|
| PSHEAR | 1 | 7 | 0.08 |
| PSHEAR | 2 | 7 | 0.08 |
| PSHEAR | 3 | 7 | 0.08 |
| PSHEAR | 4 | 7 | 0.08 |
| PSHEAR | 5 | 7 | 0.09 |
| PSHEAR | 6 | 7 | 0.13 |
| PSHEAR | 7 | 7 | 0.13 |
| PSHEAR | 8 | 7 | 0.09 |
| PSHEAR | 9 | 7 | 0.09 |
| PSHEAR | 10 | 7 | 0.09 |
| PSHEAR | 11 | 7 | 0.09 |
| PSHEAR | 12 | 7 | 0.09 |
| PSHEAR | 13 | 7 | 0.09 |
| PSHEAR | 14 | 7 | 0.09 |
| PSHEAR | 15 | 7 | 0.09 |
| PSHEAR | 16 | 7 | 0.09 |
| PSHEAR | 17 | 7 | 0.08 |
| PSHEAR | 18 | 7 | 0.08 |
| PSHEAR | 19 | 7 | 0.08 |

| | | | |
|--------|----|---|-------|
| PSHEAR | 20 | 2 | 0.365 |
| PSHEAR | 21 | 2 | 0.365 |
| PSHEAR | 22 | 2 | 0.365 |
| PSHEAR | 23 | 2 | 0.365 |
| PSHEAR | 24 | 2 | 0.365 |
| PSHEAR | 25 | 2 | 0.365 |
| PSHEAR | 26 | 7 | 0.10 |
| PSHEAR | 27 | 7 | 0.10 |
| PSHEAR | 28 | 7 | 0.10 |
| PSHEAR | 29 | 7 | 0.10 |
| PSHEAR | 30 | 7 | 0.10 |
| PSHEAR | 31 | 7 | 0.16 |
| PSHEAR | 32 | 7 | 0.09 |
| PSHEAR | 33 | 7 | 0.09 |
| PSHEAR | 34 | 7 | 0.09 |
| PSHEAR | 35 | 7 | 0.12 |
| PSHEAR | 36 | 7 | 0.12 |
| PSHEAR | 37 | 7 | 0.12 |
| PSHEAR | 38 | 7 | 0.12 |
| PSHEAR | 39 | 7 | 0.12 |
| PSHEAR | 40 | 7 | 0.12 |
| PSHEAR | 41 | 7 | 0.16 |
| PSHEAR | 42 | 7 | 0.09 |
| PSHEAR | 43 | 7 | 0.09 |
| PSHEAR | 44 | 7 | 0.09 |
| PSHEAR | 45 | 7 | 0.09 |
| PSHEAR | 46 | 7 | 0.12 |
| PSHEAR | 47 | 7 | 0.14 |
| PSHEAR | 48 | 7 | 0.12 |
| PSHEAR | 49 | 7 | 0.14 |
| PSHEAR | 50 | 7 | 0.12 |
| PSHEAR | 51 | 7 | 0.14 |
| PSHEAR | 52 | 7 | 0.12 |
| PSHEAR | 53 | 7 | 0.14 |
| PSHEAR | 54 | 7 | 0.16 |
| PSHEAR | 55 | 7 | 0.1 |
| PSHEAR | 56 | 7 | 0.105 |
| PSHEAR | 57 | 7 | 0.11 |
| PSHEAR | 58 | 7 | 0.11 |
| PSHEAR | 59 | 7 | 0.11 |
| PSHEAR | 60 | 7 | 0.11 |
| PSHEAR | 61 | 7 | 0.11 |
| PSHEAR | 62 | 7 | 0.08 |
| PSHEAR | 63 | 7 | 0.08 |
| PSHEAR | 64 | 7 | 0.10 |
| PSHEAR | 65 | 7 | 0.09 |
| PSHEAR | 66 | 7 | 0.1 |
| PSHEAR | 67 | 7 | 0.105 |
| PSHEAR | 68 | 7 | 0.1 |

| | | | | | |
|--------|---|---|----|----|----|
| CTRIA3 | 1 | 1 | 40 | 41 | 39 |
| CTRIA3 | 2 | 1 | 38 | 89 | 87 |

| | | | | |
|--------|---|---|-----|---|
| PSHELL | 1 | 4 | 0.3 | 4 |
|--------|---|---|-----|---|

| \$ | MID | E | G | NU | RHO | A |
|------|-----|--------|---|-----|-----|---|
| MAT1 | 4 | 10.3E6 | | 0.3 | 1.0 | |
| MAT1 | 2 | 30.0E6 | | 0.3 | 1.0 | |

| | | | | |
|------|---|--------|-----|-----|
| MAT1 | 1 | 10.3E6 | 0.3 | 1.0 |
| MAT1 | 7 | 10.3E6 | 0.3 | 1.0 |

| | | | | | | |
|-------|---|----|---------|-----|-----|-----|
| FORCE | 1 | 1 | -500.0 | 0.0 | 0.0 | 1.0 |
| FORCE | 2 | 5 | -1000.0 | 0.0 | 0.0 | 1.0 |
| FORCE | 3 | 6 | -200.0 | 0.0 | 0.0 | 1.0 |
| FORCE | 4 | 11 | -1500.0 | 0.0 | 0.0 | 1.0 |
| FORCE | 5 | 19 | -2500.0 | 0.0 | 0.0 | 1.0 |
| FORCE | 6 | 20 | -500.0 | 0.0 | 0.0 | 1.0 |
| FORCE | 7 | 27 | -3000.0 | 0.0 | 0.0 | 1.0 |
| FORCE | 8 | 32 | -5000.0 | 0.0 | 0.0 | 1.0 |

| | | | | | | |
|---------|-----|------|------|--------|-----|------|
| \$LOAD | SID | S | S1 | L1 | S2 | L2 |
| \$LOAD | 3 | 1.0 | 1.0 | 4 | 1.0 | 1 |
| \$ | SID | CID | G | N1 | N2 | N3 |
| \$RAV | 4 | 0 | 32.2 | 0.0 | 0.0 | -1.0 |
| EIGR | 1 | MGIV | 0.0 | 1000.0 | | 20 |
| 130 | | | | | | |
| +30 | MAX | | | | | |
| ENDDATA | | | | | | |
| // | | | | | | |

INTENTIONALLY LEFT BLANK

No. of
Copies Organization

2 Administrator
Defense Technical Info Center
ATTN: DTIC-DDA
Cameron Station
Alexandria, VA 22304-6145

1 Commander
U.S. Army Materiel Command
ATTN: AMCAM
5001 Eisenhower Ave.
Alexandria, VA 22333-0001

1 Director
U.S. Army Research Laboratory
ATTN: AMSRL-D
2800 Powder Mill Rd.
Adelphi, MD 20783-1145

1 Director
U.S. Army Research Laboratory
ATTN: AMSRL-OP-CI-AD,
Tech Publishing
2800 Powder Mill Rd.
Adelphi, MD 20783-1145

2 Commander
U.S. Army Armament Research,
Development, and Engineering Center
ATTN: SMCAR-IMI-I
Picatinny Arsenal, NJ 07806-5000

2 Commander
U.S. Army Armament Research,
Development, and Engineering Center
ATTN: SMCAR-TDC
Picatinny Arsenal, NJ 07806-5000

1 Director
Benet Weapons Laboratory
U.S. Army Armament Research,
Development, and Engineering Center
ATTN: SMCAR-CCB-TL
Watervliet, NY 12189-4050

(Unclass. only) 1 Commander
U.S. Army Rock Island Arsenal
ATTN: SMCRI-IMC-RT/Technical Library
Rock Island, IL 61299-5000

1 Director
U.S. Army Aviation Research
and Technology Activity
ATTN: SAVRT-R (Library)
M/S 219-3
Ames Research Center
Moffett Field, CA 94035-1000

No. of
Copies Organization

1 Commander
U.S. Army Missile Command
ATTN: AMSMI-RD-CS-R (DOC)
Redstone Arsenal, AL 35898-5010

1 Commander
U.S. Army Tank-Automotive Command
ATTN: ASQNC-TAC-DIT (Technical
Information Center)
Warren, MI 48397-5000

1 Director
U.S. Army TRADOC Analysis Command
ATTN: ATRC-WSR
White Sands Missile Range, NM 88002-5502

1 Commandant
U.S. Army Field Artillery School
ATTN: ATSF-CSI
Ft. Sill, OK 73503-5000

(Class. only) 1 Commandant
U.S. Army Infantry School
ATTN: ATSH-CD (Security Mgr.)
Fort Benning, GA 31905-5660

(Unclass. only) 1 Commandant
U.S. Army Infantry School
ATTN: ATSH-CD-CSO-OR
Fort Benning, GA 31905-5660

1 WLMNOI
Eglin AFB, FL 32542-5000

Aberdeen Proving Ground

2 Dir, USAMSAA
ATTN: AMXSY-D
AMXSY-MP, H. Cohen

1 Cdr, USATECOM
ATTN: AMSTE-TC

1 Dir, ERDEC
ATTN: SCBRD-RT

1 Cdr, CBDA
ATTN: AMSCB-CI

1 Dir, USARL
ATTN: AMSRL-SL-I

10 Dir, USARL
ATTN: AMSRL-OP-CI-B (Tech Lib)

**No. of
Copies Organization**

- 1 Department of the Army
U.S. Army Natick Research,
Development, and Engineering Center
Aero-Mechanical Engineering Directorate
ATTN: STRNC-UE, Andrea M. Blanas
Natick, MA 01760-5017**

- 1 Syracuse University
Department of Civil Engineering
ATTN: Professor James A. Mandel
Syracuse, NY 13244**

- 1 Syracuse University
Department of Aerospace Engineering
ATTN: Professor V. R. Murthy
Syracuse, NY 13244**

USER EVALUATION SHEET/CHANGE OF ADDRESS

This Laboratory undertakes a continuing effort to improve the quality of the reports it publishes. Your comments/answers to the items/questions below will aid us in our efforts.

1. ARL Report Number ARL-TR-99 Date of Report March 1993
2. Date Report Received _____
3. Does this report satisfy a need? (Comment on purpose, related project, or other area of interest for which the report will be used.) _____

4. Specifically, how is the report being used? (Information source, design data, procedure, source of ideas, etc.) _____

5. Has the information in this report led to any quantitative savings as far as man-hours or dollars saved, operating costs avoided, or efficiencies achieved, etc? If so, please elaborate. _____

6. General Comments. What do you think should be changed to improve future reports? (Indicate changes to organization, technical content, format, etc.) _____

CURRENT ADDRESS

Organization _____

Name _____

Street or P.O. Box No. _____

City, State, Zip Code _____

7. If indicating a Change of Address or Address Correction, please provide the Current or Correct address above and the Old or Incorrect address below.

OLD ADDRESS

Organization _____

Name _____

Street or P.O. Box No. _____

City, State, Zip Code _____

(Remove this sheet, fold as indicated, staple or tape closed, and mail.)

DEPARTMENT OF THE ARMY

OFFICIAL BUSINESS

BUSINESS REPLY MAIL

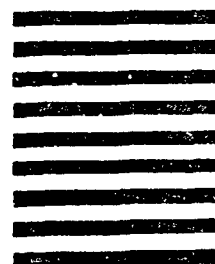
FIRST CLASS PERMIT No 0001, APS, MD

Postage will be paid by addressee

Director
U.S. Army Research Laboratory
ATTN: AMSRL-OP-CI-B (Tech Lib)
Aberdeen Proving Ground, MD 21005-5066



NO POSTAGE
NECESSARY
IF MAILED
IN THE
UNITED STATES



**END
FILMED**

DATE:

4-93

DTIC